



**HAL**  
open science

# Aptamer biosensor development for small molecule detection

Lorena Zara

► **To cite this version:**

| Lorena Zara. Aptamer biosensor development for small molecule detection. Structural Biology [q-bio.BM]. Université Grenoble Alpes [2020-..], 2020. English. NNT : 2020GRALV033 . tel-03188139

**HAL Id: tel-03188139**

**<https://theses.hal.science/tel-03188139>**

Submitted on 1 Apr 2021

**HAL** is a multi-disciplinary open access archive for the deposit and dissemination of scientific research documents, whether they are published or not. The documents may come from teaching and research institutions in France or abroad, or from public or private research centers.

L'archive ouverte pluridisciplinaire **HAL**, est destinée au dépôt et à la diffusion de documents scientifiques de niveau recherche, publiés ou non, émanant des établissements d'enseignement et de recherche français ou étrangers, des laboratoires publics ou privés.

## THÈSE

Pour obtenir le grade de

**DOCTEUR DE L'UNIVERSITE GRENOBLE ALPES**

Spécialité : **Biologie Structurale et nanobiologie**

Arrêté ministériel : 25 mai 2016

Présentée par

**Lorena Zara**

Thèse dirigée par **Corinne Ravelet, Maître de Conférences,**  
**Université Grenoble Alpes**

Co encadrée par **Jean-Jacques Toulmé, Directeur de recherche**  
**émérite INSERM et Directeur Général Novaptech**

préparée au sein du **Département de Pharmacochimie**  
**Moléculaire**

dans l'**École Doctorale Chimie et Sciences de Vivant**

# Développement de biocapteurs à base d'aptamères pour la détection de petites molécules

Thèse soutenue publiquement le **15 décembre 2020**,  
devant le jury composé de :

**Madame Claire DEMESMAY- GUILHIN**

Professeur, Université Lyon I, Rapporteur

**Monsieur Thierry NOGUER**

Professeur, Université de Perpignan, Rapporteur

**Monsieur Michael RYCKELYNCK**

Professeur, Université de Strasbourg, Examineur

**Monsieur Eric DEFRANCO**

Professeur, Université Grenoble Alpes, Président

**Madame Corinne RAVELET**

Maître de Conférences, Université Grenoble Alpes, Directrice de Thèse

**Monsieur Jean-Jacques TOULME**

Directeur Général Novaptech, Bordeaux, Tuteur entreprise

**Monsieur Eric DAUSSE**

Ingénieur de Recherche INSERM, Université de Bordeaux, Membre invité

**Monsieur Eric PEYRIN**

Professeur, Université Grenoble Alpes, Encadrant invité



*Al mio amico geniale,*

*Sabatino.*

# Acknowledgements

Je souhaiterais, tout d'abord, transmettre mes remerciements aux membres du jury de cette thèse, les professeurs **Claire Demesmay-Guilhin** et **Thierry Noguier** qui ont consacré une partie de leur temps à l'évaluation de ce travail et qui m'ont fait l'honneur d'avoir accepté la fonction de rapporteur. Je tiens également à remercier le professeur **Michael Ryckelynck** pour avoir accepté d'examiner mon manuscrit, ainsi que le professeur **Eric Defrancq**, qui a bien voulu présider le jury de ce doctorat.

Les travaux présentés dans ce manuscrit ont fait l'objet **d'une convention CIFRE** entre la **société Novaptech** de Bordeaux et le **Département de Pharmacochimie Moléculaire (DPM)** de l'Université Grenoble Alpes. Je remercie cet organisme pour mon financement.

J'adresse toute ma gratitude à madame **Marine Faussillon-Laville** présidente de Novaptech et monsieur **Jean-Jacques Toulmé** directeur général ainsi que co-encadrant de ma thèse, sans qui cette convention CIFRE n'aurait jamais vu le jour. Je tiens également à les remercier pour la confiance qu'ils m'ont accordée en acceptant de co-financer ce projet.

Je remercie tout particulièrement ma directrice de thèse, madame **Corinne Ravelet** pour sa présence constante, ses conseils et pour toutes les heures qu'elle a consacré à diriger cette recherche. Je n'oublierai pas sa disponibilité dans la relecture des documents que je lui ai adressés. Enfin, j'aimerais également lui dire à quel point j'ai apprécié ses qualités, son soutien et sa compréhension, qui m'ont profondément aidé tout au long de ces dernières années.

Je tiens également à remercier monsieur le professeur **Eric Peyrin** pour son accueil à chaque fois que j'ai sollicité son aide, ainsi que pour ses critiques et conseils constructifs. Merci aussi pour sa bonne humeur quotidienne.

Je remercie toute l'équipe NOVA, en particulier madame **Emmanuelle Fiore** pour ses conseils et sa gentillesse. Ainsi, je souhaiterais également remercier tous les membres du DPM pour leur accueil chaleureux et leur soutien surtout pour la fin de la rédaction. Merci à **Mathieu, Brayan, Pierre** et à **Silvia** qui ont changé ma vie grenobloise.

Je remercie mes collègues de l'équipe Novaptech **Laure, Raouia, Cynthia et Ellia** pour leur aide, malgré la distance. Elles ont toujours été là, chaque fois que j'en ai eu besoin. Je les remercie aussi pour leurs échanges constructifs, leur soutien et pour avoir rendu agréable le travail au sein du laboratoire, à Bordeaux.

Un grand merci à **Arghya Sett**, pour son aide dans nos projets communs, je n'oublierai pas sa positivité, sa curiosité et l'amitié qui s'est créé entre nous pendant ces années. En

outre, je tiens à transmettre toute ma gratitude à monsieur **Eric Dausse** qui a été mon mentor et qui m'a apporté son soutien sans faille.

Enfin, je tiens à remercier tous mes amis de Bordeaux qui ont toujours cru dans mes projets et mes plus chers amis italiens qui m'ont donné la détermination, le support psychologique et l'enthousiasme pour persévérer dans mes recherches.

Pour conclure, je tiens à remercier ma famille qui a toujours accepté mes décisions, la distance et qui m'a fortement encouragée à atteindre mes objectifs.

# Table of Contents

|  |            |
|--|------------|
| <b>Abbreviations</b> .....   | <b>5</b>   |
| <b>List of Figures</b> .....   | <b>7</b>   |
| <b>List of Tables</b> .....  | <b>8</b>   |
| <b>Introduction</b> .....  | <b>9</b>   |
| <b>Bibliographic review</b> .....  | <b>13</b>  |
| 1. Small molecule detection.....   | 14         |
| 1.1. Aptamers (origins, structures, affinity and specificity) and their properties.....                                | 15         |
| 1.2. Aptamers versus antibodies.....   | 17         |
| 1.3. SELEX for small molecules.....  | 19         |
| 1.4. Determination of binding affinity.....  | 24         |
| 2. Aptasensors and strategies for small molecules focused on pesticides.....   | 26         |
| 2.1 Strategies for the construction of aptamer-based biosensors.....   | 28         |
| 2.2 Aptasensors for pesticides.....  | 36         |
| 2.3 Light up aptasensors.....  | 40         |
| 3. Technologies used in the present work.....  | 43         |
| 3.1 Fluorescence anisotropy.....   | 44         |
| 3.2 Isothermal Titration Calorimetry (ITC).....  | 46         |
| <b>Experimental Section</b> .....  | <b>51</b>  |
| 1. Objectives of thesis.....   | 52         |
| 2. « Engineering light-up aptamers for the detection of RNA hairpins through kissing interaction. ».....               | 54         |
| 2.1 Strategy.....  | 54         |
| 2.2 Conclusions.....   | 70         |
| 3. « A malachite green light-up aptasensor for the detection of theophylline ».....                                    | 71         |
| 3.1 Strategy.....  | 71         |
| 3.2 Conclusions.....   | 92         |
| 4. « Anti-Pesticide DNA Aptamers Fail to Recognize their Targets with Reported Micromolar Dissociation Constants»..... | 93         |
| 4.1 Strategy.....  | 93         |
| 4.2 Conclusions.....   | 119        |
| <b>Conclusions and perspectives</b> .....  | <b>120</b> |
| <b>References</b> .....  | <b>123</b> |

# Abbreviations

|                |   |
|----------------|---|
| DNA            | Deoxyribonucleic acid   |
| GO-SELEX       | Graphene oxide-SELEX  |
| HPLC           | High-performance liquid chromatography                        |
| LC             | Liquid chromatography   |
| MS             | Mass spectrometry   |
| $K_d$          | Dissociation constant   |
| PCR            | Polymerase Chain Reaction                                     |
| RNA            | Ribonucleic acid  |
| SELEX          | Systematic Evolution of Ligands by Exponential enrichment     |
| ss             | single-stranded   |
| UV             | Ultraviolet   |
| AFB1           | Aflatoxin B1  |
| AuNPs          | Gold nanoparticles  |
| BHQ1           | Back hole quencher 1  |
| CDs            | Carbon dots   |
| D              | Dabcyl  |
| FAM/F          | Fluorescein   |
| FRET           | Fluorescence resonance energy transfer                        |
| Au/MWCNT-rGONR | multiwalled carbon nanotube-reduced graphene oxide nanoribbon |
| HIV            | Human immunodeficiency virus                                  |
| IFE            | Inner filter effect   |
| QDs            | Quantum dots  |
| SPR            | Surface Plasmon Resonance                                     |
| UCNPs          | Up-conversion nanoparticles                                   |
| EIS            | Electrochemical impedance spectroscopy                        |
| CV             | Cycle voltammetry   |
| Hemin-rGO      | Hemin- functionalized reduced graphene oxide                  |
| TAR            | Trans-activation response element                             |
| QCM            | Quartz crystal microbalance                                   |
| T01            | Thiazole orange 1   |
| DFHBI          | 3,5-difluoro-4-hydroxybenzylidene imidazolinone               |

|         |   |
|---------|---|
| MGA     | Malachite Green Aptamer                     |
| TMR     | Tetramethylrosamine                         |
| NMR     | Nuclear magnetic resonance                  |
| FP      | Fluorescence polarization                   |
| $K_a$   | association constant                        |
| (FP-DA) | Fluorescent polarization Displacement assay |
| Msw     | Malaswitch                                  |
| Tsw     | Theoswitch                                  |

# List of Figures

|  |    |
|--|----|
| <b>Fig. 1.</b> Important small species targets.  | 14 |
| <b>Fig. 2.</b> Aptamer structural motifs.  | 16 |
| <b>Fig. 3.</b> Size comparison between an antibody (human IgG) and an aptamer (anti-thrombin DNA aptamer).       | 18 |
| <b>Fig. 4.</b> SELEX process for DNA.  | 20 |
| <b>Fig. 5.</b> SELEX process for small molecules.  | 22 |
| <b>Fig. 6.</b> Schematic illustration of a biosensor.  | 27 |
| <b>Fig. 7.</b> General overview of aptasensing strategies.   | 29 |
| <b>Fig. 8.</b> Schematic representation of the optimised signalling aptamers.                                    | 30 |
| <b>Fig. 9.</b> Example of double-end labelled aptasensors.   | 31 |
| <b>Fig. 10.</b> Example of a split aptasensor before and after the addition of dopamine.                         | 32 |
| <b>Fig. 11.</b> Example of a strand-displacement strategy.   | 34 |
| <b>Fig.12.</b> Example of kissing complex.   | 35 |
| <b>Fig. 13.</b> General overview of aptasensors for pesticides.  | 37 |
| <b>Fig. 14.</b> Light up aptamer.  | 41 |
| <b>Fig. 15.</b> Predicted structures of MGA and their targets.   | 42 |
| <b>Fig. 16.</b> Allosteric light-up aptamer  | 43 |
| <b>Fig. 17.</b> Schematic representation of fluorescence anisotropy (polarization)                               | 44 |
| <b>Fig. 18.</b> Representation of depolarized and polarized emission.  | 45 |
| <b>Fig. 19.</b> Isothermal titration calorimeter. Example of results obtained by ITC.                            | 48 |
| <b>Fig. 20.</b> Illustration of the c-value on the shape of the binding isotherm.                                | 49 |
| <b>Fig. 21.</b> Schematic illustration of the phases of the project.   | 52 |
| <b>Fig. 22.</b> Representation of the fluorescent kissing-complexes design.                                      | 54 |
| <b>Fig. 23.</b> Representation of the fluorescent double-switch complex design.                                  | 71 |
| <b>Fig. 24.</b> Secondary structure of theophylline-aptamer and chemical structure of theophylline and caffeine. | 72 |
| <b>Fig. 25.</b> Secondary structure of theophylline-aptamer and chemical structure of isocarbophos and phorate.  | 93 |

# List of Tables

|   |    |
|---|----|
| <b>Table 1.</b> Comparison of aptamers and antibodies.                              | 19 |
| <b>Table 2.</b> Some examples of aptamers selected with GO-SELEX and Capture SELEX. | 24 |
| <b>Table 3.</b> Summary of the aptasensor strategies for pesticide detection.       | 40 |

# Introduction

The need to detect small molecules (<1000 Daltons)<sup>1</sup> such as residues of pesticides or drugs, toxins, antibiotics or illegal drugs becomes even more important for protecting human health and the surrounding environment. It is also important to detect these molecules with sensitive and rapid assays, under environmental conditions, e.g. in small traces and complex matrices. Traditional analytical methods used to detect small molecules imply liquid or gas chromatography coupled to mass spectrometry detection (HPLC-MS, GC-MS).<sup>2,3</sup> However, these methods are complicated, time-consuming and require qualified experimentors. Conventional binding ligands offer a valid alternative to these methods in biosensor platforms. Because of their capacity to recognize their target with high affinity and specificity, antibodies are among the most widely used as molecular recognition elements.<sup>4</sup> However, they suffer from some limits concerning their production and characterization process. To overcome these issues, more and more researchers are turning towards other types of sensors, using alternative recognition elements such as aptamers. Aptamers are single-stranded DNA or RNA oligonucleotides that bind to their target with high affinity and specificity, by folding into a three-dimensional conformation. They can be selected *in vitro*<sup>7,8</sup> against a wide variety of targets ranging from inorganic ions to cells, also including non-immunogenic and toxic compounds.<sup>9</sup>

Due to their synthetic nature, they can be easily labelled (with fluorophores, cholesteryl motif, spacer arm, etc.) or modified by chemical groups in order to improve their stability and use in complex media, such as biological fluids.

Compared to the traditional sensors such as antibody- or enzyme-based assays, aptamer-based biosensors have proved to be advantageous for small molecule detection and they have been largely adopted in a variety of applications in environmental monitoring. In the last years, many research groups were interested to develop new aptasensors for the detection of pesticide residues and, to this end, a large number of pesticide-specific aptasensors were developed. Most of them focus on fluorescence, electrochemical, and colorimetric technologies,<sup>11-13</sup> and they are principally engineered based on two approaches: the aptamer signalling and the strand displacement strategy.

In the assay format based on the aptamer signalling strategy, the aptamer interacts with the target and it undergoes significant structural changes which produce a detectable signal.<sup>10</sup> The fabrication of those aptamer-based biosensors is greatly dependent on the

conformation of the aptamers (such hairpin conformation), or the specific target-aptamer complex structure. For these reasons, this mode belongs to structure-dependent assays.

The second, most used assay-format is based on the strand displacement strategy with a complementary oligonucleotide.<sup>14</sup> The complementary sequence can be labelled with a fluorophore or employed as anchor to localize the aptamers. After incubation with the target, the duplex formed between aptamer and complementary sequences can be easily dissociated by competitive binding of the aptamer with the target. The aptamer-pesticide complex will be dissociated into the solution leading to a detectable signal. This mode is considered as structure-independent and it belongs to competitive assays.

Based on these two strategies, several pesticide-aptasensors have been developed. However, many of these aptasensors have demonstrated low selectivity and the inability to distinguish among analogous compounds. Thus, it is necessary to create new aptasensors more specific and applicable to complex matrix.

During my thesis project, the aim was to design an innovative and more specific aptasensor by coupling two strategies never used before for the pesticide detection: kissing-complex<sup>5,6</sup> and light-up. The objectives were first to create aptasensors for small molecule model in order to show their potentiality and versatility for further application to the targeted pesticides.

This manuscript consists of 2 chapters. Chapter 1 is a literature review dealing with the aptamers for small molecules in general. A first part focuses on aptamer characteristics, their properties, their selection mode and the affinity characterization methods employed. A comparison of aptamers with antibodies is also described. A second part, deals with the strategies for the design of aptamer-based biosensors for small molecules, with a focus on pesticide aptasensors. Finally, the third part displays the technologies used in the experimental work (fluorescence anisotropy and ITC) and their application for the detection of small molecules.

The chapter 2 is dedicated to the experimental part of my thesis and it will be presented in the form of three research manuscripts:

- The first manuscript titled: « Engineering light-up aptamers for the detection of RNA hairpins through kissing interaction » has been published in the *Analytical Chemistry*

journal in July 2020. The Malachite green aptamer is an imperfect hairpin displaying a central loop and a bulge that constitute the fluorogenic dye (malachite green) binding site. In this study, this aptamer was modified in such a way that it can engage loop-loop (so-called kissing) interactions with RNA hairpins. Then, the malachite green kissing aptaswitch was used as a direct sensor of RNA hairpins.

- The second one titled « A malachite green light-up aptasensor for the detection of theophylline » is submitted to Biosensors and Bioelectronics, and is currently under review. We engineered a combination of hairpin aptamers containing two recognition elements: firstly, they bind a target; secondly, they display an apical loop that can generate loop-loop (kissing) complexes with another RNA hairpin. The first hairpin is specific for the malachite green. The second hairpin is another aptamer that binds to the molecule to be detected, the theophylline compound. Interestingly, the binding sites act in a concerted manner: the specific formation of the RNA-RNA complex requires the simultaneous presence of theophylline and malachite green and leads to the fluorescence emission from the dye. Thereby, the design and the characteristics of this new type of sensor could be used for analytical purposes in different areas of chemistry biochemistry and environment area.

- The third manuscript, which focuses on the characterization of two anti-pesticide aptamers with the aim at creating fluorescent aptasensors, will be submitted shortly to a peer-review journal. This publication compares the results obtained with two aptasensors for two organophosphorous pesticides (isocarbophos and phorate) with other aptasensors, widely used in the literature towards small molecules. Finally, it was shown that pesticide aptamers do not bind to their target.

Finally, a general conclusion and the perspectives of the project will conclude the manuscript.

# **Bibliographic review**

## 1. Small molecule detection

Small molecules are chemical compounds having a molar mass lower than 1000g/mol.<sup>1,9</sup> Their small size allows them to diffuse easily across the cell membrane and directly affect the intracellular site of action. Small molecules can possess large biological functions and applications. On one hand, they are beneficial, serving as research tools, drugs in medicine, pesticides and antibiotics in the agrochemical and food industry. On the other hand, they can be harmful such as toxins, narcotics causing pollution, diseases and others abnormalities.

As such, small molecule monitoring is crucial to determine the impact of these substances on human health and environment. Medical and pharmaceutical industries require fast and sensitive detection of small molecules such as molecular biomarkers or drugs. In agri-food industries, the detection of pesticides, toxins and heavy metals are fundamental to ensure food safety.<sup>15</sup>

Since the need to detect small molecules is increasing, reliable methods are required to identify these compounds with high sensitivity, low cost and simple to use.

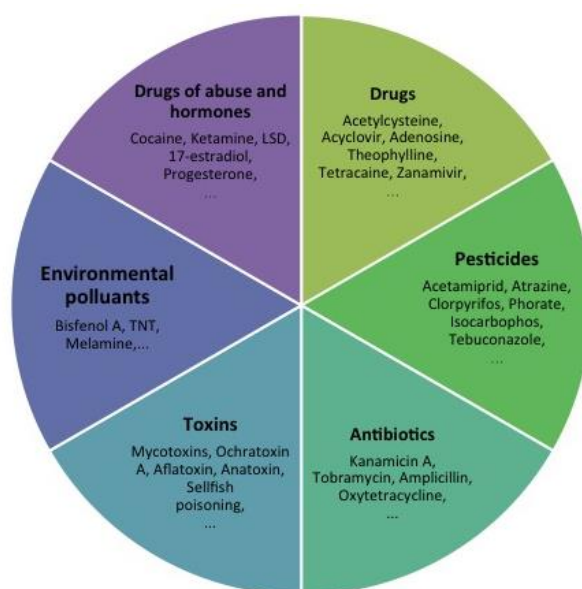


Fig. 1. Important small species targets.

Although the detection of small species is a major challenge, due in part to their small size and limited availability of functional groups.<sup>9</sup> In addition, detection of small species in

biological samples can require additional treatment steps, such as extraction, which can make difficult the outcome of the analysis.<sup>16,17</sup>

Small species can be detected in several manners.<sup>18</sup> Traditional methods used are high-performance liquid chromatography (HPLC) in combination with UV and/or fluorescence detector<sup>19</sup> or with mass spectrometry (LC-MS).<sup>2</sup> In these methods, the complex sample is often pre-treated following steps which require time and laborious process, costly equipment and highly qualified personnel. For these reasons, it is necessary to develop rapid and cost-effective assays to quantify small species.

In the last years, conventional binding elements such as antibodies and enzymes used as biosensors, have been a helpful alternative to traditional techniques. Nevertheless, these approaches have some limitations. Compounds with low molecular weight are sometimes toxic and not immunogenic so that antibodies against these targets are difficult to be generated. While, enzyme-based assays often show low specificity caused by interference of similar species present in the sample matrix.<sup>20</sup> In case of antibodies, haptens (small molecule conjugated to a carrier protein) are used to generate an immune response.<sup>4</sup> The use of protein carrier has the advantage of inducing an immune response, in turn, collaborating to produce an anti-carrier response. Antibodies thus could recognize conjugates rather than the target molecules. In addition, antibodies as proteins are sensitive to enzymatic degradation or thermal denaturation with a limited shelf-life.<sup>21</sup> Identify these issues allows to research the « ideal » molecular probe with high specificity, stable in structure, and preferably with a long shelf-life. Nearly 30 years ago, chemical antibodies also known as aptamers, have been suggested as a replacement affinity reagents.<sup>22-24</sup>

The technology of aptamers offers a great opportunity to develop non-traditional assays for a rapid detection and to engineer biosensors specific for small targets.<sup>16,20,25</sup> In the last three decades, a considerable number of aptamer sequences that bind to small molecules with high affinity and selectivity have been isolated.<sup>9</sup>

### **1.1. Aptamers (origins, structures, affinity and specificity) and their properties**

Nucleic acids are essential for any living organism. They are responsible for genetic information and protein synthesis and, in the recent decades, they have been largely used in various fields. Taking inspiration from their natural mechanisms, nucleic acids are

exploited for research, modulating gene expression and therapy. Moreover, nucleic acids can fold in a convoluted three-dimensional (3D) structure, which allows them to perform various functions including ligand binding and catalytic activity. Molecular biology now for 30 years, allows to synthesize and to select functional nucleic acids, having recognition properties towards a diverse range of analytes. These binding nucleic acids are known as *aptamers*.

Aptamers are single-stranded (ss) DNA (deoxyribonucleic acid) or RNA (ribonucleic acid) molecules able to specifically recognize their target molecule. In 1990, Gold and Ellington groups<sup>7,8</sup> contributed to the introduction of aptamers and independently developed an *in vitro* selection process, called Systematic Evolution of Ligands by Exponential enrichment (SELEX), for isolating RNA sequences against targets. These oligonucleotides are then baptized as “aptamers” derived from Latin word « *aptus* » (meaning « to fit ») and Greek suffix « *-meros* » (meaning « part »).<sup>7,8</sup>

Aptamers can bind a wide range of targets with high affinity and specificity including, proteins,<sup>26</sup> small molecules,<sup>27</sup> ions,<sup>28</sup> bacteria,<sup>29</sup> virus<sup>30</sup> and even whole cells.<sup>31</sup>

The molecular recognition of aptamers with a target compound is the result of intermolecular forces involving hydrogen bonds, stacking of aromatic rings, van der Waals forces, hydrophobic effect and electrostatic interactions.<sup>32</sup> Further, the specific interaction between an aptamer and its cognate ligand is complemented through an induced fit mechanism, which requires the aptamer to adopt a unique folded structure to its target.<sup>33</sup> Aptamers can fold into various structural motifs<sup>34</sup> including hairpin structures,<sup>35</sup> pseudoknots or G-quadruplexes.<sup>36,37</sup>

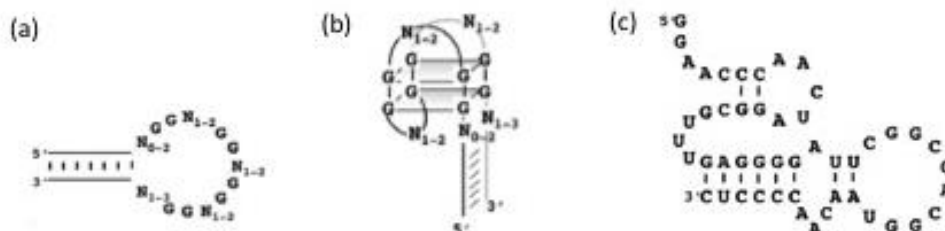


Fig. 2. Aptamer structural motifs. a) hairpin structure; b) G-quadruplex; c) pseudoknots structure.<sup>38</sup>

Thanks to their unique three-dimensional fold, aptamers can recognize their cognate ligands with affinity, expressed in terms of equilibrium dissociation constant ( $K_d$ ), in a

range from picomolar to millimolar. The ability of aptamers to recognize small molecules with high affinity has been widely demonstrated. McKeague and De Rosa have reported a list of all RNA and DNA aptamers selected against small molecules found in the literature from 1990 to 2012, including their binding affinity constants.<sup>9</sup> For a long time now, aptamers are described as ideal molecular recognition probes for small molecules<sup>39</sup> thanks to their high affinity, but also for the selectivity with which they recognize their target. The first example of a highly selective aptamer dates back to 1994, a functional oligonucleotide directed against the theophylline target.<sup>27</sup> This RNA aptamer shows an affinity for theophylline 10000 times greater than for caffeine, although the two molecules vary their structures only in a single position. More importantly, a 10-fold improvement in discriminating power was reported as compared with antibodies.<sup>27</sup> To date, such aptamer remains one of the most studied and used in different applications.<sup>40</sup> Indeed, aptamers are capable of distinguishing between closely similar structures such as enantiomers. Several aptamers have demonstrated high affinity and enantioselectivity against various L and D amino acids,<sup>39,41</sup> and some small molecule drugs such as ibuprofen or thalidomide.<sup>42,43</sup>

## **1.2. Aptamers versus antibodies**

As antibodies, aptamers are known to be able to bind to their targets with high affinity and selectivity. Due to their similar recognition properties and because they are chemically synthesised, aptamers are also considered as artificial antibodies. For many years, antibodies are standard affinity reagents and they have been widely used to detect various targets, playing a dominant role in diagnostic, therapeutic and sensitive devices.<sup>44</sup> The technology of aptamers has aroused much interest in the last years, demonstrating their inherent advantages over conventional antibodies.<sup>23</sup> Besides of their superior characteristics such as high affinity, specificity, production method and low cost, aptamers are considered as a valid alternative to antibodies (Table 1). Firstly, due to their smaller size (Fig. 3.), aptamers are more suitable for improving the efficiency of affinity reagent grafted onto desired surfaces.

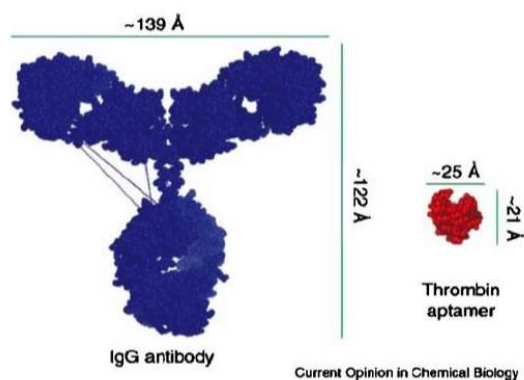


Fig. 3. Size comparison between an antibody (human IgG) and an aptamer (anti-thrombin DNA aptamer).<sup>45</sup>

In contrast with antibodies that are produced in animals, all steps of aptamer generation occur in a test tube. The *in vitro* selection, in addition to being rapid process, allows to control and optimize the aptamer binding conditions. Additionally, they are considered to be chemically sturdy to resist at different conditions, including non physiological pH, temperature and ionic strength. In contrast with antibodies, aptamers can be selected *in vitro* against almost all types of target including, non-immunogenic and toxic molecules. Aptamers can be reversibly denatured after changing surrounding conditions such as temperature or salt conditions. Once selected, aptamer sequences can be quickly resynthesized at large scale using automated chemical solid-phase synthesis.<sup>9</sup> Thereafter, for the characterization step, aptamers can be also modified with reporter molecules and shrewdly labelled at a specific position.

Despite the numerous advantages described above, aptamers also display some drawbacks. Firstly, they are susceptible to nuclease degradation which may affect their *in vivo* function. Furthermore, with their 4 nucleobases, aptamers have a lower chemical diversity than antibodies. However, to overcome these issues, some chemical modifications can be used in order to improve the nuclease resistance and increase the diversity of candidates.<sup>46-49</sup>

All these potential advances make the aptamers the prominent rivals of antibodies and powerful recognition elements for generating different types of biosensors (see below).

|                         | <b>Aptamers</b>   | <b>Antibodies</b>   |
|-------------------------|---|---|
| <b>Synthesis</b>        | In vitro SELEX,<br>take 4-6 weeks,<br>cheap to synthesize   | In vivo production<br>in more than 6 months,<br>laborious and expensive                         |
| <b>Stability</b>        | Long self life (many years)<br>Temperature resistant<br>Degradable by nucleases<br>Resistant by proteases | Limited shelf life<br>Temperature sensible<br>Resistant to nucleases<br>Degradable by proteases |
| <b>Target potential</b> | Any targets from ion to whole cells   | Targets no-toxic and must cause an<br>immune response for antibodies<br>production              |
| <b>Size</b>             | Small molecules<br>(10 <sup>4</sup> Da)   | Relatively large by comparison<br>(10 <sup>4</sup> -10 <sup>5</sup> Da)                         |
| <b>Reusability</b>      | Good reusability through a<br>reversible conformation switch  | Low reusability for the irreversible<br>conformation changes                                    |

Table 1. Comparison of aptamers and antibodies.

### 1.3. SELEX for small molecules

Aptamer oligonucleotides are selected from a large random library (typically 10<sup>13</sup>-10<sup>16</sup> single-stranded unique sequences) for a wide variety of targets ranging from small molecules to whole cells. The diversity of the library depends on the length of the random region. Each oligonucleotide in the library is composed of 40-100 nucleotides, with a central random region (commonly in the 20-60 nucleotide range) and two fixed binding primer-sequences at each extremity.

Aptamers are generated by a method called SELEX (Systematic Evolution of Ligands by EXponential enrichment).<sup>7,8</sup> This technique involves three interconnected steps: binding, partitioning and amplification (Fig. 4.). Firstly, DNA, RNA or modified nucleic acid library are incubated with the target of interest (*step 1*). After incubation, the DNA oligonucleotides specifically bound to the target are separated from the unbound ones (*step 2*). Bound sequences are collected, amplified by Polymerase Chain Reaction (PCR) (*step 3*) and then purified for subsequent re-starting the cycle. In the case of the RNA aptamer selection, the SELEX protocol further includes the transcription by T7 RNA polymerase and reverse transcription step before PCR.<sup>50</sup>

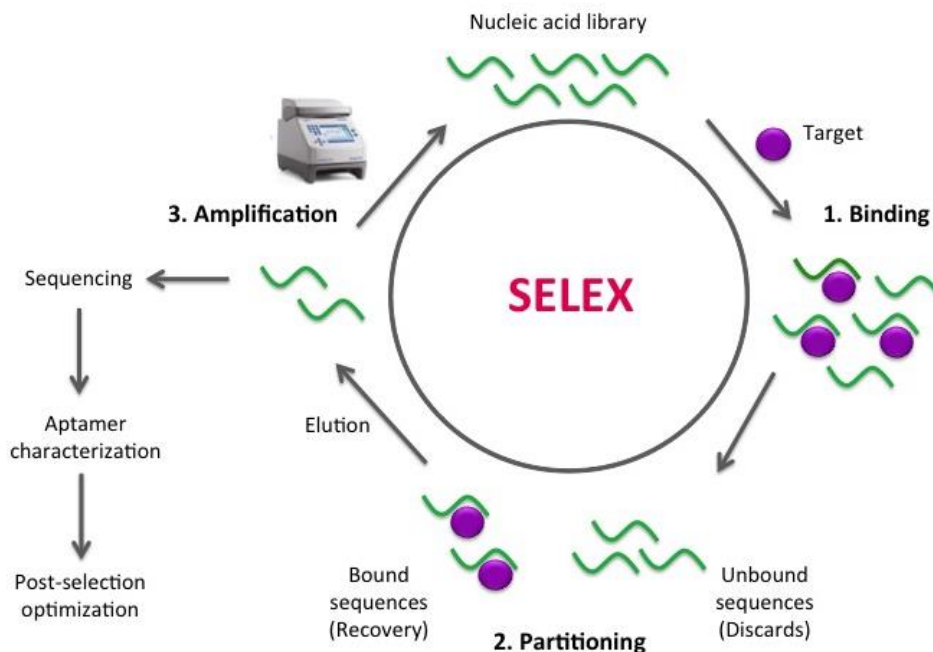


Fig. 4. SELEX process for DNA. Step1 Binding, Step 2 Partitioning, Step 3 Amplification.

For improving the binding step, negative or counter selection can be introduced. Negative selection, is the selection performed against the unmodified carriers (filter or beads) in the absence of the target; the counter selection could also be performed against some related molecule targets. This is an optional step used to discard the non-specific sequences, allowing aptamers to discriminate between very similar species.<sup>27</sup>

During the SELEX process, the evolution of the DNA pool can be monitored by quantification of target-bound oligonucleotides modified with a traceable label.<sup>51</sup> This step is important to optimise the conditions and increase efficiency of selection in a controlled way. After several cycles of selection and amplification, the diversity of the pool decreases and the affinity of the oligonucleotides for target can increase.

The selection is stopped when the target-bound candidates are predominant in the pool of oligonucleotides or when no increase is observed during the next two or three SELEX rounds. The enriched pool obtained is then analysed and the candidate aptamers are identified by cloning and sequenced individually clones, or alternatively, with high-throughput sequencing and bioinformatic analysis. (Fig. 4.)

After sequencing, the most promising candidates are synthesized to be evaluated for their potential binding of the target, and characterized under different conditions. The affinity and specificity of individual candidates are evaluated by different methods. These two important characteristics of aptamers can be influenced by the conditions of the binding assay. Best aptamers are then optimized for incorporation in diagnostic, therapeutic or analytical applications.

To date, there is no standard selection method for any type of target. During the last three decades, the SELEX process has been continuously modified to make the selection more efficient, adapting it to new separation techniques and sometimes against difficult targets such as small molecules. SELEX method can be used to isolate aptamers against almost all types of target. Nevertheless, macromolecules are the most suitable targets because they contain more functional groups and provide a large surface for interaction with aptamers. Although the demand for the detection of small molecules (<1000g/mol) recently increased, the selection of aptamers against such class of targets is less prevalent.<sup>9</sup>

Aptamers screening for small molecules is accompanied by some specific difficulties as compared with the selection against proteins or other macromolecules. First of all, small molecules have limited functional groups that reduce the possibility to interact with aptamers. A major problem of performing SELEX against small molecules lies on the separation step between bound and unbound sequences. Due to the small size of the target, there is not an evident difference between unbound candidates and aptamer-ligand complex, complicating the partitioning step in homogenous phase. Consequently, immobilization of one of the two biomolecules is required.

The first conventional DNA SELEX against small molecules was performed by Ellington and Szostak for the selection of aptamers against organic dyes. In this case, the target is immobilized to a solid support matrix.<sup>8</sup> Candidates that interact with the target are separated from sequences that do not bind after multiple washes. The sequences of interest are then eluted from the solid support and amplified by PCR for the next round. On one hand, with this method, the oligonucleotides pool is unmodified and free in solution, with no complication related to the conjugation of the pool. On the other hand, the immobilization of target generates some difficulties. As chemical modifications of the target are required to allow the immobilization, a novel epitope can be generated in such

a way that the selected aptamer may interact with the conjugate rather than the desired target. In addition, for certain small molecules, the immobilization on solid substrate is not easy to achieve.

To overcome this problem of SELEX for small-molecules, target immobilization-free aptamer screening methods have emerged, such as GO-SELEX (Graphene oxide-SELEX)<sup>52</sup> (Fig. 5 a) and capture-SELEX (Fig. 5 b).<sup>53</sup>

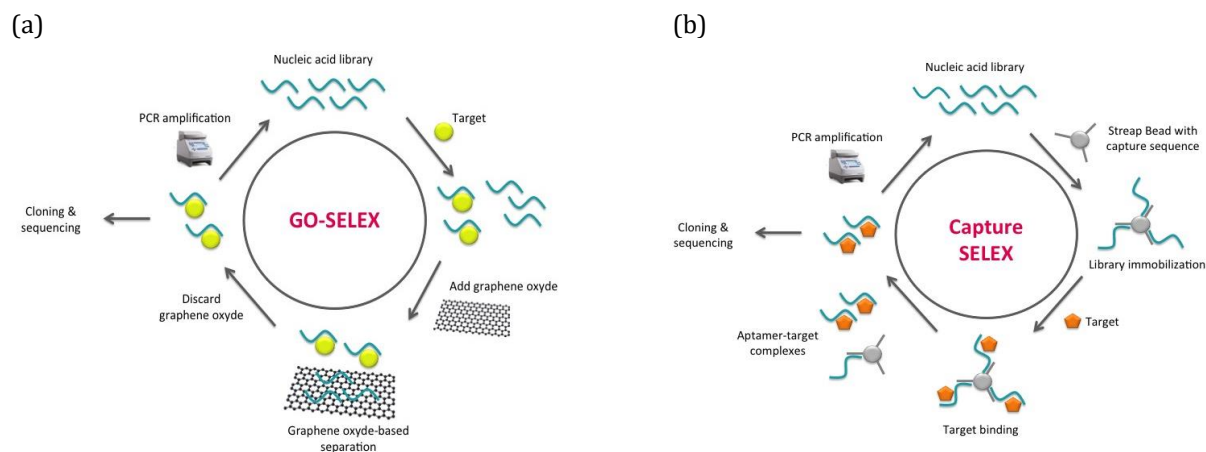


Fig. 5. SELEX process for small molecules. a) Scheme of graphene oxide-based SELEX (GO-SELEX). b) Scheme of Capture SELEX.

In GO-SELEX, the initial ssDNA library is adsorbed on graphene or graphene oxide sheets *via*  $\pi$ - $\pi$  stacking and hydrogen bonds.<sup>54</sup> The addition of the target can induce a release of sequences that interact with the target molecule and consequently, a separation from the unbound ssDNA pool still adsorbed on the graphene sheet. The separated sequences are recovered and amplified for the next selection cycles. GO-SELEX process is not based on the size difference, but on the competition among the oligonucleotides, the graphene sheets and the target molecules. It can therefore be applied to small molecule targets (Fig. 5a).

Another immobilization-free SELEX method is the Structure-Switching or Capture SELEX.<sup>53</sup> In this process, the initial ssDNA library is designed to hybridize to a complementary capture sequence anchored to the solid substrate (magnetic beads or agarose). The addition of the target causes a conformational change or “structure switching” of ssDNA that can dissociate from the hybrid complex (Fig. 5b). The sequences

are then amplified and used for the subsequent SELEX round. Since they were first described GO-SELEX (2012) and Capture SELEX (2003) have been widely used in the selection of aptamers against different types of small molecules including, dyes or antibiotics and also poorly soluble targets such as toxins or pesticides. Table 2 lists some examples of aptamers successfully selected against small molecules using GO-SELEX or Capture SELEX.

\*when is specified

| Method        | Small molecule target | Molar mass (g/mol) | $K_d$ or LOD*   | References |
|---------------|-----------------------|--------------------|-----------------|------------|
| GO-SELEX      | T-2 toxin             | 466.5              | $20.8 \pm 3$ nM | 55         |
|               | Inabenfide            | 338.8              | 191 nM (LOD)    | 56         |
|               | Tebuconazole          | 307,82             | 128 nM (LOD)    |            |
|               | Mefenacet             | 245.31             | 276 nM (LOD)    |            |
|               | Iprobenfos            | 288.34             | 1.76 $\mu$ M    | 57         |
|               | Edifenphos            | 310.4              | 38 nM           |            |
|               | Okadaic acid          | 805.01             | $40 \pm 13$ nM  | 58         |
| Capture SELEX | Phorate               | 260.4              | 1.11 $\mu$ M    | 59         |
|               | Isocarbophos          | 289.29             | 0.83 $\mu$ M    |            |
|               | Profenofos            | 373.63             | 1 $\mu$ M       |            |
|               | Omethoate             | 213.19             | 2.5 $\mu$ M     |            |
|               | Acetamiprid           | 222.67             | 4.98 $\mu$ M    | 60         |
|               | Cd (II)               | 112.41             | 40 nM (LOD)     | 61         |
|               | Kanamycin A           | 484.49             | 3.9 $\mu$ M     | 62         |
|               | Tobramycin            | 467.51             | 520 nM          | 63         |
| Geniposide    | 388.4                 | 2 $\mu$ M          | 64              |            |

Table 2. Some examples of aptamers selected with GO-SELEX and Capture SELEX.

#### 1.4. Determination of binding affinity

The characterization of candidates is a fundamental step to validate the isolated sequences. An important parameter for the characterization of aptamers is the equilibrium dissociation constant  $K_d$ . The lower the  $K_d$ , the higher the affinity of the target for the aptamer. To determine the  $K_d$ , either aptamer or its cognate target is titrated

against the other molecule. There are several methods to determine the dissociation constant of aptamers, involving spectroscopy-based methods, mass-sensitive surface-based measurements or separation-based methods.<sup>9</sup> Currently, main methods used for the characterization of aptamers, are classified in two categories: immobilization of one binding partner (aptamer or its target) and immobilization-free technology. One immobilization-based method relies on the surface plasmon resonance (SPR) technique where one partner is immobilized on a solid surface. The immobilization-free technology can include fluorescence polarization/anisotropy (FA/FP)<sup>65</sup>, Isothermal Titration Calorimetry (ITC)<sup>66</sup> and capillary electrophoresis (CE)<sup>67</sup> approaches.

For the small molecule-aptamers the characterization is not easy. Aptamers are significantly larger than small molecules and the drastic difference size is one of the major limitations for the detection of these targets. To date, there is no universal method for determining the binding affinity and select the right assay for the accurate affinity measurements constitutes a real challenge. Each assay presents some limitations, including immobilization of target or aptamer, lack of sensitivity or inability to quantitatively measure the dissociation constant. Moreover, the same aptamer, characterised with different assays, can differently behave and display different binding-affinities.<sup>68</sup> This inconsistency between  $K_d$  measuring methods could also be due to the method system (e.g. immobilization or free-solution). In order to overcome any limitation of each characterization approach, it is suitable to use multiple assays for the small molecule-aptamer characterization. The choice of surrounding conditions such as temperature, pH, or ionic strength is also fundamental for the characterization. The selection takes place in a given buffer and the functionality of the aptamers obtained could be specific for this buffer. Similarly, the aptamers are generated at a unique temperature. Because nucleic acids can fold into different conformations under different temperatures, aptamer misfolding can occur under particular conditions. For these reasons, it is recommended to maintain the same selection conditions for their characterization. Finally, two fundamental controls are required, i. e. the use of a non-binding aptamer and the use of at least one non-cognate target. Furthermore, to avoid changes that could compromise the final performance of the aptamer, it is important to choose the conditions of the SELEX according to the desired applications of biosensors.

## 2. Aptasensors and strategies for small molecules focused on pesticides

The environmental contaminants are harmful substances present in soil, air and water. These compounds can be released from human sources such as industrial manufacturing, agricultural treatment and wastewater discharge, or they can be generated naturally in form of toxins by algae and bacteria blooms.<sup>69</sup> During the last years, the increased production and use of these substances has caused serious problems for the food and environment contamination, putting the health of humanity at risk. Among these environmental contaminants, pesticides are one of the most widespread.<sup>70</sup>

Divided into three categories -fungicides, herbicides and insecticides-, pesticides include more than a thousand of active substances used to fight against organisms, which are considered as harmful (fungi, plants, insects). Their use in agriculture for the purpose of increasing crop yields and for improving the quality of agricultural products is very excessive. Consequently, the effects on the population exposed to pesticides have become devastating. The most detected pathologies are neurological diseases, damages to reproductive function, developmental alterations and cancers.<sup>71</sup> This great threat to mankind is getting more and more attention from governments which impose stringent laws to minimize the usage of these substances in food and agricultural production.

To safeguard both human and ecosystem health, contaminant monitoring and, if possible, their removal is necessary.<sup>72</sup> Many of these contaminants, such as pesticides, toxins, antibiotics and drugs, are small molecules (1000 g / mol) that are difficult to detect. Therefore, the development of methods that allow a rapid and specific detection of low-weight contaminants has become a real urgency. The limitations of traditional techniques have encouraged the development of new technologies, among them *biosensors*.<sup>16</sup>

A biosensor (Fig. 6) is a small analytical device which combines a biological molecular recognition element with a physicochemical transducer<sup>73</sup> that can signal the presence of the analyte of interest. The sensitive biological component interacts with the target and the transducer element transforms this interaction into a measurable signal. The biological component can be made up of antibody, enzyme, nucleic acid, etc. while a transducer may be optical, electrochemical, thermal, mass sensors, etc. A biosensor that

utilizes an aptamer as recognition molecular component is called *aptasensor*.<sup>22,74</sup>

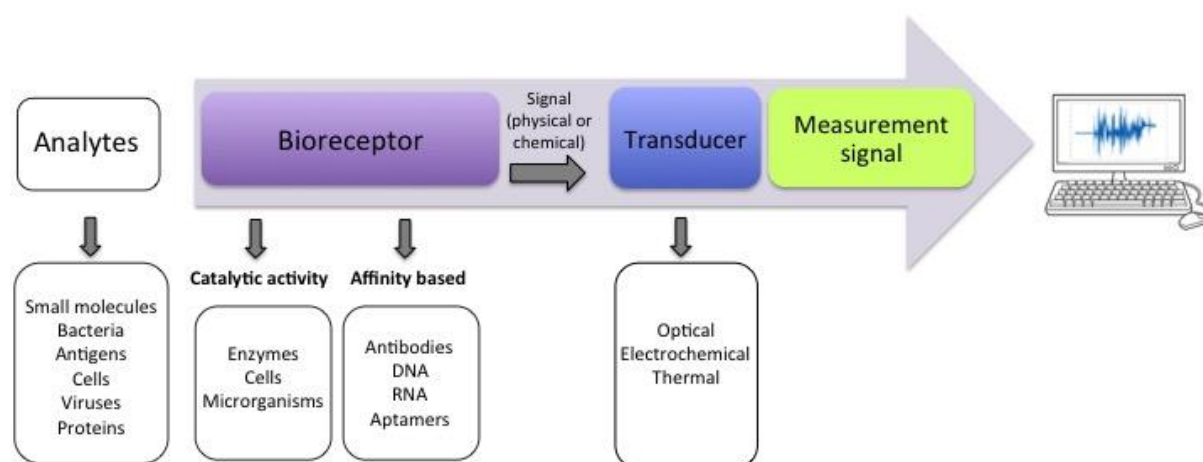


Fig. 6. Schematic illustration of a biosensor. Upon binding of a bioreceptor towards an analyte, the transducer collects this interaction and converts it into a measurable signal.<sup>16</sup>

Biosensors for small molecule targets have not been extensively studied as much as those for protein targets because it is difficult to develop a recognition element for low-weight compounds. Although antibody- or enzyme-based assays are considered as standard sensing platform for the detection of proteins and small targets, they are not available for all compounds. A sandwich assay format, one of the most used methods in immunoassays, is not suitable for the detection of small molecules as these targets are generally embedded in the cleft of the first capturing probes, leaving a too small space for the interaction with the second detector probe.<sup>74</sup>

Another important issue for an assay development is related to the detector platform for signal production. To detect small molecules, mass-dependent detection methods such as quartz crystal microbalance (QCM) or surface plasmon resonance (SPR) are hardly advisable due to the small mass change produced upon molecular interaction.<sup>20</sup>

To address the challenges associated with the signal generation, aptamer-based biosensors have been developed and extensively adopted in a large variety of applications in environmental monitoring. Aptamers can selectively bind to analytes with affinity constants comparable to those of antibodies.<sup>75</sup> However, aptasensors for pesticide

determination have recently gained considerable attention due to their advantages over antibodies. Hence, aptasensors are very promising and have made significant breakthroughs in the development of highly sensitive assays for small molecules detection.

### **2.1 Strategies for the construction of aptamer-based biosensors**

In order to be used in aptasensors, an aptamer must have some fundamental requirements. Firstly, to be introduced to an aptasensor platform, an aptamer must be modified in such a way that it will be able to interact with the target and signal the target-binding event, simultaneously. Accordingly, it has to maintain the affinity and selectivity of the native aptamer and must quickly recognize the target molecule. Regarding the design process, a minimal knowledge of the secondary and tertiary structure of the aptamer-target complex is often necessary. It should be versatile and applicable to different readout methods. However, the choice of the design strategy to be adopted is a crucial point for the success of an aptasensor.

Since the first aptasensor was created in 2000 by Ellington and colleagues, many aptasensing strategies have been designed and developed to make aptasensors simpler, applicable to various methods and versatile for all types of targets.<sup>76</sup> The principal strategies developed are: a) signalling aptamer b) double end-labelled aptasensor, c) split aptasensor d) label-free aptasensor e) strand displacement strategy f) kissing complex.

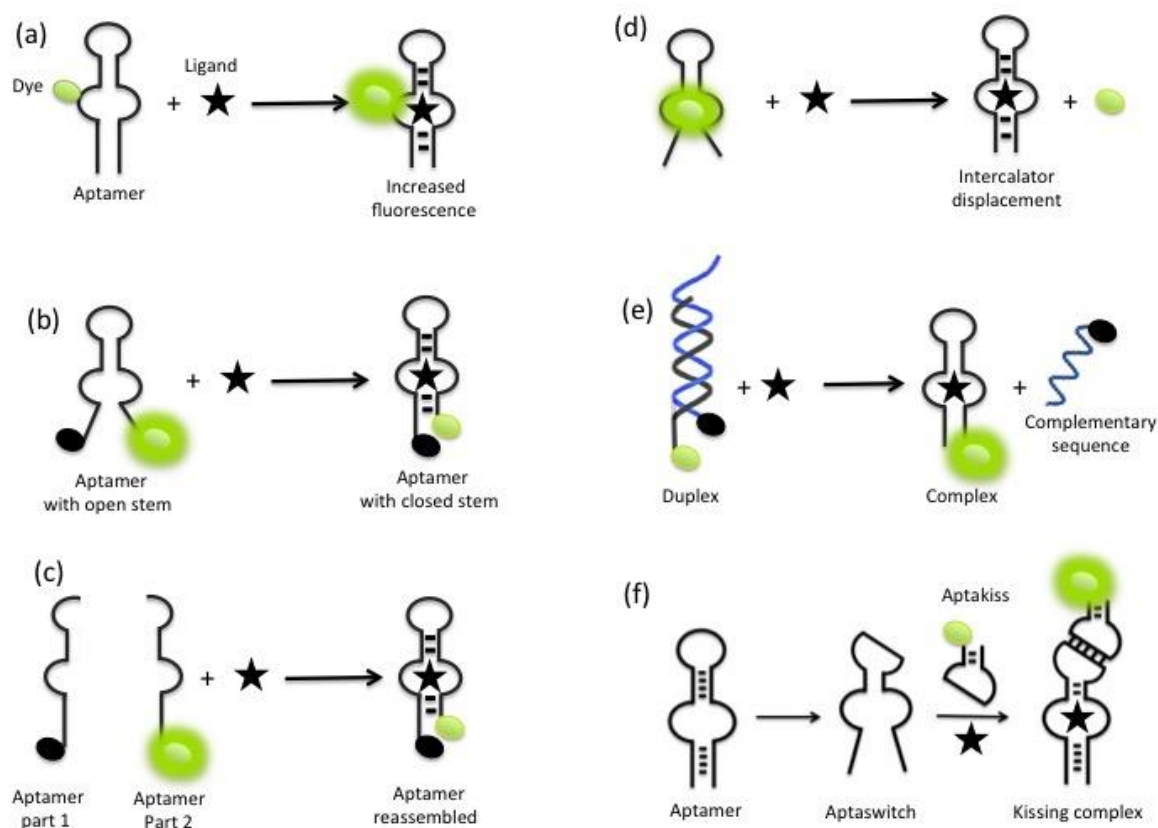


Fig. 7. General overview of aptasensing strategies. a) signalling aptamer b) double end-labelled aptasensor, c) split aptasensor d) label-free aptasensor e) strand displacement strategy f) kissing complex.

There are several examples of aptasensors based on these strategies designed for the detection of small molecules; most of these are proof-of-concept systems using ATP, theophylline or cocaine aptamers. In the next sub-chapters, more detailed information will be given on each aptasensing strategies.

### *Signalling aptamer*

In aptasensors based on the signalling aptamer strategy, the signal transduction depends on the molecular recognition mechanism. The binding of the target causes a conformational change which will be used to generate a measurable signal (Fig. 7a). Although signalling aptamers have often shown a good affinity for the target, this approach has some limitations. Since many aptamers possess partially folded structure, the signal gain produced with this strategy is often low. In addition, in case of small molecules, the target can interact with aptamer without causing a large detectable conformational change. The application of this strategy is limited to some aptamers.<sup>76</sup>

Therefore, several research groups have investigated alternative methods to enhance the target-induced structural change and applied this approach to the small molecule detection. The first aptasensor design published in the literature was a signalling aptamer directed against ATP.<sup>77</sup> In this aptasensor system, the aptamer is labelled with a fluorescent dye in proximity to the ligand-binding pocket. In the presence of the target, the structure of aptamer changes, increasing the fluorescent signal. Some years later, Ruta and colleagues described a small molecule aptamer assay based on this strategy (Fig. 8), using a directed fluorescence anisotropy (FA) technique.<sup>78</sup> For this approach they engineered a biosensor based on the anti-tyrosinamide aptamer, labelled by a single fluorescent dye at one extremity. The presence of the target induces the conformational change of the aptamer, which modify the local motional freedom of the fluorescent label, resulting in an increase of fluorescence anisotropy signal. Based on this strategy Perrier and coworkers designed another signalling aptasensor with an anti-adenosine aptamer as a model. They rationally engineered the instability of the secondary structure of the aptamer which allows to demonstrate the conformational change of the aptamer in the presence of the target.<sup>79</sup>

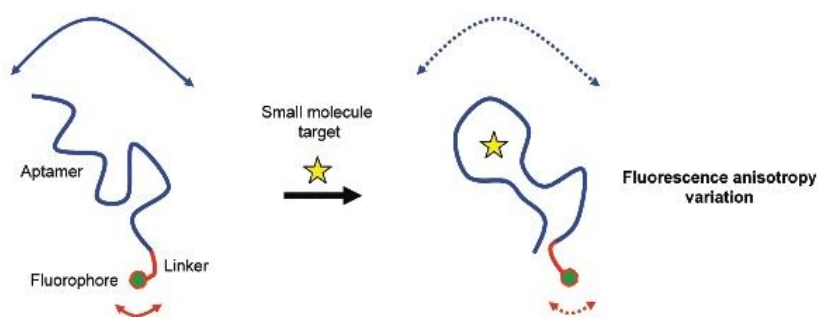


Fig. 8. Schematic representation of the optimised signalling aptamer. The conformational change in the presence of the target molecule is translated into an increase of fluorescence anisotropy signal.<sup>78</sup>

### *Double-end labelled aptasensors*

Afterwards, in order to engineer aptasensors with higher signal gain, aptasensor designs relying on a FRET pair rather than a single dye reporter have been developed. FRET aptasensors have been engineered based on a molecular beacon probe.<sup>80</sup> A molecular beacon is a fluorescently bi-labelled DNA hairpin probe designed to bind complementary DNA or RNA sequences. It can report the presence of targets in a homogeneous solution. The extremities of the probes contain a FRET pair (or a fluorophore-quencher pair) whose

fluorescence signal changes (or is restored) when the beacon opens upon binding to the complementary target sequence. Other aptasensor strategies have been designed on the basis of this format.

Stojanovic and colleagues first implemented the molecular beacon-like format in a double end-labelled aptasensor (Fig. 9).<sup>10</sup> They re-engineered the anti-cocaine aptamer, introducing an instability in one stem of a three-way junction that forms the cocaine-binding pocket and labelling the resulting short terminal stem with a fluorophore and quencher pair. In the presence of cocaine, the formation of the three-way junction leads to the stem closure in such way that the fluorophore and quencher are brought in close proximity. This structural change causes the fluorescence decrease, which reports the presence of the cocaine. Moreover, this aptasensor has been tested in serum, demonstrating its selectivity over cocaine's metabolites. By using this strategy to engineer an aptasensor, they have demonstrated that this design can provide a new set of analytical tool to detect small molecules in different media.

Recently, the same strategy has been used to engineer a new aptasensor against aflatoxin B1.<sup>81</sup> Inspired by the Ellington model, they engineered the aptamer anti-aflatoxin 1 (AFB1) into a double-end labelled aptamer beacon (using a fluorophore and quencher pair). This aptamer molecular beacon assay showed high specificity for AFB1 (tested against other mycotoxins) and a potential detection (in the nanomolar range) in real samples. In the last years, the use of double end-labelled aptasensors has allowed the development of aptamer based fluorescent molecular beacon assays for the detection of small molecules such as cocaine or adenosine triphosphate (ATP), based on binding-induced structure change with the subsequent fluorescence increase or decrease.<sup>81,82</sup>

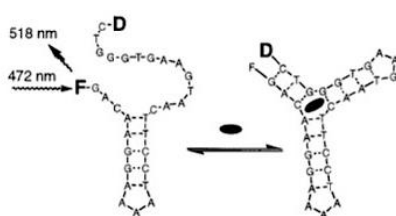


Fig. 9. Example of double-end labelled aptasensors.<sup>10</sup> When the target molecule, in this case cocaine, is present in solution, a conformational change of the aptamer brings closer fluorescein and a quencher, leading to a fluorescent decrease.

### Split aptasensor

Biosensors can be in general classified into two groups, competitive and sandwich assays. In the sandwich assays, two probes such as antibodies or aptamers, are used simultaneously to capture the target through the recognition and binding of two distinct regions. The sandwich assay is mainly used for the macromolecule detection, especially proteins, with high sensitivity and specificity resulting from this dual recognition mechanism. However, it cannot be used for the detection of low molecular weight analytes for the reasons described above. To overcome this issue, Stojanovic and colleagues<sup>83</sup> developed a split-aptamer-based strategy, in which the aptamer sequence was divided into two subunits that form a ternary complex in the presence of the target. To obtain a signal, the two subunits (labelled, for example, with a FRET or fluorescent-quencher pairs) have to be close enough to each other to allow signal transmission, which occurs only in the presence of a target. To transform an aptamer into a split aptasensor, it is fundamental to know the aptamer–target complex structure and understand the role of each nucleobases.<sup>84</sup> This approach has been adopted for the detection of various ligands, especially small molecular targets, using different transduction methods including fluorescence, colorimetric, and electrochemical techniques,<sup>85–87</sup> many based on anti-cocaine and ATP aptamers.<sup>84</sup> Recently, a novel dual-signal ratiometric electrochemical biosensor based on a split aptamer for the detection of dopamine has been also engineered (Fig. 10).<sup>88</sup> In this study, Guo and co-workers have demonstrated the efficiency of the split-aptasensor strategy in small molecule detection with good affinity (in micromolar range) while maintaining satisfactory reliability and sensitivity similar to those of the native aptamer.

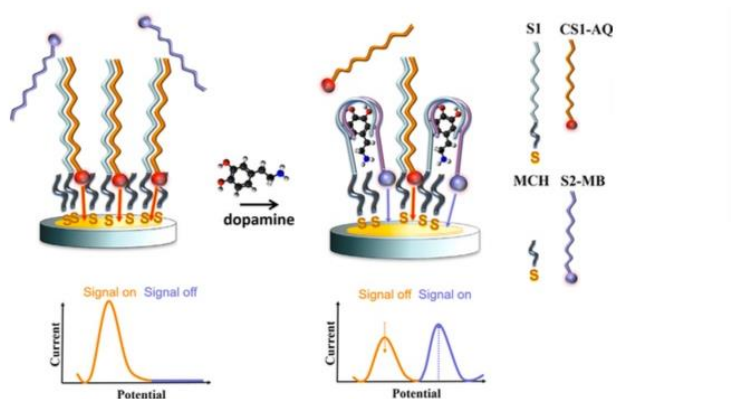


Fig. 10. Example of a split aptasensor before and after the addition of dopamine.<sup>88</sup>

### *Label-free aptasensors*

The label-end strategy may suffer of some limitations. In some cases this target-induced fluorescence change results in a high detection limit, even under optimal conditions. This could originate from an inefficient proximity quenching,<sup>89</sup> or the chemical modification of the aptamers.<sup>90</sup> To overcome these concerns, label-free aptamer probes have been developed as an alternative strategy. This approach is dependent on the conformational change of the aptamers before and after binding to its target. This approach requires a ssDNA aptamer probe without any labelling and a fluorescent reporter such as double-stranded DNA (dsDNA) intercalators, single-stranded DNA (ssDNA) binding dye, or fluorescent conjugated polymer. The most common signal reporters for label-free fluorescence aptasensors is related to the use of DNA intercalation dyes. In aqueous solution, these dye molecules show a low fluorescence intensity while a strong fluorescence signal occurs when they intercalate into dsDNA.

Using the (Ru (phen)<sub>2</sub>(dppz)) intercalator dye, the Wang's group has developed a label-free aptasensor for detecting ATP with high selectivity and high sensitivity, down to 1nM in homogeneous solution.<sup>91</sup> Some other fluorescent dyes such as SYBR Green I<sup>92</sup> have been also used as a transducer for the aptamer-target recognition devoted to small molecules.

Label-free aptasensors can be similarly created using fluorogenic dyes (or fluorogens) such as Thiazole Orange,<sup>93</sup> Hoescht,<sup>94</sup> Malachite Green (MG)<sup>95</sup> DFHBI,<sup>96</sup> Patent blue<sup>97</sup>. Among them, MG shows extremely low fluorescence in homogeneous solution and strong fluorescence intensity (~2400-fold) after binding with its RNA aptamer.

Light-up aptamers are RNA sequences that specifically interact with a fluorogen to form a fluorescent complex. Based on the MG light-up aptamer, taking advantage of the unique fluorescence property of MG, Stojanovic and Kolpashchikov firstly proposed a modular aptameric sensor to detect various small molecules analytes (ATP, flavin mononucleotide and theophylline).<sup>98</sup> These aptasensor designs consist of MG aptamer as signal domain, other aptamers (ATP, flavin mononucleotide or theophylline) as recognition domain and a connector module between the recognition and signal domains. The interaction of each aptamer with its cognate target leads to the exposure of the MG aptamer so that MG binds its aptamer and emits a high fluorescence intensity.

Recently other light-up aptamers were successfully selected. By taking advantage of their sensitive properties, they could be used to develop new label-free aptasensors to detect other small molecules.

### *Strand displacement strategy*

The design of the above described aptasensors strategies cannot be applied to all aptamers. For instance, many aptamers do not form a defined stem structure with a terminal hairpin. Likewise, most aptamers do not have a secondary structure that can be easily split into two fragments without affecting the aptamer functionality.

To overcome these drawbacks, a strategy based on the structure-switching concept was introduced in 2003 and is still today one of the most used in aptamer selection and aptasensor design for small molecules.<sup>14</sup> This strategy is based on the target induced dissociation of a hybrid complex between an aptamer and a partially complementary sequence. It does not require any -or only minimal- aptamer modifications.<sup>53,99</sup> This mechanism is based on the ability of aptamers to bind to both complementary sequence and their specific target. In the presence of the target, the aptamers can then switch from a nucleic acid helix to an aptamer-target complex. In « structure-switching » assays, the dissociation caused by the competitive binding of the aptamer to the target is converted into a measurable signal that detect the presence of the target.<sup>100</sup> For instance, the aptamer can be functionalized with a fluorophore while the complementary sequences can be labelled with a quencher. In the absence of the target, the two nucleic acid strands form a duplex, leading to low fluorescence (Fig. 11). In the presence of target, the aptamer-target complex is formed and the complementary quenched sequence is displaced, leading to the fluorescence signal.

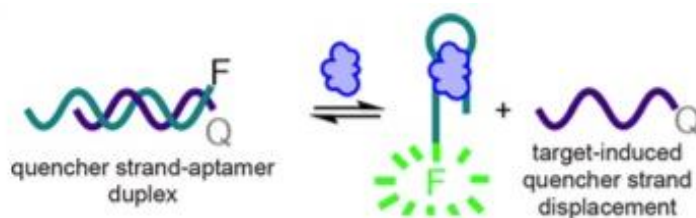


Fig. 11. Example of a strand-displacement strategy. In the absence of the target molecule, the aptamer, functionalized with a fluorophore, is hybridized with a complementary DNA strand, labelled with a quencher. After the addition of the target molecule, the displacement of the quencher strand leads to a fluorescence signal.<sup>101</sup>

Li and co-workers have shown the first proof-of-concept for strand displacement assay based on aptamers against ATP and thrombin.<sup>14</sup> Since then, this strategy has been widely used to detect various types of targets, being the most used for the small molecule signalling. Actually, it is considered as a highly generalizable method to engineer all aptamers into biosensor and it is introduced into a very different sensors.<sup>91,102</sup>

### *Kissing complex*

This strategy is based on the engineering an aptasensor for the detection of small molecules involved in the kissing complex system. The term « kissing complex » appeared for the first time in 1984, to describe the regulatory mechanism for the replication of the bacterial plasmid ColE1<sup>103</sup> and it has been observed in the regulation of numerous biological process such as virus assembly and plasmid replication.<sup>103-105</sup> Kissing or loop-loop interaction is formed between two RNA *via* complementary base pairing and is greatly dependent on loop parameters (base composition, sequence and size) in combination with the loop-loop helix - stem junctions (Fig. 12). More than 20 years ago, this mechanism has been used to generate an RNA aptamer for the TAR-RNA element of HIV-1 and to select DNA aptamers specific for a DNA hairpin structure.<sup>106-108</sup>

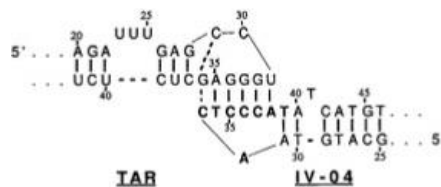


Fig. 12 Example of kissing complex. Aptamer anti-TAR and HIV-1 TAR hairpin.<sup>108</sup>

More recently, a novel aptamer biosensing concept based on the kissing complex strategy has been described by Toulmé and Peyrin groups.<sup>5,6</sup> They introduced a new type of aptasensor to detect small molecules based on a dual recognition mechanism that includes a signalling partner that contributes to increase the stability of the complex with the target. This assembly is constituted by two partners: an aptamer called *aptaswitch*, able to shift its conformation from unfolded to folded (hairpin) structure in the presence of the target, and a second short RNA hairpin named *aptakiss*.

For the aptaswitch design, the apical loop of the native aptamer is substituted with a short RNA sequence able to recognize the aptakiss through loop-loop interactions forming a

kissing complex. Therefore, the resulting structure is formed when both partners are structured in hairpin structures, *i.e.* in the presence of the target. Aptakiss is then used as a transducer and it can be adapted to various kinds of aptaswitches. This strategy was conceived in order to enhance the specificity and the resulting signal gain of the biosensor. In recent years, this approach has been employed in the rational design of new small molecule biosensors. Toulmé and Peyrin groups designed some new aptasensors exploiting the formation of kissing complexes for sensing the presence of small molecules specifically recognized by their hairpin aptamers.<sup>5,6</sup> The new aptaswitches rationally designed, baptized as Adenoswitch, GTPswitch, Theoswitch and Vasoswitch (specific for adenosine, GTP, theophylline and vasopressine respectively) have been largely studied with different detection systems including SPR, fluorescence anisotropy,<sup>109</sup> colorimetry with AuNPs<sup>110</sup> and HPR with an ELAKCA system (Enzyme linked aptamer kissing complex assay).<sup>111</sup> In addition, this last approach has been successfully applied to colorimetric tests, to detect the presence of theophylline in human plasma samples.

All these kissing-complex approaches have demonstrated a high sensitivity and specificity for the small molecules. The new kissing-aptasensors have proved to be a promising system also applied to multiple target sensing.

## **2.2 Aptasensors for pesticides**

Due to their large application in agriculture, pesticides can be transported to the surface water and easily contaminate the agricultural product for the human consumption. Over the past years, various aptasensors have been successfully exploited for the detection of pesticide residues for the environmental monitoring.<sup>112,113</sup> Most of these aptasensors are engineered based on two approaches: the aptamer signalling and the strand displacement strategy.

Based on these two strategies, the three most widely used types of the aptasensors are focused on fluorescence,<sup>114</sup> electrochemical,<sup>115</sup> and colorimetric<sup>116</sup> technologies. (Fig. 13). For developing electrochemical and fluorescent aptasensors, a number of nanomaterials such as quantum dots (QDs), carbon dots (CDs), up-conversion nanoparticles (UCNPs), AuNPs, Graphene oxide (GO) and so on, have been employed for the detection of pesticide residues.

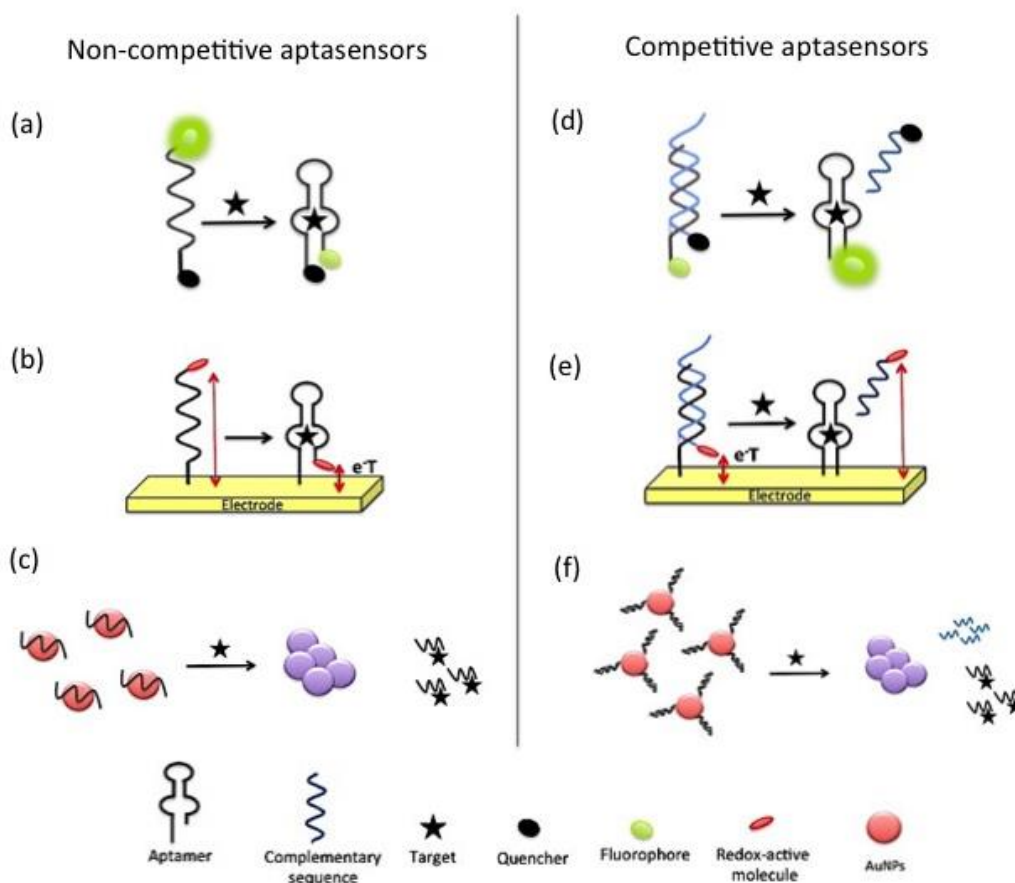


Fig. 13. General overview of aptasensors for pesticide. a) and d) fluorescent aptasensors, b) and e) electrochemical aptasensors, c) and f) colorimetric aptasensors.

### Fluorescent aptasensors

Due to its high sensitivity and efficiency, the fluorescence technique is one of the most common approach for the analysis aptamer-target interactions.<sup>117</sup> Generally, there are two sensing mechanisms in developing fluorescent aptasensors, *i.e.*:

-“signal-on” mechanism, where the presence of the target causes a recovery or great increase of fluorescence intensity, while in the absence it is quenched or minimal;

-“signal-off” mechanism where the presence of the target causes the quenching or a great decrease of the fluorescence intensity, while in the absence it is strong.

The change in the fluorescence intensity allows the quantitative detection of pesticides. Wang and his co-workers reported a non-competitive fluorescent aptasensor for the detection of acetamiprid pesticide based on the inner filter effect (IFE) of AuNPs toward

fluorescent carbon dots (CDs).<sup>118</sup> This aptasensor system displayed high selectivity and excellent accuracy for acetamiprid detection with a linear range from 22.5 nM to 0.45  $\mu$ M and a detection limit of 4.85 nM. In another study, Zhang and colleagues reported a FRET competitive aptasensor based on molecular beacon for the quantification of phorate, profenofos, isocarbophos and omethoate.<sup>13</sup> The molecular beacon was labelled with FAM and DABCYL at the 5' and 3' end respectively, and contained a sequence partially complementary to the aptamer. Upon adding the pesticides, the aptamer preferably binds the targets, inducing the molecular beacon opening and a restore of fluorescence intensity. The limit of quantification (LOQ) detected for phorate, profenofos, isocarbophos, and omethoate reached 19.2, 13.4, 17.2, and 23.4 nM, respectively. Various other types of fluorescent aptasensors have been developed for the pesticide detection.<sup>119,120,121</sup>

#### *Electrochemical aptasensors*

In the past years, electrochemical aptasensors have shown great potential for pesticide detection due to their ability to multiplexed analysis, fast response, and low cost.<sup>122,123</sup>

Fei and co-workers developed an electrochemical aptasensor for the detection of acetamiprid residues using gold nanoparticles (AuNPs) decorated with multiwalled carbon nanotube-reduced graphene oxide nanoribbon (Au/MWCNT-rGONR) composites.<sup>124</sup> This aptasensor, based on the variation of electron transfer resistance, was relevant to the formation of acetamiprid–aptamer complex on the modified electrode surface. This non-competitive electrochemical aptasensor showed excellent performances for the acetamiprid detection into a linear range of 50 fM to 10  $\mu$ M and an extremely low detection limit of 17 fM. Rapini and colleagues developed a simple electrochemical DNA aptasensor for the detection of acetamiprid based on a competitive format and disposable screen-printed arrays.<sup>125</sup> The dose–response curve was constructed between 0.25 and 2.0 mM acetamiprid concentration range with a limit of detection of 0.086 mM. Furthermore, the efficacy of this aptasensor has also been demonstrated in various fruit juice samples showing high recovery percentage. All these characteristics make this aptasensor particularly promising for the realization of a commercial kit.

### *Colorimetric aptasensors*

Colorimetric methods have been extensively applied for the detection of pesticide contaminants.<sup>112,126</sup> Gold nanoparticles (AuNPs) are the most commonly used probes for the colorimetric sensing assays due to their facile preparation and surface modification. By using AuNPs, Wang and co-workers reported a simple non-competitive colorimetric aptasensor for the detection of omethoate.<sup>127</sup> This system was based on the principle that single-stranded DNA (ssDNA)-wrapped gold nanoparticles (AuNPs) are resistant to salt-induced aggregation. In the presence of the target, the aptamer binds to omethoate and is released from the AuNP surface. The consequent aggregation of AuNPs changes the color of the sample from purple to red. This aptasensor showed good linearity between 0.1 and 10  $\mu\text{M}$ , with a low detection limit of 0.1  $\mu\text{M}$ . In addition, Abnous et al. recently developed a competitive colorimetric aptasensor to determine the presence of pesticide malathion.<sup>128</sup> In the absence of the target, aptamer forms a double-strand DNA structure (dsDNA) with a complementary sequence and protect AuNPs against salt-induced aggregation. Upon malathion addition, the aptamer folds into a hairpin structure to form aptamer-malathion complex, releasing the complementary strands into the solution. As a result, the AuNPs underwent salt-induced aggregation, leading to a solution colour change from red to purple. The efficiency of this aptasensor has also been demonstrated in spiked human serum samples, showing its high sensibility to malathion with a rapid response (35 min) and a detection limit of 1 pM.

Several other pesticide-specific aptasensors have been developed, also demonstrating a lower limit of quantification (LOQ) and some of them are listed in the table 3.

| Pesticide residue   | Assay   | LOD  | References |
|---|---|--|------------|
| Phorate,<br>profenophos,<br>isocarbophos,<br>omethoate                        | Fluorimetric<br>FRET: FAM and DABCYL                    | 19 nM,<br>13 nM<br>17 nM,<br>23 nM         | 113        |
| Phorate,<br>profenophos,<br>isocarbophos,<br>omethoate                        | Fluorimetric<br>FRET: FAM and AuNPs                     | 35 nM,<br>134 nM<br>384 nM<br>2.35 $\mu$ M | 129        |
| Acetamiprid   | Fluorimetric<br>FRET: QDs and Au NPs                    | 7 nM                                       | 130        |
| Acetamiprid   | Fluorimetric<br>FRET: UCNPs and<br>colorimetric AuNPs   | 3 nM                                       | 131        |
| Isocarbophos,<br>dursban phosalone,<br>methamidophos,<br>acephate trichlorfon | Colorimetric<br>AuNPs aggregation                       | Isocarbophos:100 ppb,<br>others: 2000 ppb  | 132        |
| Acetamiprid   | Colorimetric<br>hemin-rGO                               | 40 nM                                      | 133        |
| Acetamiprid   | Electrochemical<br>AuNPs modified electrode;<br>EIS, CV | 1 nM                                       | 134        |

Table 3. Summary of some the aptasensor strategy for pesticide detection.

### 2.3 Light up aptasensors

Light-up aptamers are generated for specific binding and activate their cognate fluorogenic ligand (small non-fluorescent dye that becomes fluorescent). In free unbound form, when the fluorogen molecule is excited, its energy is dissipated by non-radiative pathway, such as molecular vibration. However, when it binds to the aptamer, the planar

structure of the small molecule dye is stabilized and radiative decay pathways can prevail, leading to a large fluorescence enhancement (Fig. 14).

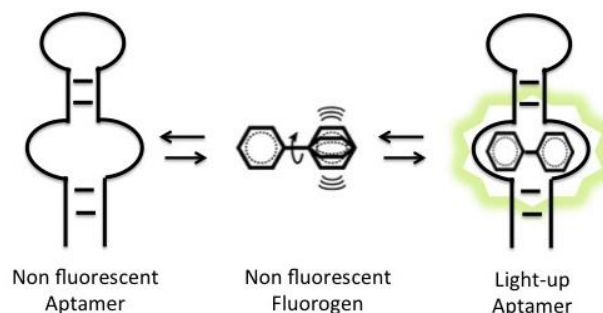


Fig. 14. Light up aptamer.

In the light-up system, the fluorogen molecule contributes through two roles: it gives brightness and photostability (the response of the molecule against the exposure to solar, UV, and visible light that leads to a physical or chemical change).<sup>135</sup> The fluorescence intensity at a given concentration depends on the dissociation constant ( $K_d$ ) and on the fluorescence quantum yield of the fluorogen with its specific aptamer.

The first light-up RNA aptamer was selected against Malachite Green (MG) by Grate and Wilson in 1999.<sup>95</sup> It was generated to confine the formation of radicals on RNA upon laser activation, leading to the rapid degradation of such RNA. This light-up aptamer was demonstrated to display a high affinity for MG, with a dissociation constant ( $K_d$ ) of 117 nM. A ~2400-fold increase in fluorescence was observed upon binding to the cognate target.<sup>129</sup> Some years later, other light-up aptamers against several fluorogenic dyes, above-mentioned- have been selected and largely used for both *in vivo* and *in vitro* applications.<sup>136</sup> They all have their unique fluorogen-binding pocket. This binding zone constitutes an extended planar platform that stabilizes the planar structure of the fluorogen, allowing the fluorescence enhancement. In almost all light-up aptamers, the binding pocket is made from two or more G-quartets stabilized by potassium ions.<sup>136,137</sup> However, the Malachite Green aptamer (MGA) is characterized by a binding pocket made from a mixed quadruple base that is structured only upon MG binding (Fig. 15).<sup>138</sup> Among all developed RNA light-up aptamers, MGA is one of the most characterized. Its structure has been determined by X-ray crystallography and NMR spectroscopy, displaying the

complex between MGA and MG and its analog tetramethylrosamine (TMR).<sup>138,139</sup> TMR differs from MG by a bridging oxygen between two phenyl rings, which constrains them into a plane. More recently, Trachman and colleagues described in detail the structure of the fluorogen-binding pocket of MGA formed in the presence of TMR, as reported in Fig. 15.<sup>137</sup>

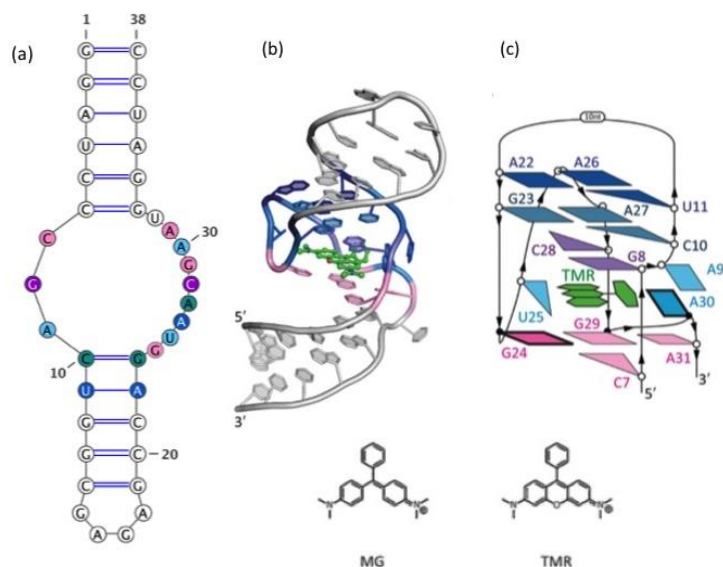


Fig. 15: Predicted structures of MGA and their targets. Chemical structure of malachite green (MG) and tetramethylrosamine (TMR). a) Predicted secondary structure of MGA. b) Tertiary structure of MGA with TMR. c) Illustration of binding-pocket structure of MGA with TMR. Colour coding for both the secondary and tertiary structure schematics is as follows: TMR, green; the G24 A31 G29 C7 base quadruple that accommodate the fluorogen, pink; the canonical G8:C28 base-pair that capped the fluorogen, purple; the perpendicularly stacking A9 and A30 adenosines, magenta; U25, the uridine involved in the U-turn: light blue; the two base triples A26 U11-A22 and A27 C10-G23 are respectively dark blue and petrol blue.

One of the limitations of the RNA-malachite green probe system is the cytotoxicity of MG, with a limiting toxic concentration in human cell detected around 0.1 and 1  $\mu\text{M}$ .<sup>140</sup> Nonetheless, the Malachite Green aptamer represents a powerful model system to understand the factors that stabilize the RNA structure. MGA can also be used for monitoring the recognition of small molecules. Indeed, light-up aptamers can be converted into biosensors, applying different strategies to create fluorogen reporters for detection of nucleic acid sequences,<sup>141,142</sup> target proteins<sup>143</sup> or small species.<sup>98,144</sup> As previously described, Stojanovic was the first to create a light-up aptasensor for the small molecule detection.<sup>86</sup>

In order to develop an efficient light-up biosensor, fluorogen and aptamer must have some fundamental requirements. Firstly, aptasensors should maintain a high affinity for

both fluorogen and the target. Accordingly, with the major advantage of light-up system, fluorogens must emit no fluorescence in the free state while generating high fluorescence upon target binding. Finally, fluorogens have to ensure the photostability of the system.

An allosteric light-up aptamer consists of two connected aptamers: one that binds to the analyte of interest (recognition domain) and the other that recognizes the fluorogen (reporting domain), held together through a labile connecting stem (communication module) (Fig. 16). The light-up aptasensor is engineered to introduce an instability on the structure of the fluorogen-binding site. In the presence of target, a « cascade mechanism » is triggered. The binding of the analyte target to its domain stabilizes the connecting stem, which in turn stabilizes the binding of the fluorogen to the signalling module. As a result, a stable complex is formed and a large fluorescence signal is produced.

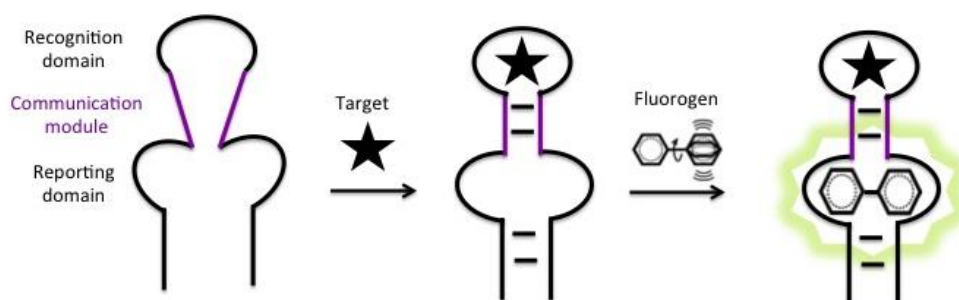


Fig. 16. Allosteric light-up aptamer

The thorough investigation of the MGA structure allowed us to modify this aptamer and to design new light-up aptasensors (see later).

### 3. Technologies used in the present work

In order to rationally design a new aptasensor, it is crucial to characterize the aptamer affinity for the target. The development of sensitive, selective, and controllable small target recognition sensors remains as a tough challenge. Moreover, as previously described, choosing the most suitable technique is not easy, especially in the case of small molecule targets often weakly soluble (including pesticides). Ideally, it is important to compare various techniques and apply all necessary controls.

During my thesis project, in order to design a new dual recognition aptasensor for the

pesticide detection, a thorough study on the recognition ability of aptamers was conducted using two common homogeneous-phase techniques such as fluorescence anisotropy and ITC. In this sub-chapter, the principle and applications of these two techniques in the characterization of small molecule-aptamer complexes will be described.

### 3.1 Fluorescence anisotropy

Fluorescence anisotropy (FA) is a powerful technique largely used to study the molecular interactions. It measures the rotational mobility of the fluorescent molecule that is excited with polarized light. In literature, the terms fluorescence anisotropy (FA) and fluorescence polarization (FP) are frequently used and they can be interchanged. FA and FP values can be determined by measuring emission intensities based on both horizontal and vertical polarization planes (Fig. 17.).

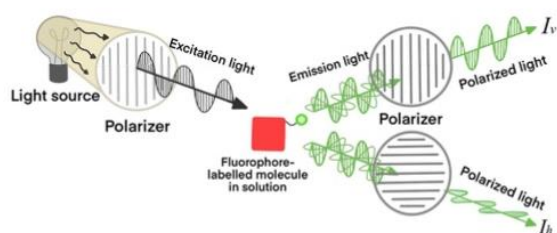


Fig. 17. Schematic representation of fluorescence anisotropy (polarization)<sup>145</sup>

Anisotropy ( $r$ ) and polarization ( $P$ ) values are defined by the equation 1 and 2 respectively:

$$1) \quad r = \frac{I_v - I_h}{I_v + 2I_h} \qquad 2) \quad P = \frac{I_v - I_h}{I_v + I_h}$$

where  $I_v$  is the fluorescence intensity in the vertical polarization plane and  $I_h$  in the horizontal polarization plane. The fluorescence polarization and the fluorescence anisotropy contain the same information, but anisotropy is preferred because it is normalized by the total intensity  $I_T = I_v + 2I_h$ , resulting in a simplified relationship (see below).

Firstly described by Perrin, FA is defined by the following mathematical equation, where the fluorophore is assimilated to a spherical molecule:

$$r = r_0 / (1 + \tau / \theta)$$

In this equation,  $r$  is the measured anisotropy,  $r_0$  is the fundamental fluorescence anisotropy (also called intrinsic or limiting anisotropy),  $\tau$  is the excited state lifetime of the fluorophore and  $\theta$  the rotational correlation time of the labelled molecule.

Also note that  $\theta$  can be described as:

$$\theta = \eta V / RT$$

where  $\eta$  is the solution viscosity,  $R$  is the gas constant,  $T$  is the temperature, and  $V$  is the effective molar volume of the rotating unit. This relation implies that the molecular size affects the polarization of fluorescence emission (Fig. 18). Therefore, fast rotation in solution generates a lower  $r$  value compared to biggest molecules that have a slow rotation.

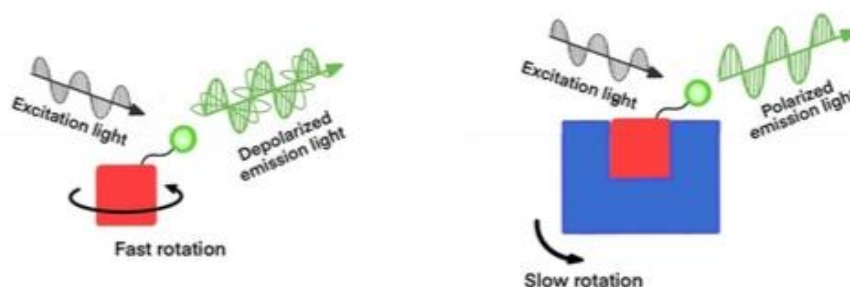


Fig. 18. Representation of depolarized and polarized emission. A small fluorescent molecule has a fast rotation. In this case, the planes from which fluorescence is emitted, is rotated compared to the plane of excitation, consequently the light emitted is depolarized. The  $r$  value will be low. On the other hand, when the small fluorophore or labelled molecule binds a larger molecule, the molecular volume increases and the rotational motion slow down. In this situation, the planes from which the light is emitted, deviates less from the plane for excitation, resulting in polarized fluorescence.  $r$  value will be higher.<sup>145</sup>

Two theoretical situations can be retrieved. The first one occurs when the measurement time is very long compared to the rotational correlation time of the fluorophore ( $\tau \gg \theta$ ). In this case, during the experiment, fluorophores emit light during the measurement process in all directions without any specific preference. The measurement system will not record a specific polarization direction in such way that the emitted light is depolarized. The second case occurs when the measurement time is very short compared to the rotational correlation time of the fluorophore ( $\tau \ll \theta$ ). In this case, even if fluorophores are rotating, they will be “snapped” by the measurement system at a specific

time with a specific orientation, emitting a light with a specific polarization.

Anisotropy, based on a ratiometric intensity measure, is dimensionless and independent of the fluorophore concentration. Moreover, it can be used to obtain information on size, shape and flexibility of macromolecules.

#### *Fluorescence Anisotropy for small molecules aptamers*

Fluorescence anisotropy can be used to measure the binding constants and kinetics of reactions that cause a change in the rotational time of the molecules. Due to its simple operation, rapid measurement, high sensitivity and reproducibility, FA has been largely used to characterize the aptamers and to study interactions with their targets. In particular, for the aptamer binding to small molecules, different FA-based strategies can be applied. Perrier and colleagues<sup>146</sup> classified these approaches in three strategies:

- The first strategy is based on the modification of the rotational correlation time  $\theta$  due to the increase in the apparent mass of the fluorophore. This approach is the most widely used and can be applied to the strategies based on split aptasensor,<sup>147</sup> duplexed aptamer biosensor,<sup>148</sup> and kissing complex.<sup>109</sup>
- The second strategy, also based on the modification of the rotational correlation time ( $\theta$ ), depends on the modification of the local mobility of the fluorophore and can be applied to the design of signalling aptamers.<sup>78,79</sup>
- The third strategy relies on excited state lifetime ( $\tau$ ) changes. This method, described for the first time by Chovelon and colleagues can be applied using the SYBR Green for the label-free assay devoted to the small molecule detection.<sup>149</sup>

During my thesis, I applied the fluorescence anisotropy for the detection of pesticides based on either the first approach for the duplex aptamer biosensor or the third approach for a label-free assay. In the next chapter, these approaches will be described in more details.

### **3.2 Isothermal Titration Calorimetry (ITC)**

Isothermal titration calorimetry (ITC) is a label-free quantitative technique used to study a wide variety of biomolecular interactions. In particular, it has become a very popular method to study the binding ability of aptamers to their targets of different size.<sup>66,150–152</sup>

ITC relies on the fact that the formation of the aptamer-target complex is typically an exothermic process that releases heat. From one single ITC experiment, it is possible to determine the thermodynamic parameters of the molecular interaction including the enthalpy change ( $\Delta H$ ), the equilibrium binding constant ( $K_a$ ) and the stoichiometry ( $N$ ). From these initial measurements, the Gibbs free energy change ( $\Delta G$ ) can be calculated from the following equation:

$$\Delta G = - RT \ln K_a$$

where  $R$  is the gas constant and  $T$  is the Temperature in Kelvin. The entropy changes ( $\Delta S$ ) can be also calculated as follows:

$$\Delta G = \Delta H - T\Delta S$$

Understanding the interaction from a thermodynamic perspective allows us efficient characterization of aptamers. When such binding occurs, heat is either released or absorbed, which is measured by a calorimeter.

The isothermal titration calorimeter is composed of two cells, one is the reference cell filled with water or buffer and another is the sample cell with either the ligand or aptamer. (Fig. 19 a). The cells are placed in an adiabatic jacket, at identical temperature, maintained constant by a heater tool around the sample cell. In the typical ITC experiment, the ligand is titrated into the aptamer by a syringe, with defined injections. Each injection causes heat changes of a few millionths of a degree Celsius detected and measured. The quantity of heat measured is in direct proportion to the amount of aptamer-ligand binding.

In an exothermic reaction, the temperature in the sample cell increases upon addition of ligand, causing the decrease in the power to the heater and a downward peak in the signal (Fig. 19 b). As the temperature of the two cells comes back to being equal, the signal returns back to baseline, become stable until the next injection. Through a series of ligand injections, the molar ratio between the ligand and aptamer is gradually increased, leading to a titration curve (Fig. 19 b). During the measurement, the ligand is being increasingly saturated and less binding of the ligand occurs so that the heat change starts to decrease until the sample cell contains an excess of ligand with respect to aptamer, causing the reaction towards saturation. The area of each peak is then integrated and plotted versus the molar ratio of ligand to aptamer.

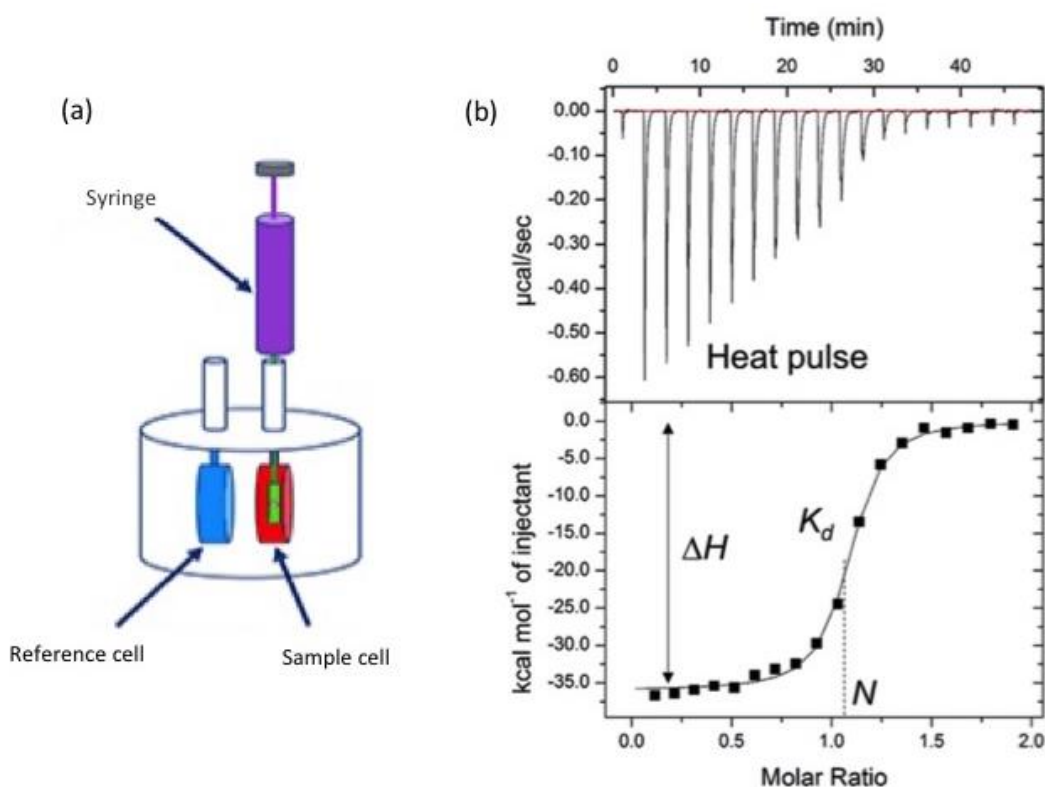


Fig. 19 a) Isothermal titration calorimeter. b) Example of results obtained by an ITC.<sup>146</sup>

Enthalpy value ( $\Delta H$ ) can be measured directly during ITC measurement. It reflects the energy change of the system when the aptamer binds to the ligand, resulting from the formation of non-covalent interactions (e.g., van der Waals interactions, hydrogen bonds, ion pairs) at the binding interface. The dissociation constant ( $K_d$ ) can be calculated by fitting a suitable binding model to the ITC isotherm.

The binding constant  $K_a$ , with the product of stoichiometry ( $N$ ) and the concentration of aptamer  $[M]$  provides the value of the  $c$  parameter (determining the profile of the curve) calculated using the equation:

$$c = N \times K_a \times [M]$$

A high  $c$  value ( $\sim 1000$ ) leads to the generation of a too-step binding curve (Fig. 20), which allows determining the stoichiometry and enthalpy parameters, but not the affinity. If the  $c$  value is  $< 10$ , the architecture of the binding isotherm is too shallow, which not allows an accurate determination of affinity, enthalpy and stoichiometry values. Hence, to get a good sigmoidal shape of the binding isotherm, the optimal  $c$  value should be between 20 and 100.<sup>153</sup> Moreover, the  $c$  value can be adjusted by varying the

concentration of the aptamer, which also affects the stoichiometry value.

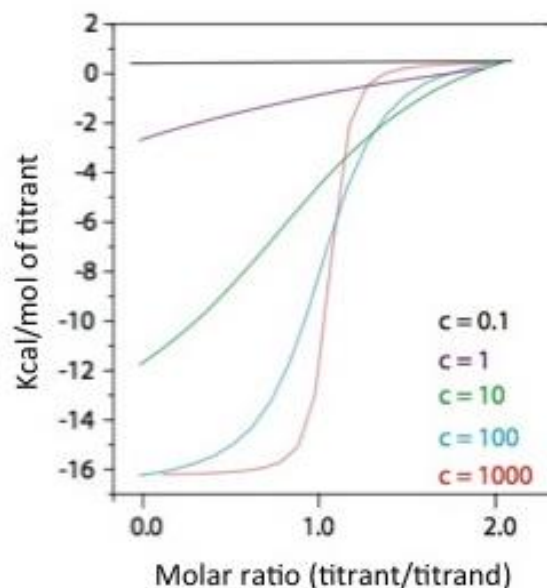


Fig. 20. Illustration of the c-value on the shape of the binding isotherm.<sup>154</sup>

In order to evaluate the dilution effects caused by each injection, it is important to perform a control experiment and titrate the ligand into the buffer without the aptamer. Another important control consists in the titration of buffer into the aptamer, without the ligand. In both cases, the values obtained are subtracted from the experimental raw data. Finally, the data obtained are analysed with the manufacturer software the, which calculates the thermodynamic parameters.

#### *ITC for small molecules aptamers*

ITC is widely used to characterize the aptamers selected against proteins <sup>152</sup> or small molecules<sup>155</sup> determine their thermodynamic parameters, and also study the binding interaction using aptamer variants or similar targets.

Neves and coworkers<sup>155</sup> used ITC measurements to explore the optimal reaction condition for the cocaine aptamer-binding affinity. They studied how ionic strength and pH can affect the cocaine-aptamer binding affinity. According to the experimental results, they confirmed that the highest binding affinity can be achieved in the absence of sodium chloride at pH 7.4.

A few years later, Slavkovic and coworkers studied the structure-affinity of the same MN4 aptamer able to recognize the cocaine likewise the alkaloid quinine.<sup>150</sup> They used ITC methods to study the interaction on the cocaine-binding aptamer to a different cocaine metabolites and quinine analogs. Affinity and thermodynamic parameters of ligands enabled to determine which groups of cocaine and quinine molecules are important for high-affinity binding. Firstly, the high affinity for cocaine was confirmed, and secondly, the importance of the bicyclic aromatic ring with a methoxy group at the 6th position of quinine was demonstrated.

Recently, Zhang et al. applied ITC to study the binding ability of the adenosine aptamer.<sup>156</sup> As the adenosine aptamer has two binding sites, the authors aimed at investigating whether the aptamer maintains its binding affinity and specificity if one of the binding sites is removed. They measured the binding parameters of the original aptamer using ITC. They subsequently deleted one of the two binding sites for creating the mutant aptamer. As compared with the parent aptamer, the mutated DNA molecule showed similar binding affinity and the stoichiometry was reduced by half.

# **Experimental Section**

## 1. Objectives of thesis

The role of aptasensors lies in integrating them for detecting pesticide residues trying to avoid the use of standard methods and their drawbacks. Compared to the large number of existing pesticides, to date only few aptamers have been generated (reviewed by Liu 2019 recently)<sup>112</sup> and some of them lack selectivity and are unable to discriminate among analogous species. To allow monitoring pesticide residues on a larger scale, it is necessary to develop more specific aptasensors. On the one hand, they need to be generated by SELEX method, on the other hand, innovative strategies capable of developing more sensitive aptasensors – through the rational re-engineering of aptamers- must be put into practice. Besides, it is necessary to designate aptasensors that can be used in real complex samples and capable of resisting to disturbances of interfering substances present in the sample.

During my thesis project, my goal was to engineer new smart and more specific aptasensors, combining two strategies never used before for the pesticide detection, i. e. involving light-up and kissing complex concepts.

Indeed, taking advantage of these two approaches (described in the previous chapter), we firstly developed some proof-of-concept aptasensors for demonstrating their functionality towards small molecules and for demonstrating that our approach could be applied to pesticide detection. The final objective was to realize a sensitive aptasensor for the monitoring of pesticides, based on a fluorescent double-switch complex, as shown below (Fig. 21).

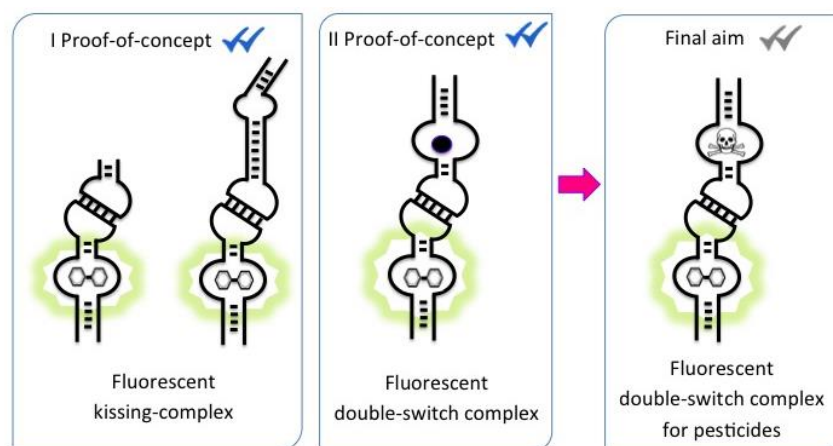


Fig. 21. Schematic illustration of the project phases.

In this chapter, our work will be presented in the form of three research manuscripts. The covered topics are the following:

- design of new signalling aptasensors based on the anti-Malachite Green aptamer and detection of RNA hairpins through kissing interaction. This work has been published in the *Analytical Chemistry* journal in July 2020.

- design of a dual-aptasensor for the detection of theophylline, based on the combination of the Malachite-Green aptamer and the theophylline aptamer. This work is submitted to *Biosensors and Bioelectronics*, and is currently under review.

- characterization of two anti-pesticide aptamers through different homogenous-phase techniques. This work will be submitted shortly to a peer-review journal.

Design of aptasensors against small RNA hairpins and dual-aptasensor works have been conceptualized and carried out in collaboration with the ARNA laboratory from the University of Bordeaux.

## 2. « Engineering light-up aptamers for the detection of RNA hairpins through kissing interaction. »

### 2.1 Strategy

The strategy described in this part is based on the development of a new light-up aptasensor for the detection of two microRNA precursors: let-7b<sup>157</sup> and miR206.<sup>158</sup>

As described in the part 2.3, the malachite green RNA aptamer (MGA) presents an imperfect hairpin conformation, in which the apical loop is not involved in the binding pocket for the recognition of the fluorogen.<sup>95</sup> Taking advantage of its properties, the MGA has been modified in such a way that it can recognize a second RNA hairpin through the loop-loop interaction. The binding to the second hairpin (aptakiss) stabilizes the binding zone, allowing the interaction with the fluorogen that in turn results in the fluorescence emission.

New MG aptaswitches, that we called Malaswitches (Msw in short), have been generated. Firstly, we rationally engineered two series of Malaswitch variants destabilizing the stem-loop portion of the native aptamer (MGA): 16 Msw variants for the aptakiss corresponding to the pre-mi-RNA let-7b and 8 Msw variants of the short RNA corresponding to the apical loop of the pre-miR206. Then, the best variants screened for each aptakiss was used with their respective full-length micro-RNA precursors. The screening has been carried out with fluorescence measurements (Fig. 22).

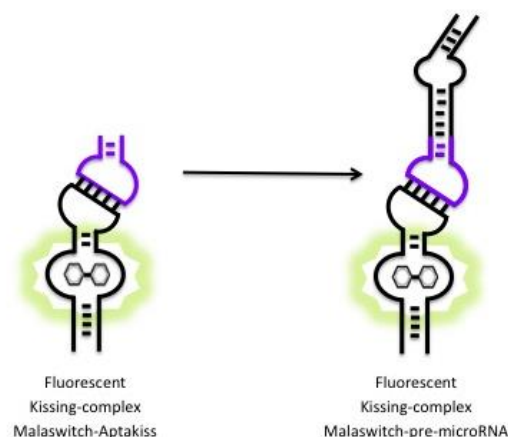


Fig. 22. Representation of the fluorescent kissing-complexes design. Malaswitch binds MG and forms a loop-loop interaction with the aptakiss (left) and the corresponding pre-miR (right), leading a fluorescent emission.

For the first time the aptaswitch-aptakiss system was designed to detect two microRNAs. The fluorogen small molecule helps to sense the formation of ternary complex and allows the label free biosensing of pre-miRNA.

## Engineering light-up aptamers for the detection of RNA hairpins through kissing interaction.

Arghya Sett, Lorena Zara, Eric Dausse, and Jean-Jacques Toulme

*Anal. Chem.*, **Just Accepted Manuscript** • DOI: 10.1021/acs.analchem.0c01378 • Publication Date (Web): 04 Jun 2020

Downloaded from [pubs.acs.org](https://pubs.acs.org) on June 5, 2020

### Just Accepted

“Just Accepted” manuscripts have been peer-reviewed and accepted for publication. They are posted online prior to technical editing, formatting for publication and author proofing. The American Chemical Society provides “Just Accepted” as a service to the research community to expedite the dissemination of scientific material as soon as possible after acceptance. “Just Accepted” manuscripts appear in full in PDF format accompanied by an HTML abstract. “Just Accepted” manuscripts have been fully peer reviewed, but should not be considered the official version of record. They are citable by the Digital Object Identifier (DOI®). “Just Accepted” is an optional service offered to authors. Therefore, the “Just Accepted” Web site may not include all articles that will be published in the journal. After a manuscript is technically edited and formatted, it will be removed from the “Just Accepted” Web site and published as an ASAP article. Note that technical editing may introduce minor changes to the manuscript text and/or graphics which could affect content, and all legal disclaimers and ethical guidelines that apply to the journal pertain. ACS cannot be held responsible for errors or consequences arising from the use of information contained in these “Just Accepted” manuscripts.

# Engineering light-up aptamers for the detection of RNA hairpins through kissing interaction.

Arghya Sett,<sup>a</sup> Lorena Zara,<sup>a, b</sup> Eric Dausse,<sup>a</sup> and Jean-Jacques Toulmé<sup>a, b\*</sup>

<sup>a</sup> ARNA Laboratory, Inserm U1212, CNRS UMR5320, University of Bordeaux, 33076 Bordeaux, France

<sup>b</sup> Novaptech, 146 rue Léo Saignat, 33076 Bordeaux

[jean-jacques.toulme@inserm.fr](mailto:jean-jacques.toulme@inserm.fr)

---

**ABSTRACT:** Aptasensors are biosensors that include aptamers for detecting a target of interest. We engineered signaling aptasensors for the detection of RNA hairpins from the previously described malachite green (MG) RNA aptamer. The top part of this imperfect hairpin aptamer was modified in such a way that it can engage loop-loop (so-called kissing) interactions with RNA hairpins displaying partly complementary apical loops. These newly derived oligonucleotides named malaswitches bind their cognate fluorogenic ligand (MG) exclusively when RNA-RNA kissing complexes are formed whereas MG does not bind to malaswitches alone. Consequently, the formation of the ternary target RNA-malaswitch RNA-MG complex results in fluorescence emission and malaswitches constitute sensors for detecting RNA hairpins. Malaswitches were designed that specifically detect precursors of microRNAs let7b and miR-206.

---

**KEYWORDS.** *Aptamer, Light-up, Malachite green fluorescence, RNA hairpin, Kissing complex.*

Aptamers -known as chemical antibodies- are single-stranded oligonucleotides that bind with strong affinity and high selectivity to a target molecule.<sup>1,2</sup> Aptamers are known to change conformation upon binding to their cognate target. Such a structural change of natural aptamers found in riboswitches is used by prokaryotic cells for regulating gene expression.<sup>3</sup> Structure switching is also exploited for the selection of aptamers through capture-SELEX, a procedure based on the release of candidates hybridized to an immobilized capture oligonucleotide following a structural change induced by the addition of the target.<sup>4-7</sup> The conformation change associated to the binding of the target to its cognate aptamer is also exploited in aptasensors that translate this change into a signal detected by fluorescence, SPR or electrochemistry.<sup>8-12</sup> To this end, advantage can be taken from kissing interactions that involve the formation of a short double-stranded hybrid between complementary loops of two RNA hairpins. We used conditional kissing interactions for the detection of purine derivatives thanks to the combination of two partners: a structure-switching aptamer and a short hairpin named aptakiss that gives rise to a kissing complex in the presence -and only in the presence- of the ligand.<sup>13-15</sup> This ternary complex quantitatively signals the presence of the target.

The need for tools allowing the detection of RNA molecules led to the design of so-called light-up aptamers *i.e.* aptamers that bind to fluorogenic dyes, consequently inducing their fluorescence emission. The malachite green fluorogenic aptamer was one of the first probe that was developed. Many other light-up aptamers were then

selected specific for DFHBI, thiazole orange, etc.<sup>16-20</sup> Spinach, Broccoli, Mango among other light-ups constituted the basis for the design of sensors that respond to the presence of metabolites such as ADP, SAM or 5-hydroxytryptophan: the fluorogenic dye and the metabolite cooperatively bind to the aptaswitch thus leading to fluorescence emission.<sup>21,22</sup>

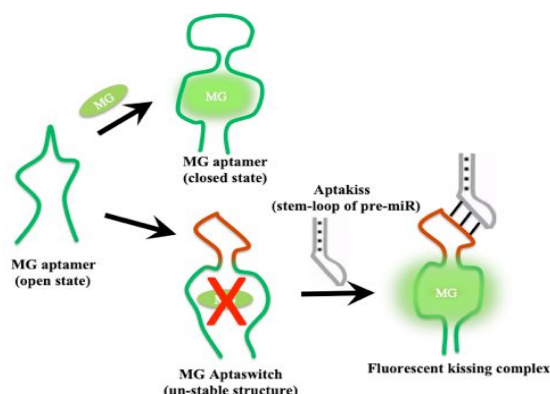
We previously identified a repertoire of hairpins Ki and Ki' with partly complementary loops. Ki-Ki' combinations gave rise to highly stable kissing complexes. These motifs constituted building blocks for engineering kissing aptaswitches.<sup>23</sup> We applied the same concept for engineering a switching aptasensor for RNA hairpins on the basis of the malachite green (MG) aptamer in which we introduced a kissing motif: the non-fluorescent MG-aptaswitch combination is stabilized by the target hairpin through kissing interaction (Scheme 1).<sup>24,25</sup> The presence of this target is quantitatively detected through the MG fluorescence emission. Application of such sensors is described for the detection of microRNA precursors.

## MATERIALS AND METHODS

### Chemicals and oligonucleotides

All chemicals used for this study were commercially available. Malachite green, HEPES, sodium acetate, potassium acetate, magnesium acetate for buffer preparation were purchased from Sigma. Oligodeoxynucleotides and 2'-O-methyl-modified oligoribonucleotides were synthesized and purified by polyacrylamide gel electrophoresis by Eurogentec (Liège,

Belgium). Sequences are given in supplementary Tables S1 and S2.



Scheme 1. MG aptamer and aptaswitch. Binding of MG to the aptamer results in fluorescence emission (top). The apical part of the MG aptamer was changed (red line), generating an aptaswitch that no longer binds to MG. The formation of a loop-loop complex with the aptakiss or the pre-miR hairpin allows MG binding and leads to fluorescence emission.

### Preparation of RNA

The RNA candidates were generated by T7-Flashscribe™ transcription kit (Cellscript). DNA templates containing the reverse complementary sequence of the T7 promoter site (5'-TAATACGACTCACTATAGGG-3') were used to prepare RNA by in vitro transcription. In a standard 20  $\mu$ l transcription mixture, 1  $\mu$ g of DNA template along with a 3-fold excess of T7 promoter were mixed with 100 mM of ATP, CTP, UTP, and GTP (1.8  $\mu$ l each), 100 mM DTT (2  $\mu$ l), 10 x T7-Flashscribe transcription buffer (2  $\mu$ l), 2U of T7 RNA polymerase and 0.5  $\mu$ l of RNase inhibitor. The reaction mixture was kept at 37°C for 2 hours followed by DNase (1U) treatment for 20 minutes. The RNA produced was then purified by polyacrylamide gel extraction. The RNA stock solutions were prepared in pure water (nuclease free) and stored at -20°C until use.

### Fluorescence measurements

Prior to fluorescence measurements, aptaswitch variants in the presence or in the absence of aptakiss or microRNA precursors were heated for 2 minutes at 65°C and then kept on ice for 5 minutes. SE x5 buffer was then added to the mixture and kept at room temperature for 15 minutes. (The SE x1 buffer contains 20 mM HEPES pH 7.4, 20 mM sodium acetate, 140 mM potassium acetate and magnesium acetate as required for the assay. Following this folding treatment, malachite green (2  $\mu$ M) was added to the aptaswitch alone (0.1  $\mu$ M) or mixed with the aptakiss (2  $\mu$ M) in SE x1 buffer. After 2 hours incubation at 4°C in the dark, the fluorescence of 50  $\mu$ l samples (in triplicate) was carried out in microtiter plates. Blank wells were filled with SE x1 buffer and background was subtracted to fluorescence measurements. The fluorescence signal was measured on a Tecan Infinite M1000 microplate reader. Excitation and emission wavelengths were set at 610 nm and 650 nm, respectively.

Fluorescence titration curves of aptaswitch-aptakiss mixtures by MG and of aptaswitch-MG mixtures by K4, K206, or miR precursors were fitted by non-linear regression plot (Graphpad Prism 7).

### Titration of malaswitch kissing complexes by malachite green

To obtain the dose response curves, the concentration of malachite green was varied from 0 to 10  $\mu$ M whereas the malaswitch and RNA hairpin concentrations were kept constant at 0.1  $\mu$ M and 2  $\mu$ M respectively. The fluorescence signal was measured in the SE x1 buffer containing 10 mM magnesium on a Tecan Infinite M1000 microplate reader. The fold change of intensity was expressed as the ratio between the fluorescence signals in the presence and absence of the RNA hairpin respectively. The saturation plot was fitted by non-linear regression plot (Graph pad Prism 7®).

### Effect of magnesium on the kissing interaction

The malaswitch candidate-RNA hairpin mixtures were folded (heated at 65°C for 2 minutes followed by freeze-thawing at ice for 5 minutes) in water. Then SE x5 buffer containing either 10 mM or 50 mM magnesium acetate was added and the samples were incubated at room temperature for 15 minutes to stabilize the ionic interaction. Malachite green was added to the mixture at the final concentration of 2  $\mu$ M and incubated at 4°C in the dark for 2 hours. Then, the fluorescence intensity was measured using Tecan Infinite M1000 microplate reader as described above.

### Fluorimetric titration of MG-malaswitch mixtures by RNA hairpins

The concentration of the aptakiss/pre-miRNA was varied from 0 to 10  $\mu$ M whereas malaswitch and ligand concentrations were kept constant at 0.1  $\mu$ M and 2  $\mu$ M, respectively. Fluorescence signal was measured in the SE buffer containing 10 mM magnesium on a Tecan Infinite M1000 microplate reader as described above.

### Statistical analysis

All the fluorescence measurements were performed in triplicate ( $n=3$ ). Standard error was calculated ( $SE = \text{Standard deviation} / \sqrt{\text{sample size } (n = 3)}$ ) by Graphpad Prism® and Microsoft Excel® spreadsheet analysis tool and indicated accordingly in each graph.

## RESULTS AND DISCUSSION

The MG aptamer is an imperfect hairpin displaying a central loop and a bulge that constitute the dye binding site; it forms layers of stacked nucleotides in pairs, triples, as well as a base quadruple to encapsulate the chromophore.<sup>24</sup> A 5 base pair (bp) stretch connects this region to the apical loop, the two bp next to the central loop being part of the MG recognition site (Figure 1). The apical loop of the aptamer is not involved in the recognition of the dye. In order to generate a MG aptaswitch (we name it malaswitch, Msw in short) we substituted the K4' motif 5'ACAUCAC to the apical tetraloop of the MG aptamer allowing the potential formation of a 7 bp duplex with the K4 loop 5'GUGAUGU.<sup>23</sup> For kissing aptaswitches, the connector between the

binding site of the target and the kissing loop plays a critical role in the switching ability.<sup>13,14,23</sup> For malaswitches, the 5 bp connector of the parent aptamer should be weakened to such an extent that binding of MG to the aptaswitch is abolished or strongly reduced. The top part of the aptaswitch will be stabilized by K4 through interaction between the loop-loop helix and the connector base pairs, thus contributing to the binding of the dye and consequently resulting in fluorescence emission.<sup>26</sup> We therefore reduced the connector between the apical loop and the body of the aptamer to the CG and UA pairs next to the central loop, thus generating Msw1.1 (Figure 1). We derived Msw variants (Figure 1 and supplementary Table S1) by changing the loop size and the base

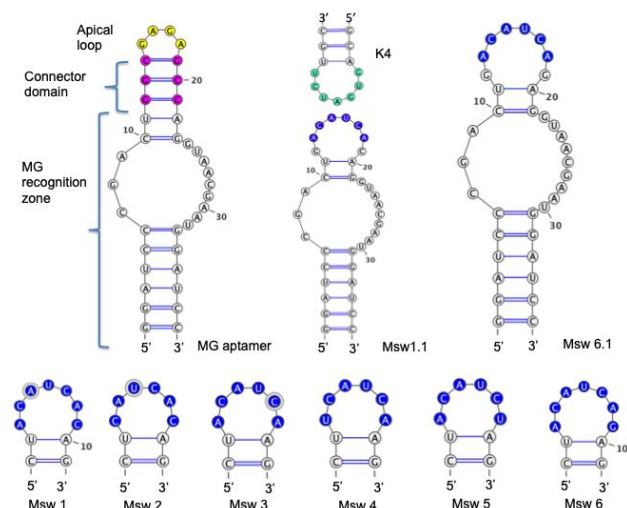


Figure 1. Predicted secondary structures of the MG aptamer, of malaswitches 1.1 and 6.1 (top) and of the apical part of malaswitch variants (bottom). For the MG aptamer, nucleotides in the apical loop are in yellow and the connector domain in pink. For Msw malaswitches, nucleotides in blue are potentially involved in kissing interaction with the aptakiss K4 (green bases). The full oligonucleotide sequences are given in the supplementary table S1.

composition, parameters that are known to contribute to the kissing complex stability.<sup>27-30</sup>

The screening of 16 Msw variants was carried out by fluorescence assay at a single malachite green concentration. Fluorescence intensity was measured in the absence and in the presence of K4. All the variants are pretty poor light-ups (1.3 to 1.5 fold fluorescence increase) in the absence of the aptakiss compared to the parent aptamer that showed about 35-fold fluorescence increase under the same conditions. The addition of K4 induces less than a 5-fold increase of the fluorescence emission with most of the variants whereas Msw6.1 shows a much larger fluorescence enhancement (about 16 fold) and a higher signal than any other variant (Figure 2 left). Msw6.1 is one of the two variants with Msw1.1 for which 8 nucleotides were inserted in the top part, all others displaying either a 6 or 7-membered apical loop.

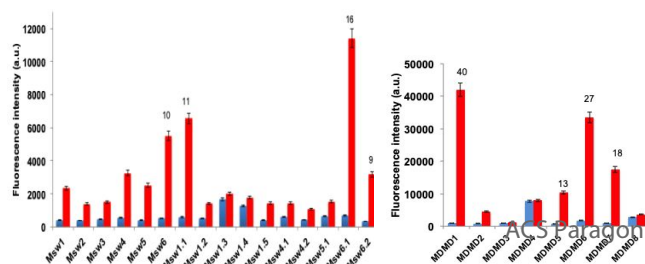


Figure 2. Fluorescence properties of malaswitch variants to K4 (left) and K206 RNA hairpins (right). Fluorescence emission ( $\lambda_{Exc} = 610$  nm,  $\lambda_{Em} = 650$  nm) of 2  $\mu$ M MG in the presence of 0.1  $\mu$ M of the different Msw variants either in the absence (blue bars) or in the presence (red bars) of either K4 or K206 (2  $\mu$ M). Measurements were performed in triplicate at room temperature in SE buffer containing 3 mM magnesium. The fold change of fluorescence increase is indicated next to red bars for the best light-ups.

Interestingly the only difference between Msw6.1 and Msw1.1 resides in the nature of the residue on the 3' side of the insert, G and C, respectively. For Msw1.1, the insert might generate a GC pair and consequently a 3 base pair connector making it less prone to switching and/or less potent for kissing if the terminal C is part of the loop-loop interaction. Indeed Msw1.1 that shows an 11-fold fluorescence increase is less potent light-up than Msw1 that has a 2 bp connector and a motif fully available for kissing complex formation (Figure 1). One can in addition point out that in Msw6.1 the loop is closed by a G-G combination. The interest of purine-purine loop closing combinations was previously demonstrated for kissing complexes.<sup>23,28</sup> It actually looked like a non-canonical base pair allowing stacking between the loop-loop helix and the lower stem of the kissing complex.<sup>31,32</sup>

Titration of K4-malaswitch complex by malachite green was performed for the variant Msw6.1 (Figure 3). The  $K_d$  for the binding of the dye to the kissing complex is in the micromolar range for the variants tested (Msw1, 4, 5, 6 and 6.1), a value 10 to 100 fold higher than that for the binding to the parent aptamer.<sup>33</sup>

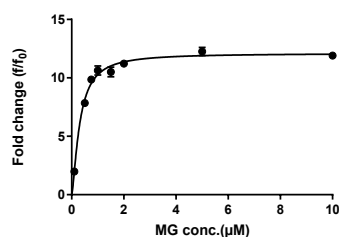
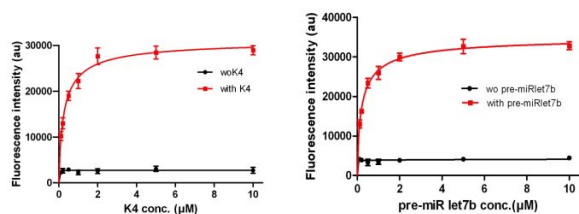


Figure 3. Titration of the Msw6.1-K4 complex with malachite green. The fold change of fluorescence in presence (f) and in absence of K4 ( $f_0$ ) at different malachite green concentrations. Msw6.1 and K4 concentrations were kept constant at 0.1 and 2  $\mu$ M respectively. Measurements were performed in triplicate ( $\lambda_{Exc} = 610$  nm,  $\lambda_{Em} = 650$  nm).

In the perspective of using the Msw/MG combination for monitoring the presence of RNA hairpins in a quantitative manner, an increasing amount of K4 was added to a malaswitch-dye mixture (Figure 4 left). Under the conditions used for this experiment, a plateau was reached at about 2  $\mu$ M of K4.

The loop of the K4 aptakiss is actually identical to the one displayed by the let7b microRNA precursor. miR-let7b is one of the 'master-regulator' of various cellular processes due to its interaction with messenger RNAs coding for DUSP9, NDST2, HDHD1A etc., thus modulating the translation process.<sup>34-36</sup> We therefore used the Msw6.1-MG sensor for the measurement of the full-length pre-miR-let7b in solution. The variation of the MG fluorescence obtained with this 83 nt long miRNA

precursor (supplementary Figure S1) is similar to the one observed with the aptakiss K4 (Figure 4 right): we observed a 15-fold increase of the MG emission under saturating pre-miR-let7b concentration.



**Figure 4.** Fluorimetric titration of a MG (2  $\mu\text{M}$ ) and Msw6.1 (0.1  $\mu\text{M}$ ) mixture by K4 (left) and the let-7b microRNA precursor (right) ( $\lambda_{\text{Exc}} = 610 \text{ nm}$ ,  $\lambda_{\text{Em}} = 650 \text{ nm}$ ). Black and red lines represent the signal in the absence and in the presence of the target RNA hairpin, respectively. Measurements were performed in triplicate at room temperature in SE buffer (see supplementary information).

We then extended this strategy to the detection of another RNA hairpin. We engineered a new series of malaswitches for detecting the precursors of miR206, a microRNA that is unbalanced in Duchenne Muscular Dystrophy (DMD) muscle cells.<sup>36</sup> Pre-miR206 is folded as an imperfect hairpin with an 11 nt apical loop (supplementary Figure S1). We substituted the 7 nt apical loop of Msw1 by an 11 nt insert giving rise potentially to a 9 base pair loop-loop duplex with the apical loop of pre-miR206, thus generating the malaswitch DMD1 (MDMD1; Figure 5 and supplementary table S2). We engineered 8 variants, MDMD1 to 8, with different loop sequence and size. For all of them, the loop was closed by a purine-purine combination that was shown to contribute to the efficiency of Msw6.1 for the detection of premiR-let7b. We investigated the binding of these 8 malaswitch variants to a short RNA hairpin, K206, corresponding to the top part of the pre-miR206, by monitoring the MG fluorescence emission. Variants 3, 4 and 8 did not show any fluorescence increase, but several variants displayed over 10-fold increase; a 40-fold enhancement of the MG fluorescence was observed with the MDMD1 upon addition of K206 (Figure 2 right). It was previously demonstrated that stacking interactions between successive nucleic acid bases were crucial at the stem-loop-loop helix junctions.<sup>37</sup> Of note the non-responding variants 3, 4 and 8 display a CG dinucleotide on the 5' side of the loop that cannot pair with the K206 loop. We might speculate that this disrupts the stacking between the connector and the loop-loop helix, thus depriving the malaswitch-MG complex of the contribution brought by the kissing interaction. Apparently, a single unpaired nucleotide either on the 3' side or in the middle of the loop is less detrimental (variants 5, 6 and 7). In contrast to what was observed for the Msw6.1-K4 complex for which no variation was seen over the 10 to 50 mM  $\text{Mg}^{2+}$  concentration range (not shown) a very different behaviour is seen for the MDMD variants: at 50 mM  $\text{Mg}^{2+}$  the variant 1 does not respond any longer to the addition of K206 (supplementary figure S2). Strong magnesium binding sites were demonstrated to be present on loop-

loop complexes, releasing the electrostatic repulsion between the backbone phosphate groups brought in close proximity through kissing interaction.<sup>26,28,38,39</sup> These results might be related to different conformations of the kissing complexes. Not surprisingly, MDMD1 was able to sense the full-length premiR206 (Figure 6).

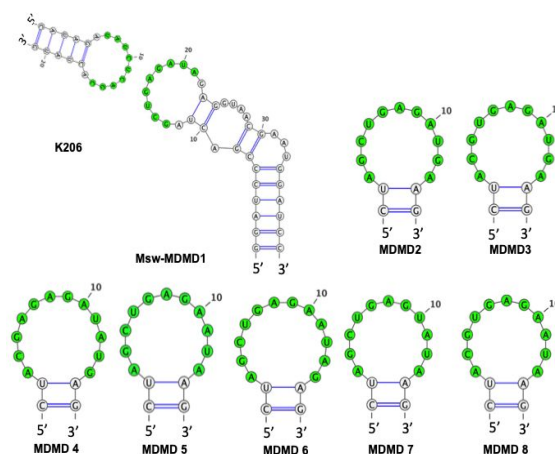


**Figure 5.** Predicted secondary structure (Mfold) of pre-miR206 aptaswitch Msw-MDMD1. The full length MDMD1 and K206 (apical part of pre-miR206) and the top part of pre-miR206 (MDMD2 to 8) are shown. The apical loops are indicated in green.

The formation of kissing complexes is known to be highly specific; a single point mutation in the loop is detrimental to the interaction.<sup>40</sup> We checked that our malaswitches displayed specific interaction. Indeed, there is no cross reactivity between Msw6.1 and pre-miR206 or between MDMD1 and pre-miRlet7b (supplementary Figure S3).

In the perspective of assays in biological media containing nucleases, it was of interest to investigate the properties of nuclease resistant analogues of malaswitches. The fully 2'-O-methyl-modified MDMD1.1 does not show MG fluorescence enhancement upon addition of the full length pre-miR206; either the conformation of the MG binding pocket was different from the one in the parent RNA malaswitch or the loss of some 2'OH group was detrimental to the interaction with the dye. In contrast, the MDMD1.2 oligomer in which only the residues in the apical loop were substituted for 2'-O-methyl analogues does retain the sensing properties (supplementary Figure S4). Such modified loops mimicking the RNA backbone are known to promote kissing interaction.<sup>26,41</sup>

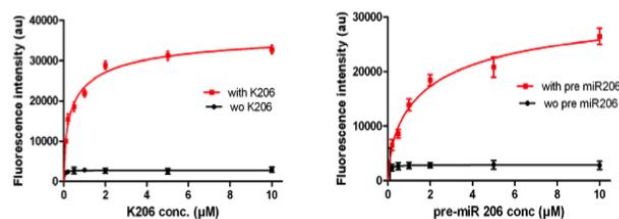


**Figure 6.** Titration of MDMD1. Fluorimetric titration of MDMD1 by (a) K206 and (b) pre-miR206 in the absence (black dots) or in the presence (red squares) of the kissing partner. The concentration of the malaswitch and of malachite green was adjusted at 0.1  $\mu\text{M}$  and 2  $\mu\text{M}$ , respectively. Measurements were performed in triplicate. ( $\lambda_{\text{Exc}} = 610 \text{ nm}$ ,  $\lambda_{\text{Em}} = 650 \text{ nm}$ )

## CONCLUSION

In conclusion we engineered a light-up aptaswitch from the MG aptamer by destabilizing the top part of this imperfect hairpin thus weakening the binding of the fluorogenic dye. The substitution of the apical loop of the parent aptamer by a sequence promoting the formation of a kissing complex provides an additional contribution that stabilizes the aptaswitch-MG complex, resulting in fluorescence emission. The design of such kissing aptaswitches is quite versatile; indeed, we previously engineered sensing aptaswitches for several purine derivatives.<sup>13</sup> In the present case the MG kissing aptaswitch is a direct sensor of RNA hairpins. Appropriately designed malaswitches detected specifically let-7b and 206 microRNA precursors. However, the sensitivity of the sensor remained too low for detecting these species in biologically relevant media. We explored a very limited subset of loop/connector combinations for generating aptaswitches. Aptasensors of increased sensitivity could likely be obtained through functional screening of larger pools by particle display or microfluidics.<sup>42,43</sup> Work along this line is in progress.

The strategy can be applied to the detection of any RNA hairpin. Malaswitches specific for viral RNA hairpins could be easily designed, for instance for the trans-acting responsive element of HIV-1 for which a kissing motif was characterized that could be introduced in the apical part of the MG aptamer.<sup>26,44</sup> Such fluorogenic tools might also be of interest for the design of inducible assembly of fluorescent nanostructures.

## ASSOCIATED CONTENT

### Supporting Information

The Supporting Information is available free of charge on the ACS Publications website.

Sequences of oligonucleotides (Malachite green aptamer, all malaswitch variants, miRNA precursors) and additional data as noted in text ([PDF](#)).

## AUTHOR INFORMATION

### Corresponding Author

E-mail: [jean-jacques.toulme@inserm.fr](mailto:jean-jacques.toulme@inserm.fr)

Phone : +33 (0)557 57 10 17

### Author Contributions

The manuscript was written through contributions of all authors.

## Notes

There are no conflicts to declare.

## ACKNOWLEDGMENT

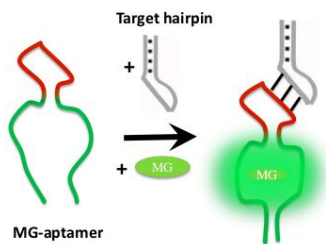
We acknowledge the support of the Agence Nationale pour la Recherche in the frame of the ERA-NET EuroNanoMed-II, project number ER-2016-2360733 and of the Conseil Régional de Nouvelle Aquitaine (grant 2017-1R30107-00013224).

## REFERENCES

- Ellington, A. D.; Szostak, J. W. In Vitro Selection of RNA Molecules That Bind Specific Ligands. *Nature* **1990**, *346* (6287), 818.
- Tuerk, C.; Gold, L. Systematic Evolution of Ligands by Exponential Enrichment: RNA Ligands to Bacteriophage T4 DNA Polymerase. *Science* (80). **1990**, *249* (4968), 505–510.
- Bédard, A.-S. V.; Hien, E. D. M.; Lafontaine, D. A. Riboswitch Regulation Mechanisms: RNA, Metabolites and Regulatory Proteins. *Biochim. Biophys. Acta (BBA)-Gene Regul. Mech.* **2020**, 194501.
- Nutiu, R.; Li, Y. In Vitro Selection of Structure-switching Signaling Aptamers. *Angew. Chemie Int. Ed.* **2005**, *44* (7), 1061–1065.
- Stoltenburg, R.; Nikolaus, N.; Strehlitz, B. Capture-SELEX: Selection of DNA Aptamers for Aminoglycoside Antibiotics. *J. Anal. Methods Chem.* **2012**, 2012.
- Nutiu, R.; Li, Y. Structure-Switching Signaling Aptamers. **2003**, *18* (11), 4771–4778.
- Yang, K.-A.; Pei, R.; Stojanovic, M. N. In Vitro Selection and Amplification Protocols for Isolation of Aptameric Sensors for Small Molecules. *Methods* **2016**, *106*, 58–65.
- Stojanovic, M. N.; De Prada, P.; Landry, D. W. Aptamer-Based Folding Fluorescent Sensor for Cocaine. *J. Am. Chem. Soc.* **2001**, *123* (21), 4928–4931.
- Hamaguchi, N.; Ellington, A.; Stanton, M. Aptamer Beacons for the Direct Detection of Proteins. *Anal. Biochem.* **2001**, *294* (2), 126–131.
- Paige, J. S.; Nguyen-Duc, T.; Song, W.; Jaffrey, S. R. Fluorescence Imaging of Cellular Metabolites with RNA. *Science* **2012**, *335* (6073), 1194.
- Baker, B. R.; Lai, R. Y.; Wood, M. S.; Doctor, E. H.; Heeger, A. J.; Plaxco, K. W. An Electronic, Aptamer-Based Small-Molecule Sensor for the Rapid, Label-Free Detection of Cocaine in Adulterated Samples and Biological Fluids. *J. Am. Chem. Soc.* **2006**, *128* (10), 3138–3139.
- Citartan, M.; Tang, T.-H. Recent Developments of Aptasensors Expedient for Point-of-Care (POC) Diagnostics. *Talanta* **2019**.
- Durand, G.; Lisi, S.; Ravelet, C.; Dausse, E.; Peyrin, E.; Toulmé, J. J. Riboswitches Based on Kissing Complexes for the Detection of Small Ligands. *Angew. Chemie - Int. Ed.* **2014**, *53* (27), 6942–6945.
- Chovelon, B.; Durand, G.; Dausse, E.; Toulmé, J.-J.; Faure, P.; Peyrin, E.; Ravelet, C. ELAKCA: Enzyme-Linked Aptamer Kissing Complex Assay as a Small Molecule Sensing Platform. *Anal. Chem.* **2016**, *88* (5), 2570–2575.
- Goux, E.; Dausse, E.; Guieu, V.; Azéma, L.; Durand, G.; Henry, M.; Choïnard, L.; Toulmé, J. J.; Ravelet, C.; Peyrin, E. A Colorimetric Nanosensor Based on a Selective Target-Responsive Aptamer Kissing Complex. *Nanoscale* **2017**, *9* (12), 4048–4052.
- Dolgosheina, E. V.; Jeng, S. C. Y.; Panchapakesan, S. S. S.; Cojocar, R.; Chen, P. S. K.; Wilson, P. D.; Hawkins, N.; Wiggins, P. A.; Unrau, P. J. RNA Mango Aptamer-Fluorophore: A Bright, High-Affinity Complex for RNA Labeling and Tracking. *ACS Chem. Biol.* **2014**, *9* (10), 2412–2420.
- Filonov, G. S.; Moon, J. D.; Svendsen, N.; Jaffrey, S. R. Broccoli: Rapid Selection of an RNA Mimic of Green Fluorescent Protein by Fluorescence-Based Selection and Directed Evolution. *J. Am. Chem. Soc.* **2014**, *136* (46), 16299–16308.

- (18) Ouellet, J. RNA Fluorescence with Light-Up Aptamers. *Front. Chem.* **2016**, *4* (June), 1–12.
- (19) Autour, A.; Jeng, S. C. Y.; Cawte, A. D.; Abdolazadeh, A.; Galli, A.; Panchapakesan, S. S. S.; Rueda, D.; Ryckelynck, M.; Unrau, P. J. Fluorogenic RNA Mango Aptamers for Imaging Small Non-Coding RNAs in Mammalian Cells. *Nat. Commun.* **2018**, *9* (1), 656.
- (20) Kim, H.; Jaffrey, S. R. A Fluorogenic RNA-Based Sensor Activated by Metabolite-Induced RNA Dimerization. *Cell Chem. Biol.* **2019**.
- (21) Strack, R. L.; Song, W.; Jaffrey, S. R. Using Spinach-Based Sensors for Fluorescence Imaging of Intracellular Metabolites and Proteins in Living Bacteria. *Nat. Protoc.* **2014**, *9* (1), 146.
- (22) You, M.; Litke, J. L.; Jaffrey, S. R. Imaging Metabolite Dynamics in Living Cells Using a Spinach-Based Riboswitch. *Proc. Natl. Acad. Sci.* **2015**, *112* (21), E2756–E2765.
- (23) Durand, G.; Dausse, E.; Goux, E.; Fiore, E.; Peyrin, E.; Ravelet, C.; Toulmé, J. J. A Combinatorial Approach to the Repertoire of RNA Kissing Motifs; Towards Multiplex Detection by Switching Hairpin Aptamers. *Nucleic Acids Res.* **2016**, *44* (9), 1–10.
- (24) Baugh, C.; Grate, D.; Wilson, C. 2.8 Å Crystal Structure of the Malachite Green Aptamer. *J. Mol. Biol.* **2000**, *301* (1), 117–128.
- (25) Grate, D.; Wilson, C. Laser-Mediated, Site-Specific Inactivation of RNA Transcripts. *Proc. Natl. Acad. Sci.* **1999**, *96* (11), 6131–6136.
- (26) Bouchard, P.; Legault, P. A Remarkably Stable Kissing-Loop Interaction Defines Substrate Recognition by the Neurospora Varkud Satellite Ribozyme. *Rna* **2014**, *20* (9), 1451–1464.
- (27) Paillart, J.-C.; Westhof, E.; Ehresmann, C.; Ehresmann, B.; Marquet, R. Non-Canonical Interactions in a Kissing Loop Complex: The Dimerization Initiation Site of HIV-1 Genomic RNA1. *J. Mol. Biol.* **1997**, *270* (1), 36–49.
- (28) Duongé, F.; Di Primo, C.; Toulmé, J. J. Is a Closing “GA Pair” a Rule for Stable Loop-Loop RNA Complexes? *J. Biol. Chem.* **2000**, *275* (28), 21287–21294.
- (29) Brunel, C.; Marquet, R.; Romby, P.; Ehresmann, C. RNA Loop-Loop Interactions as Dynamic Functional Motifs. *Biochimie* **2002**, *84* (9), 925–944.
- (30) Chen, A. A.; García, A. E. Mechanism of Enhanced Mechanical Stability of a Minimal RNA Kissing Complex Elucidated by Nonequilibrium Molecular Dynamics Simulations. *Proc. Natl. Acad. Sci.* **2012**, *109* (24), E1530–E1539.
- (31) Lebars, I.; Legrand, P.; Aimé, A.; Pinaud, N.; Fribourg, S.; Di Primo, C. Exploring TAR–RNA Aptamer Loop-Loop Interaction by X-Ray Crystallography, UV Spectroscopy and Surface Plasmon Resonance. *Nucleic Acids Res.* **2008**, *36* (22), 7146–7156.
- (32) Beaurain, F.; Di Primo, C.; Toulmé, J. J.; Laguerre, M. Molecular Dynamics Reveals the Stabilizing Role of Loop Closing Residues in Kissing Interactions: Comparison between TAR–TAR\* and TAR–Aptamer. *Nucleic Acids Res.* **2003**, *31* (14), 4275–4284.
- (33) Babendure, J. R.; Adams, S. R.; Tsien, R. Y. Aptamers Switch on Fluorescence of Triphenylmethane Dyes. *J. Am. Chem. Soc.* **2003**, *125* (48), 14716–14717.
- (34) Lee, H.; Han, S.; Kwon, C. S.; Lee, D. Biogenesis and Regulation of the Let-7 miRNAs and Their Functional Implications. *Protein Cell* **2016**, *7* (2), 100–113.
- (35) Huang, J. C.; Babak, T.; Corson, T. W.; Chua, G.; Khan, S.; Gallie, B. L.; Hughes, T. R.; Blencowe, B. J.; Frey, B. J.; Morris, Q. D. Using Expression Profiling Data to Identify Human MicroRNA Targets. *Nat. Methods* **2007**, *4* (12), 1045.
- (36) Hu, J.; Kong, M.; Ye, Y.; Hong, S.; Cheng, L.; Jiang, L. Serum miR-206 and Other Muscle-specific Micro RNAs as Non-invasive Biomarkers for Duchenne Muscular Dystrophy. *J. Neurochem.* **2014**, *129* (5), 877–883.
- (37) Lee, A. J.; Crothers, D. M. The Solution Structure of an RNA Loop-Loop Complex: The ColE1 Inverted Loop Sequence. *Structure* **1998**, *6* (8), 993–1007.
- (38) Weixlbaumer, A.; Werner, A.; Flamm, C.; Westhof, E.; Schroeder, R. Determination of Thermodynamic Parameters for HIV DIS Type Loop-Loop Kissing Complexes. *Nucleic Acids Res.* **2004**, *32* (17), 5126–5133.
- (39) Li, P. T. X.; Tinoco Jr, I. Mechanical Unfolding of Two DIS RNA Kissing Complexes from HIV-1. *J. Mol. Biol.* **2009**, *386* (5), 1343–1356.
- (40) Gago, S.; De la Peña, M.; Flores, R. A Kissing-Loop Interaction in a Hammerhead Viroid RNA Critical for Its in Vitro Folding and in Vivo Viability. *RNA* **2005**, *11* (7), 1073–1083.
- (41) Di Primo, C.; Rudloff, I.; Reigadas, S.; Arzumano, A. A.; Gait, M. J.; Toulmé, J. J. Systematic Screening of LNA/2'-O-Methyl Chimeric Derivatives of a TAR RNA Aptamer. *FEBS Lett.* **2007**, *581* (4), 771–774.
- (42) Autour, A.; Bouhedda, F.; Cubi, R.; Ryckelynck, M. Optimization of Fluorogenic RNA-Based Biosensors Using Droplet-Based Microfluidic Ultrahigh-Throughput Screening. *Methods* **2019**, *161*, 46–53.
- (43) Wang, J.; Yu, J.; Yang, Q.; McDermott, J.; Scott, A.; Vukovich, M.; Lagrois, R.; Gong, Q.; Greenleaf, W.; Eisenstein, M. Multiparameter Particle Display (MPPD): A Quantitative Screening Method for the Discovery of Highly Specific Aptamers. *Angew. Chemie Int. Ed.* **2017**, *56* (3), 744–747.
- (44) Duongé, F.; Toulmé, J.-J. In Vitro Selection Identifies Key Determinants for Loop-Loop Interactions: RNA Aptamers Selective for the TAR RNA Element of HIV-1. *Rna* **1999**, *5* (12), 1605–1614.

Table of Contents



1  
2  
3  
4  
5  
6  
7  
8  
9  
10  
11  
12  
13  
14  
15  
16  
17  
18  
19  
20  
21  
22  
23  
24  
25  
26  
27  
28  
29  
30  
31  
32  
33  
34  
35  
36  
37  
38  
39  
40  
41  
42  
43  
44  
45  
46  
47  
48  
49  
50  
51  
52  
53  
54  
55  
56  
57  
58  
59  
60

## Engineering light-up aptamers for the detection of RNA hairpins through kissing interaction.

Arghya Sett,<sup>a</sup> Lorena Zara,<sup>a, b</sup> Eric Dausse,<sup>a</sup> and Jean-Jacques Toulmé<sup>a, b\*</sup>

<sup>a</sup> ARNA Laboratory, Inserm U1212, CNRS UMR5320, University of Bordeaux, 33076 Bordeaux, France

<sup>b</sup> Novaptech, 146 rue Léo Saignat, 33076 Bordeaux

### Corresponding Author

E-mail: [jean-jacques.toulme@inserm.fr](mailto:jean-jacques.toulme@inserm.fr)

Phone : +33 (0)557 57 10 17

Table S1: Sequences of the parent MG aptamer, pre-miR let7b, K4 and malaswitch (Msw) variants.

Table S2: Sequences of pre-miR 206, K206 and MDMD malaswitch variants.

Figure S1: Predicted secondary structures (Mfold) of full-length pre-miRNAs.

Figure S2: Effect of magnesium on the fluorescence of MDMD-MG-K206 complexes.

Figure S3: Specificity of Msw6.1 and MDMD1 malaswitches.

Figure S4: Test of sensing properties of chemically modified MDMD1.2

| Candidates    | Sequences (5' to 3')  |
|---------------|---|
| MG aptamer:   | GGAUCCCGACUGGC <u>GAGA</u> GCCAGGUAACGAAUGGAUCC   |
| pre-miR let7b | CGGGGUGAGGUAGUAGGUUGUGUGGUUUCAGGGCA <u>GUGAUGU</u><br>UGCCCCUCGGAAGAUAAUAACAACCUACUGCCUCCUG |
| K4            | GCA <u>GUGAUGU</u> UGC  |
| Msw1          | GGAUCCCGA CU <u>ACAUCAC</u> AG GUAACGAAUGGAUCC  |
| Msw2          | GGAUCCCGA CU <u>CAUCAC</u> AG GUAACGAAUGGAUCC   |
| Msw3          | GGAUCCCGA CU <u>ACAUCA</u> AG GUAACGAAUGGAUCC   |
| Msw4          | GGAUCCCGA CU <u>UCAUCA</u> AG GUAACGAAUGGAUCC   |
| Msw5          | GGAUCCCGA CU <u>ACAUCU</u> AG GUAACGAAUGGAUCC   |
| Msw6          | GGAUCCCGA CU <u>ACAUCAG</u> AG GUAACGAAUGGAUCC  |
| Msw1.1        | GGAUCCCGA CU <u>GACAUCAC</u> AG GUAACGAAUGGAUCC   |
| Msw1.2        | GGAUCCCGA CU <u>ACAUCAC</u> CG GUAACGAAUGGAUCC  |
| Msw1.3        | GGAUCCCGA UU <u>ACAUCAC</u> AA GUAACGAAUGGAUCC  |
| Msw1.4        | GGAUCCCGA AU <u>ACAUCAC</u> AG GUAACGAAUGGAUCC  |
| Msw1.5        | GGAUCCCGA CG <u>ACAUCAC</u> AG GUAACGAAUGGAUCC  |
| Msw4.1        | GGAUCCCGA CU <u>GCAUCAU</u> AG GUAACGAAUGGAUCC  |
| Msw4.2        | GGAUCCCGA CC <u>CAUCAU</u> GG GUAACGAAUGGAUCC   |
| Msw5.1        | GGAUCCCGA CU <u>GACAUCU</u> AG GUAACGAAUGGAUCC  |
| Msw6.1        | GGAUCCCGA CU <u>GACAUCAG</u> AG GUAACGAAUGGAUCC   |
| Msw6.2        | GGAUCCCGA CG <u>ACAUCAG</u> AG GUAACGAAUGGAUCC  |

**Table S1:** Sequences of the parent MG aptamer, pre-miR let7b, K4 and malaswitch (Msw) variants. Predicted apical loops are underlined.

| Candidates  | Sequences (5' to 3')   |
|-------------|--|
| Pre-miR 206 | CCAGGCCACAUGCUCUUUUUAUCCUCAUAG <u>AUAUCUCAGCA</u><br>CUAUGGAAUGUAAGGAAGUGUGUGUUUUUGG |
| K206        | CAUAG <u>AUAUCUCAGCA</u> CUAUG   |
| MDMD1       | GGAUCCCGA CU <u>AGCUGAGAUAG</u> AG GUAACG AAUGGAUCC                                  |
| MDMD2       | GGAUCCCGA CU <u>AGCUGAGAUAG</u> AG GUAACG AAUGGAUCC                                  |
| MDMD3       | GGAUCCCGA CU <u>ACGUGAGAUAG</u> AG GUAACG AAUGGAUCC                                  |
| MDMD4       | GGAUCCCGA CU <u>ACGAGAGAUAG</u> AG GUAACG AAUGGAUCC                                  |
| MDMD5       | GGAUCCCGA CU <u>AGCUGAGAAUA</u> AG GUAACG AAUGGAUCC                                  |
| MDMD6       | GGAUCCCGA CU <u>AGCUGAGAAUA</u> AG GUAACG AAUGGAUCC                                  |
| MDMD7       | GGAUCCCGA CU <u>AGCUGAGUAUA</u> AG GUAACG AAUGGAUCC                                  |
| MDMD8       | GGAUCCCGA CU <u>ACGUGAGAAUA</u> AG GUAACG AAUGGAUCC                                  |
| MDMD1.1     | <b>GGAUCCCGA CU <u>AGCUGAGAUAG</u> AG GUAACG AAUGGAUCC</b>                           |
| MDMD1.2     | <b>GGAUCCCGA CU <u>AGCUGAGAUAG</u> AG GUAACG AAUGGAUCC</b>                           |

**Table S2:** Sequences of pre-miR 206, K206 and MDMD malaswitch variants. Predicted apical loops are underlined. For MDMD 1.1 and 1.2 bold letters indicate 2'-O-methyl nucleotides.

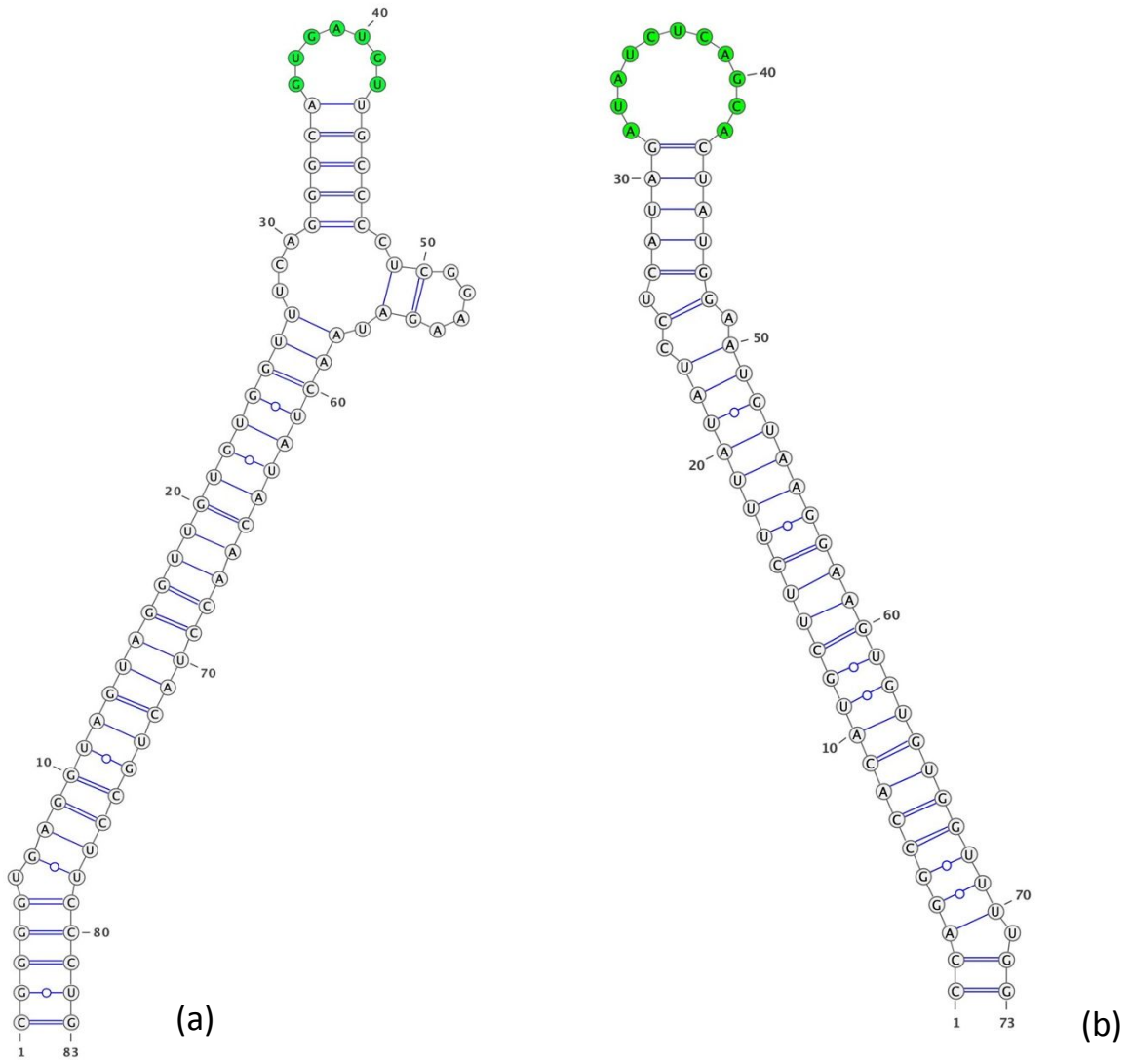


**Figure S1:** Predicted secondary structures (Mfold) of full-length pre-miRNAs (a) pre-miR-let7b (b) pre-miR206. Nucleotides of the apical loops are indicated in green.

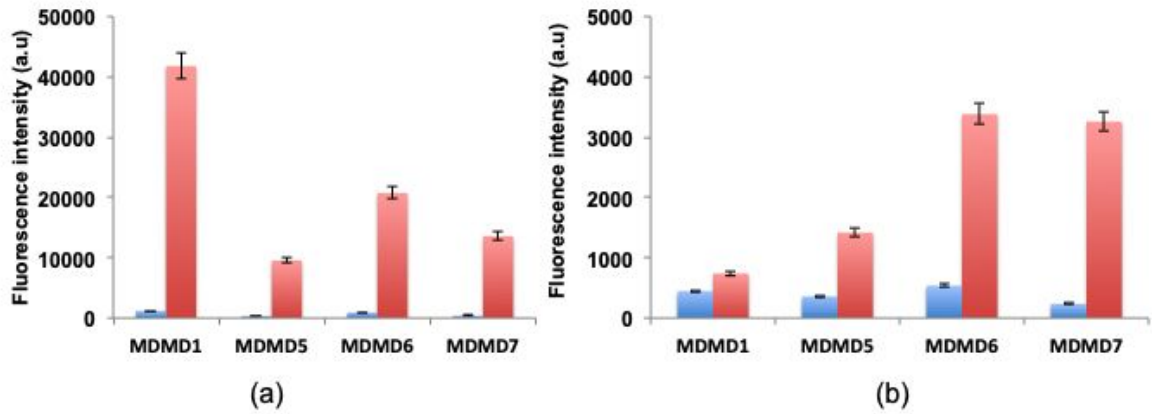


**Figure S2:** Effect of magnesium on the fluorescence of MDMD-MG-K206 complexes. (a) 10mM magnesium, (b) 50mM magnesium. MDMD, MG and K206 concentrations were adjusted to 0.1  $\mu$ M, 2  $\mu$ M and 2  $\mu$ M, respectively. Blue and red bars correspond to measurements in SE buffer without and with aptakiss K206, respectively. ( $\lambda_{Exc}$  = 610 nm,  $\lambda_{Em}$  = 650 nm). Measurements were performed in triplicate and standard error was calculated accordingly.

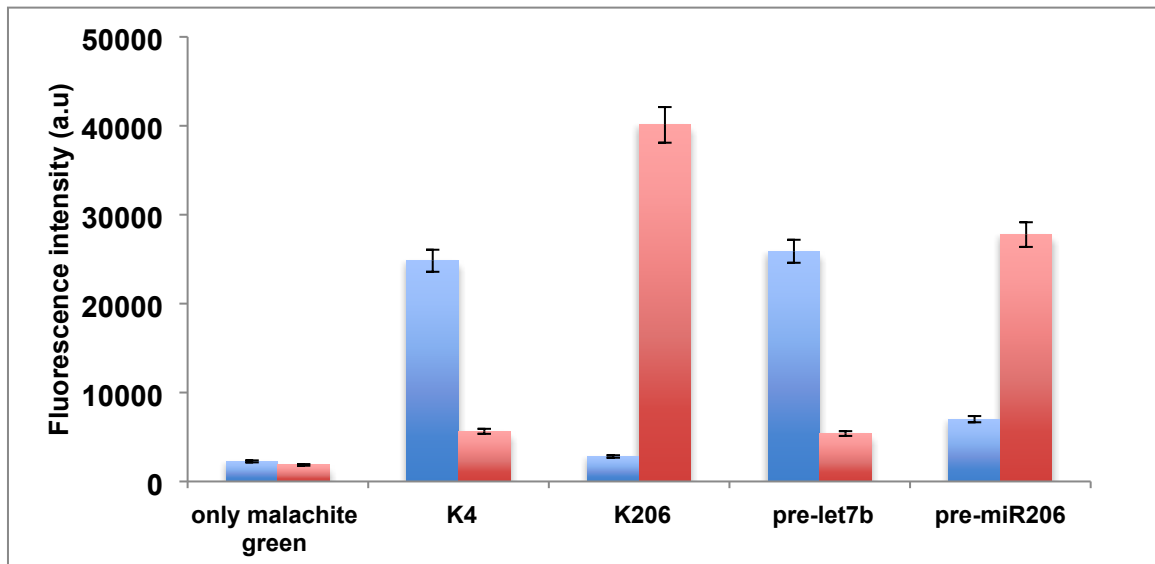


**Figure S3:** Specificity of Msw6.1 and MDMD1 malaswitches. 0.1  $\mu$ M of both malaswitches were treated with 2  $\mu$ M of hairpin loops and miRNA precursors. Blue and red bars correspond to Msw6.1 and MDMD1 malaswitches, respectively. All the measurements were performed in triplicate and standard error was calculated accordingly.

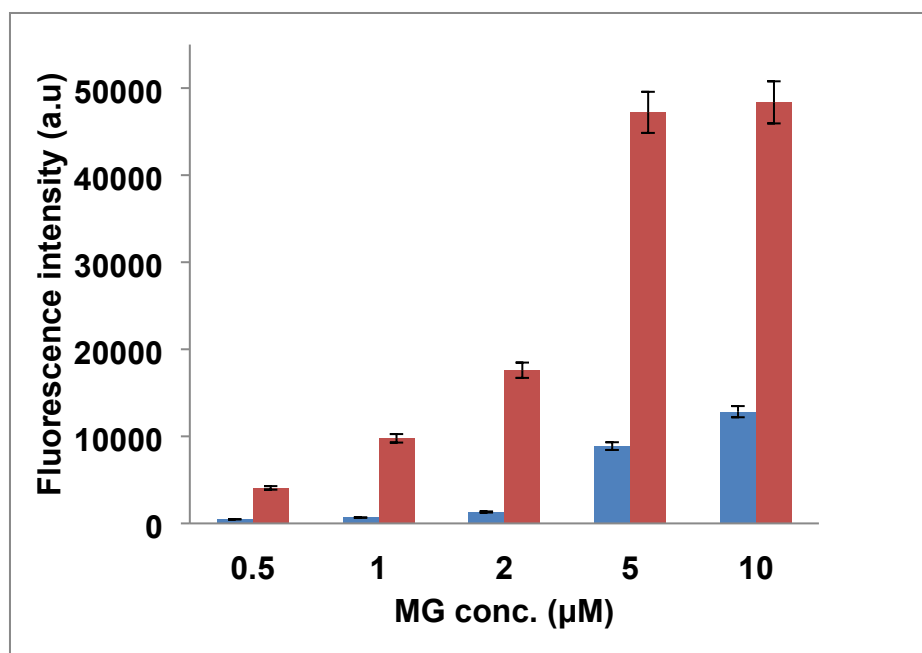


**Figure S4:** Test of sensing properties of chemically modified MDMD1.2 (see Table S2 for modifications). Fluorimetric titration of MDMD1.2 – pre-miR206 complexes by malachite green (MG) in SE buffer. MDMD1.2 and pre-miR206 were adjusted at 0.1 and 2  $\mu\text{M}$ , respectively. Measurements were performed in triplicate. ( $\lambda_{\text{Exc}} = 610 \text{ nm}$ ,  $\lambda_{\text{Em}} = 650 \text{ nm}$ ) Blue and red bars correspond to the signal obtained in absence and presence of pre-miR206, respectively.

## 2.2 Conclusions

Herein, it has been demonstrated that light up aptasensors could be integrated in a multiplex assay platform to detect the pre-miRNAs in biological environment.

We observe that the flexibility of the aptaswitch (given by the composition and length of the connector) affects the stability of the complex in the presence of the target, and therefore the efficiency of the light-up.

The engineered apical loop is shown to be specific for each aptakiss with similar results for the corresponding full-length miRNA precursors.

The introduction of the kissing complex could enhance the efficiency of the aptasensor as compared to the original aptamer (especially for the Msw-K206 where the increase in fluorescence intensity is 40-fold higher relative to the native aptamer). Likewise, both kissing-complex systems show high specificity and affinity with a  $K_d$  for the dye in the micromolar range. Despite this, the aptasensor displays low sensitivity for the detection of species in biological media. Nonetheless, the system can be applied to various types of aptamers for the application in biological specimens.

In conclusion, this label free system made it possible to detect the presence of the target in free solution using unlabelled aptaswitch and aptakiss. In addition, it can be applied to other pairs of aptaswitch-aptakiss for creating new systems able to detect any RNA hairpins.

### 3. « A malachite green light-up aptasensor for the detection of theophylline »

#### 3.1 Strategy

Herein, we present a new aptasensor based on the light-up kissing complex strategy, able to detect theophylline. We designed a fluorescent double-switch aptasensor constituted of two new aptaswitches: one based on malachite green aptamer (called Malaswitch as above mentioned) and the other one based on the theophylline aptamer (called Theoswitch – in short Thsw).

Based on the rationale of the first light-up kissing complex presented in part 3.2,<sup>159</sup> we generated a new malaswitch-aptakiss kissing complex. Initially, the apical loop of the malachite green aptamer was re-engineered with 4 different stem-loop combinations likely to form a loop-loop interaction with a small hairpin K3 (aptakiss). Among all candidates (called respectively K3', G12A20, C12 and G12), the malaswitch G12 was shown to form specific interactions with K3, detected with a fluorescence enhancement. Subsequently, we rationally engineered a specific theoswitch able to detect the small molecule theophylline forming the kissing complex with the malaswitch G12.

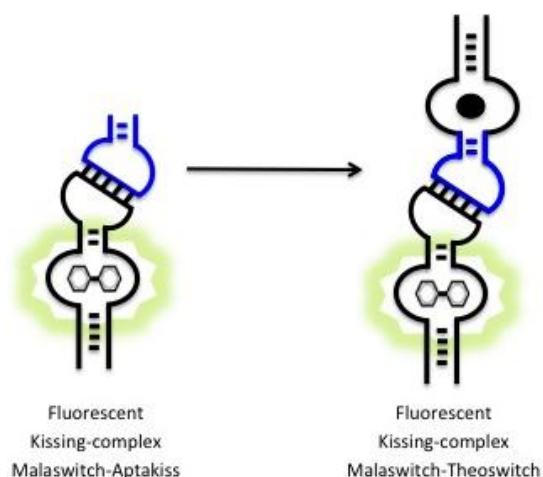


Fig. 23. Representation of the fluorescent double-switch complex design. Left: Malaswitch forms a loop-loop interaction with K3 aptakiss (blue) and binds the MG allowing the increase of the fluorescent signal. Right: K3 kissing motif is introduced in the apical part of theophylline aptamer in order to recognize the malaswitch. Theoswitch and malaswitch form a stable kissing-complex in presence of MG and theophylline simultaneously, leading a fluorescence emission.

The theophylline-aptamer was isolated by Janison and coworkers in 1994 since then its structure has been largely described and used in several applications.<sup>27,40</sup> Similarly to the malachite-green aptamer, the anti-theophylline aptamer presents an apical loop structure suitable to be converted in aptaswitch.<sup>160</sup>

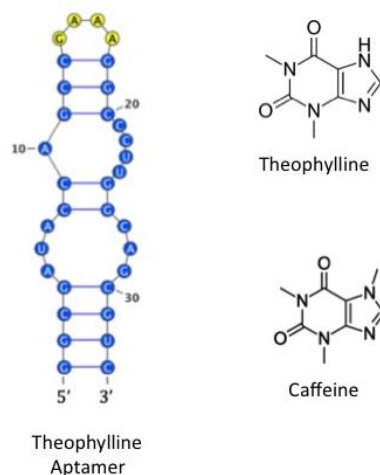


Fig. 24. Secondary structure of theophylline-aptamer and chemical structure of theophylline and caffeine.

Taking advantage of this, the hairpin portion of the anti-theophylline RNA aptamer (in yellow on the figure 24) was functionalized with a stem-loop sequence able to hybridize to the top apical part of new malaswitch G12 and form an RNA-RNA kissing-loop complex. This would ensure their conformational rearrangement only in presence of both malachite green and theophylline ligands. The sensitivity of the kissing-complex was detected by the malachite green fluorescence resulting from binding. Twenty theoswitch variants have been designed and tested with malaswitch G12 in the presence of both theophylline and malachite green. Besides, in order to prove the sensitivity of this complex, we performed specificity studies with the caffeine, which has a chemical structure very similar to that of theophylline (Fig. 24).

1 **Title: A malachite green light-up aptasensor for the detection of**  
2 **theophylline**

3  
4 Arghya Sett,<sup>a#</sup> Lorena Zara,<sup>a, b#</sup> Eric Dausse,<sup>a</sup> and Jean-Jacques Toulmé<sup>a,c\*</sup>

5 <sup>a</sup> Univ Bordeaux, CNRS, Inserm, ARNA, UMR5320, U1212, F-33000 Bordeaux, France

6 <sup>b</sup> Present address: Novaptech, 33600, Pessac, France

7 <sup>c</sup> Novaptech, 33600, Pessac, France

8 # These authors contributed equally to the work

9

10 *\*Corresponding author* [jean-jacques.toulme@inserm.fr](mailto:jean-jacques.toulme@inserm.fr)

11

12 **Abstract**

13 Biosensors are of interest for the quantitative detection of small molecules (metabolites,  
14 drugs and contaminants for instance). To this end fluorescence is a widely used technique  
15 that is easily associated to aptamers. Light-up aptamers constitute a particular class of  
16 oligonucleotides that, specifically induce fluorescence emission when binding to cognate  
17 fluorogenic ligands such as malachite green (MG). We engineered a dual aptasensor for  
18 theophylline (Th) based on the combination of switching hairpin aptamers specific for MG on  
19 the one hand and for Th on the other hand, hence their names: malaswitch (Msw) and  
20 theoswitch (Thsw). The two aptaswitches form a loop-loop or kissing Msw-Thsw complex  
21 only in the simultaneous presence of Th and MG, subsequently generating a fluorescent  
22 signal. The combination of the best Msw and Thsw variants results in a 20-fold fluorescence  
23 enhancement at saturating theophylline concentration. This aptasensor is specific: no signal  
24 is observed with caffeine that differs from theophylline by only one methyl group. Kissing  
25 aptaswitches derived from light-up aptamers constitute a novel sensing device.

26

27 **Keywords:** aptamer, malachite green, fluorescence, RNA hairpin, kissing complex, biosensor

28

29 **Introduction:**

30 Since the onset of aptamers, scientists are exploring the application of aptamers as sensor  
31 modules for diagnostic and various analytical applications (Ellington and Szostak, 1990;  
32 Hayat et al., 2014; Pfeiffer and Mayer, 2016; Tombelli et al., 2007; Tuerk and Gold, 1990).  
33 Since last decade, RNA aptamers were developed which induce fluorescence enhancement  
34 after binding to their cognate fluorogen molecule (Bouhedda et al., 2018; Dolgosheina et al.,  
35 2014; Grate and Wilson, 1999; Neubacher and Hennig, 2019; Paige et al., 2012, 2011).  
36 Such “light up” aptamers are promising tools for monitoring cellular functions and for

37 tracking metabolites in cultured cells (Autour et al., 2018; Bouhedda et al., 2020; Guet et al.,  
38 2015; Ouellet, 2016; Strack et al., 2014; Zhang et al., 2015). Light-up aptamers actually  
39 constitute an alternative to fluorescent reporter proteins (GFP, YFP etc.) of special interest  
40 for detecting RNA species (Paige et al., 2012; Sett et al., 2020).

41

42 Generally, light up RNA aptamers for organic fluorphores like DFHBI, malachite green,  
43 thiazole orange possess some structural flexibility. Structural studies of these RNA  
44 aptamers showed that the dye generally interacts with parallel/antiparallel G-quadruplexes  
45 although the structure of flanking region also influences the fluorescence emission  
46 (Neubacher and Hennig, 2019; Shelke et al., 2018; Umar et al., 2019). Jaffrey and  
47 coworkers developed a sensor-based riboswitch by integrating SAM, GTP or ADP aptamers  
48 in the 'stem' sequence of the Spinach light-up aptamer (Paige et al., 2012).

49

50 Malachite green (MG) is an organic tri-phenyl methane dye with a quantum yield of  $7.9 \times 10^{-5}$   
51 *i.e.* almost non-fluorescent when alone in aqueous solution (Baugh et al., 2000). An RNA  
52 aptamer for malachite green was discovered that induces more than 2,000 fold fluorescence  
53 increase upon binding to the dye (Babendure et al., 2003; Baugh et al., 2000; Grate and  
54 Wilson, 1999). In contrast to DFHBI or thiazole orange light-up aptamers, the malachite  
55 green aptamer folds into an imperfect hairpin. Structural insights of malachite green  
56 aptamer identified the nucleotides and the MG groups involved in the interaction between  
57 the dye and the oligonucleotide (Baugh et al., 2000; Wang et al., 2016).

58

59 We took advantage of this hairpin structure for engineering a new type of aptasensor.  
60 Indeed, we previously demonstrated that the formation of loop-loop RNA complexes (so-  
61 called "kissing" complexes) can be exploited for sensing different ligands (Chovelon et al.,  
62 2016; Durand et al., 2014, 2016; Sett et al., 2020; Takeuchi et al., 2016). We recently  
63 converted the malachite green RNA aptamer into a switching aptamer (we called it an  
64 aptaswitch). In response to kissing interactions the aptamer switches between an open  
65 (unfolded) and a closed (folded) structure. Only the folded one binds the dye, thus allowing  
66 the specific detection of hairpin precursors of microRNAs by fluorescence (James et al.,  
67 2017; Sett et al., 2020).

68

69 In the present study we used a similar strategy for engineering malachite green-based  
70 fluorescent sensors for the detection of a small molecule: theophylline. To this end two  
71 modules specific for malachite green that will generate the signal on the one hand and for

72 the target ligand theophylline on the other hand should be designed, that will interact  
73 through kissing interactions depending on the simultaneous presence of the two cognate  
74 ligands.

75

76 The theophylline RNA aptamer, first isolated by Jenison and co-workers in 1994, was so  
77 specific toward its target that it could differentiate the chemical analogue caffeine which is a  
78 methyl derivative of theophylline (Jenison et al., 1994). Since then, this RNA hairpin  
79 aptamer was widely used in cellular engineering, synthetic biology and other diagnostic  
80 applications (Pu et al., 2020; Wrist et al., 2020). We converted the malachite green and the  
81 theophylline hairpin aptamers into aptaswitches (malaswitch and theoswitch, respectively)  
82 by modifying the apical part of the parent oligomers that is not involved in the recognition of  
83 their targets. First a kissing prone sequence was substituted to their apical loop. Second the  
84 double-stranded connector between this loop and the target-binding site (a central loop)  
85 was shortened in such a way that the modified aptamers do no longer bind their target. The  
86 affinity for the dye or for theophylline is restored by loop-loop interaction, likely through  
87 stacking interaction between the loop-loop nucleic acid base pairs and the aromatic moiety  
88 of the target molecules. We report here the engineering of such a kissing biosensor that  
89 quantitatively and specifically translates the recognition of theophylline into malachite green  
90 fluorescence.

91

## 92 **Materials and Methods:**

### 93 ***Oligonucleotides and chemicals:***

94 Synthetic oligodeoxynucleotides purified by polyacrylamide gel electrophoresis were  
95 purchased from Eurogentec. The concentration of oligonucleotide solutions was measured  
96 on a Nanodrop spectrophotometer. Theophylline, caffeine, malachite green and other  
97 chemicals (HEPES buffer, sodium acetate, potassium acetate, magnesium acetate) were  
98 purchased from Sigma-Aldrich.

### 99 ***In vitro transcription:***

100 RNA aptaswitch candidates were in-vitro transcribed by T7-Flashscribe™ transcription kit  
101 (Cellscript). In a standard 20 µl reaction volume, 1 µg of DNA templates containing the  
102 complementary sequence of the T7 promoter (5' TAATACGACTCACTATAG 3 ') at the 3'  
103 end of the template were transcribed with ATP, UTP, GTP and CTP (100 mM of each), 100  
104 mM DTT (2 µl), Type I RNase Inhibitor (0.5 µl ), T7 reaction buffer (10x) and 2 U of T7 RNA  
105 polymerase. The reaction mixture was kept at 37 °C for 2 hours followed by DNase (1U)

106 treatment for 20 minutes. Gel purified RNA transcripts were verified on 20% denaturing  
107 polyacrylamide gel electrophoresis and stored at -20°C in water for further use.

#### 108 ***Fluorescence measurements:***

109 Malaswitch variants were heated for 2 minutes at 65°C and then kept on ice for 5 minutes.  
110 SE 5x buffer was added to the mixture and incubated at room temperature for 15 minutes.  
111 (SE x1 buffer contains 20 mM HEPES pH 7.4, 20 mM sodium acetate, 140 mM potassium  
112 acetate and 3 mM magnesium acetate). Deionized water was added to adjust the required  
113 concentration of the aptaswitch candidates. Following the folding of malaswitches,  
114 malachite green was added. In parallel, RNA hairpin K3 and theoswitch variants were also  
115 folded according to the protocol described above. Malaswitch-K3 or malaswitch-theoswitch  
116 mixtures were incubated for 2 hours at 4°C in the dark and the fluorescence measurements  
117 of 50 µl sample were performed in triplicate. Background signal was subtracted to  
118 fluorescence measurements.

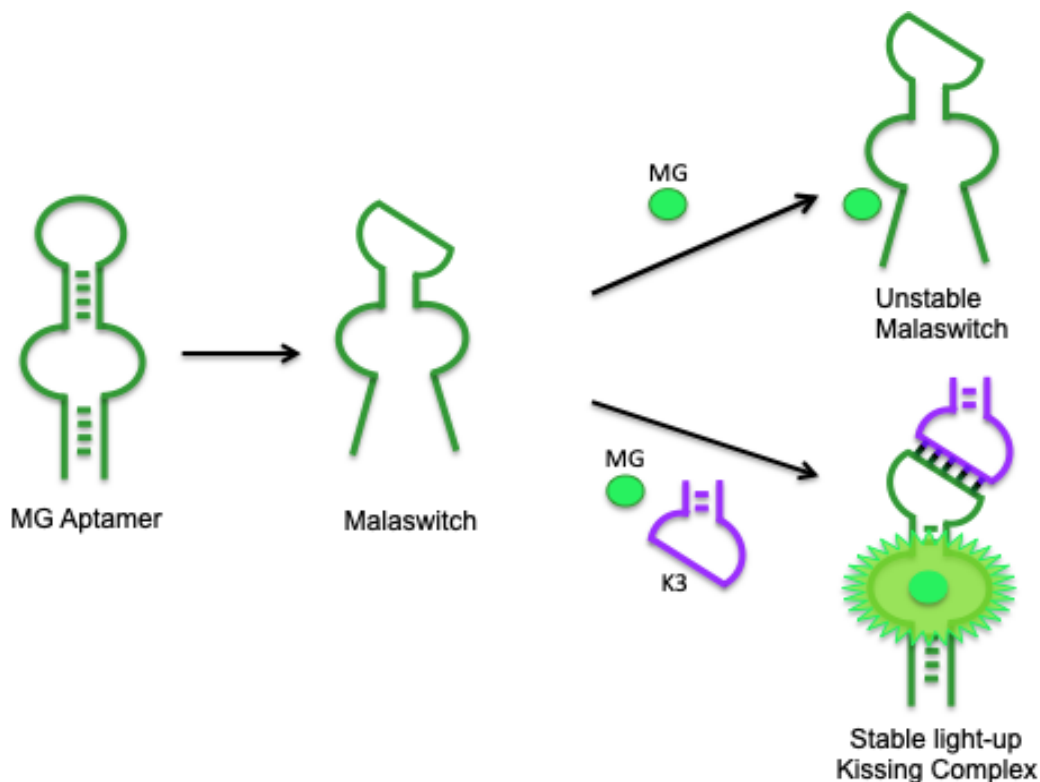
119 The properties of theoswitch variants were tested in the presence or in the absence of  
120 theophylline. 4 µM of theoswitch variants in SE buffer were folded with or without 8 mM of  
121 theophylline and 0.1 µM malaswitch was folded with 1 µM of malachite green. All  
122 fluorescence measurements were performed at 650 nm in triplicate on a Tecan Infinite  
123 M100 spectrofluorometer, following excitation at 610 nm.

124

#### 125 **Results and Discussion:**

##### 126 *Rationale engineering of an aptaswitch for malachite green (malaswitch):*

127 We converted the malachite green specific RNA aptamer into a structure-switching  
128 aptaswitch (we name it 'malaswitch') (Grate and Wilson, 1999). We used the same rationale  
129 as the one previously used for generating malaswitches able to sense precursors of  
130 microRNAs (Scheme 1) (Sett et al., 2020). The original apical loop of the malachite green  
131 aptamer that is not involved in the recognition of the dye was substituted by a sequence  
132 prone to loop-loop interaction with the small RNA hairpin K3: 5'CGAGCCUGGGAGCUCG3'  
133 (Figure 1).



134

135 *Scheme 1: The apical part of the MG aptamer was changed in such a way to promote the*  
 136 *formation of a loop-loop complex with its kissing partner K3. The stable light-up kissing*  
 137 *complex formation occurs only in the simultaneous presence of K3 and malachite green.*

138

139 We investigated the binding behaviour of 4 variants in which the motif 5'-XCCCAG-3'  
 140 (X=C,G,U), complementary to part of the K3 loop, was introduced. In addition we  
 141 destabilized the top part of the aptamer in such a way that it cannot any longer bind the  
 142 malachite green alone (Durand et al., 2016). To this end, the connector between the apical  
 143 loop and the internal loop corresponding to the dye binding site was restricted to 2 base  
 144 pairs, (UA and CG). The 4 variants MswK3', MswG12A20, MswC12 and MswG12 are  
 145 shown on the Figure S1 and their sequence is given in Table S1.

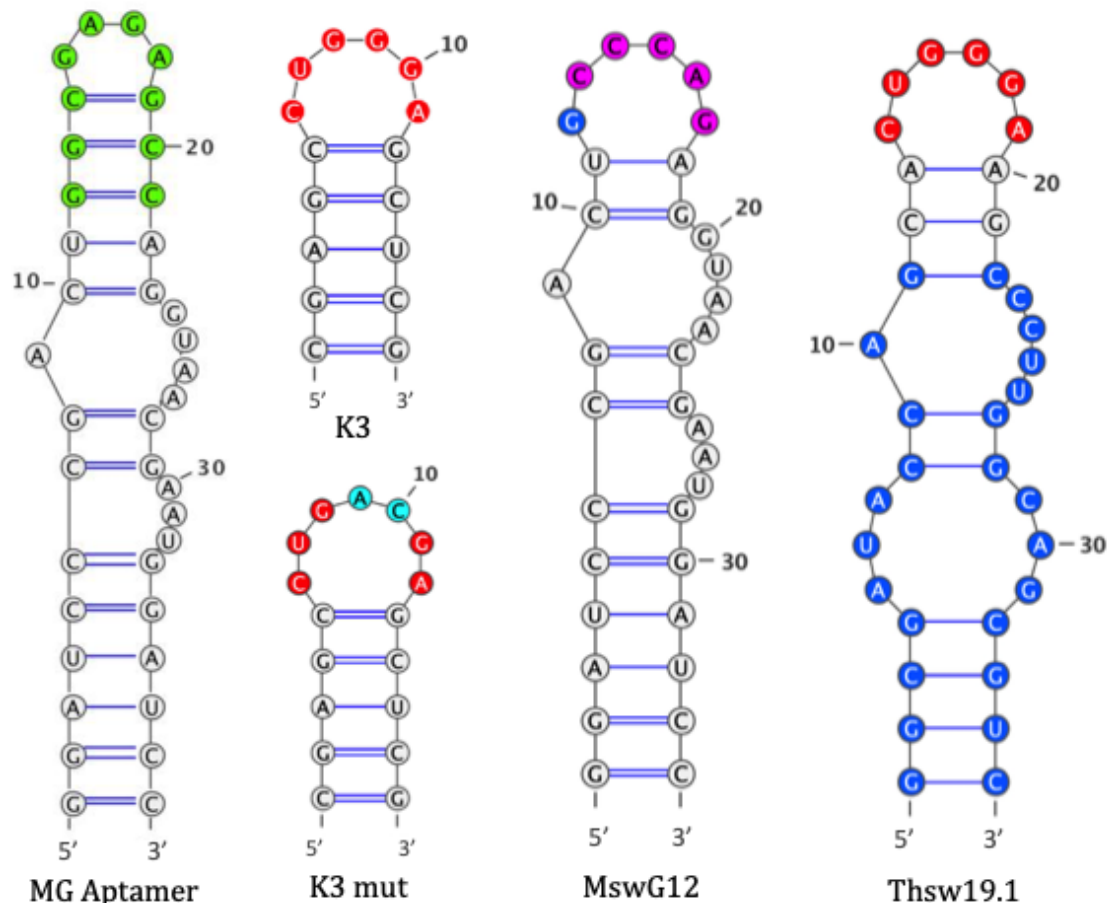
146

147 Compared to the parent aptamers all 4 variants induced a very poor fluorescence emission  
 148 of the dye (Figure 2) likely due to the destabilisation of the top part of the aptamer that does  
 149 not provide a sufficient contribution to the formation of the dye-RNA complex. This is indeed  
 150 what we expected from our design.

151

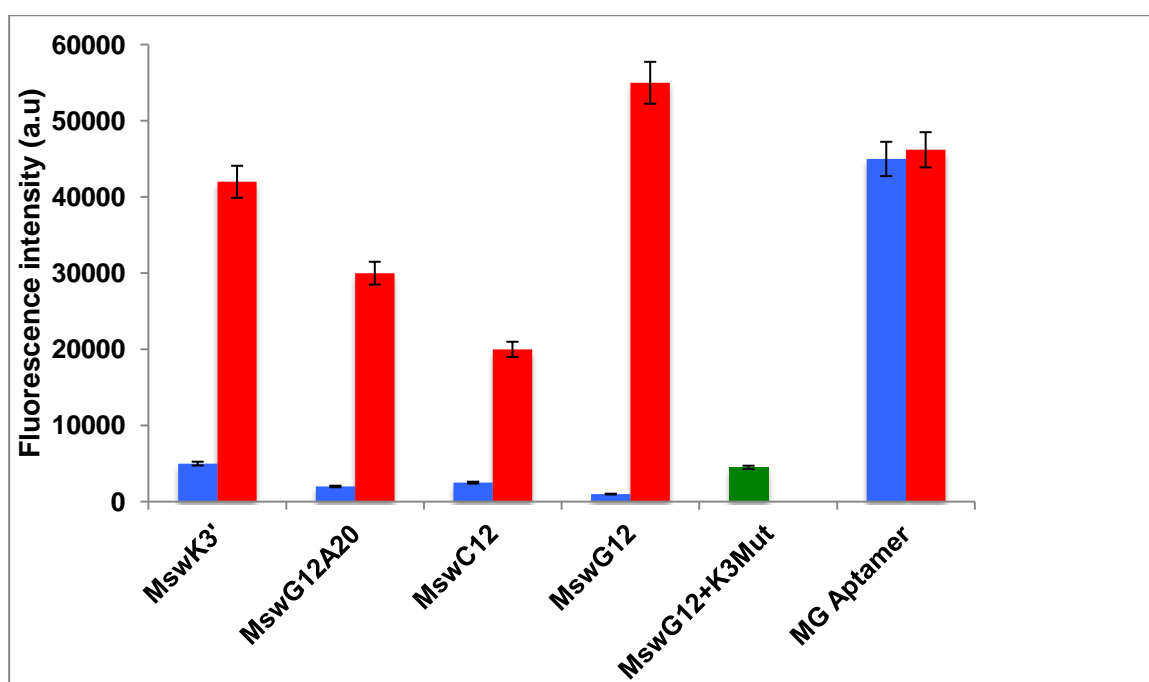
152 We then evaluated the effect of K3 on the malachite green-aptamer interaction. All 4  
 153 variants responded to the simultaneous addition of the dye and of K3 by a fluorescence

154



156 *Figure 1. Predicted secondary structure of the malachite green aptamer (Baugh et al., 2000)*  
 157 *and sequences of the malaswitch variant MswG12 and theoswitch Thsw19.1. The hairpins*  
 158 *K3 and K3mut are also shown. The apical part of the MG aptamer that was deleted for*  
 159 *generating the malaswitch variants is shown in green. The complementary bases*  
 160 *susceptible to generate a loop-loop helix are highlighted in pink for MswG12 and in red (K3*  
 161 *and Thsw19.1). The mutations are indicated in cyan for K3 mut. In Thsw19.1 the*  
 162 *nucleotides present in the parent theophylline aptamer are shown in blue.*

163  
 164 enhancement. For a mixture of 0.1  $\mu\text{M}$  of the different malaswitch variants with 2  $\mu\text{M}$  of  
 165 malachite green the fluorescence was increased 12, 18 and 10 fold for MswK3',  
 166 MswG12A20 and MswC12, respectively, upon addition of 2  $\mu\text{M}$  of K3 (Figure 2). The largest  
 167 enhancement (50 fold) was observed with MswG12 that displayed under these conditions a  
 168 fluorescence signal even higher than the parent aptamer (Figure 2). This is very likely  
 169 related to the stabilisation of the aptamer-malachite green complex by the kissing interaction.  
 170 Indeed no such an increase was observed when K3Mut was substituted to K3 in the ternary  
 171 mixture (Figure 2). The loop sequence of K3 mut 5'CUGACGA (Figure 1) did not allow the  
 172 formation of a loop-loop helix with MswG12 due to the presence of two point mutations.



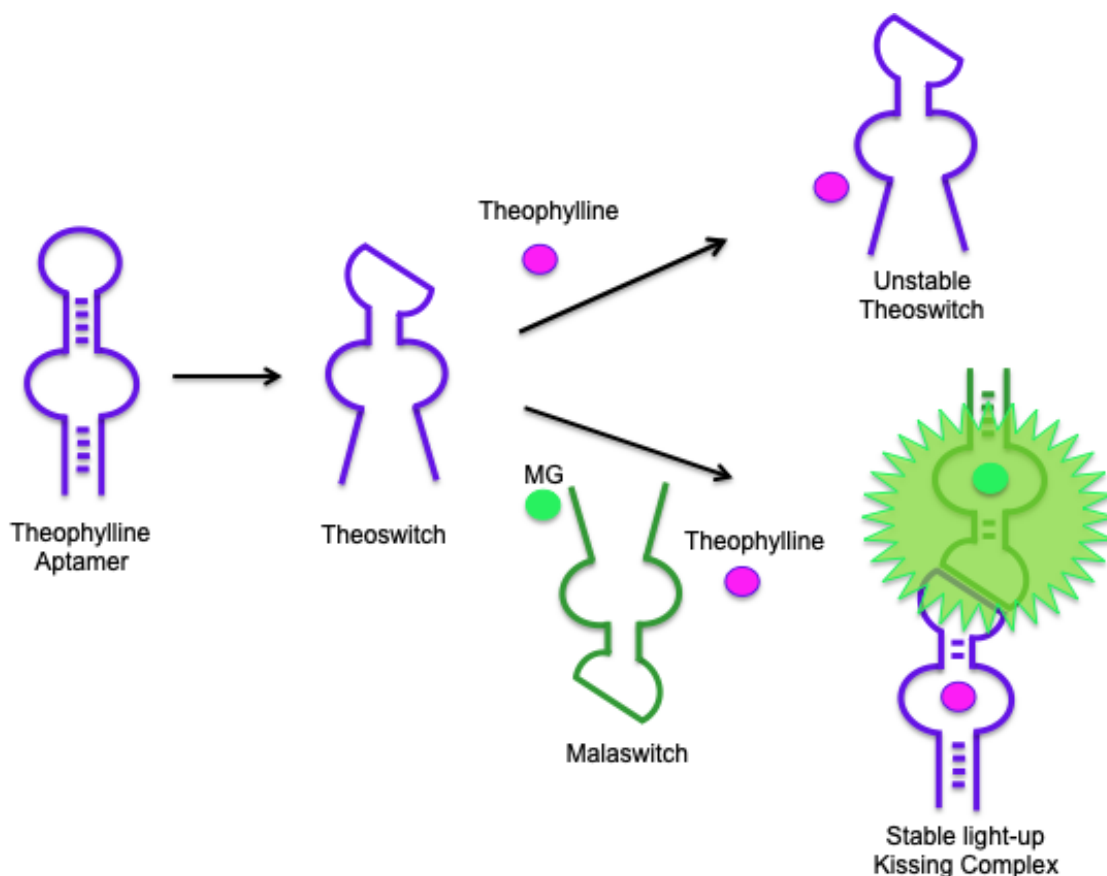
174

175 *Figure 2. Fluorescence of malachite green with the MG aptamer or with malaswitch variants in*  
 176 *the absence (blue bars) or in the presence of either K3 (red bars) or K3 mut (green bar).*  
 177 *Measurements ( $\lambda_{Exc} = 610 \text{ nm}$ ,  $\lambda_{Em} = 650 \text{ nm}$ ) were performed in triplicate at room temperature in*  
 178 *the SE buffer containing 3 mM magnesium.*

179

### 180 Engineering an aptaswitch for theophylline (theoswitch)

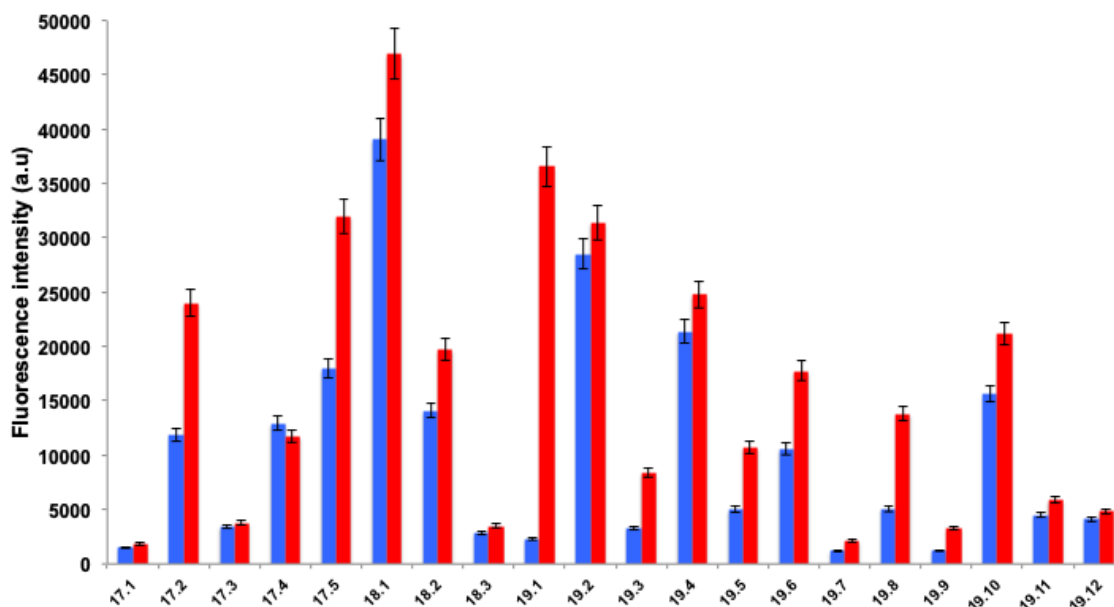
181 In order to sense the presence of theophylline through MG signalling we substituted a  
 182 specific aptaswitch to the hairpin K3. The idea was to convert the theophylline aptamer  
 183 (Zimmermann et al., 2000, 1997) into a theoswitch *i.e.* an aptaswitch responding to  
 184 theophylline. The parent theophylline RNA aptamer that is an imperfect hairpin should be  
 185 engineered in such a way that it forms a kissing interaction with the malaswitch described  
 186 above in the presence, and only in the presence of both theophylline and malachite green.  
 187 The kissing association of the theoswitch and of the malaswitch in a medium containing  
 188 malachite green will result in a theophylline-dependent fluorescence emission (Scheme 2).  
 189 To this end the top part of the theophylline aptamer was modified: the K3 kissing motif  
 190 5'CUGGGA3' complementary to the MswG12 loop was introduced into the apical loop and  
 191 the connector domain between the loop and the theophylline binding site was destabilized.



192

193 *Scheme 2. Design of the malaswitch-theoswitch fluorescent sensor.*

194



195

196 *Figure 3. Fluorescence of malachite green for different MswG12-theoswitch variants.*  
 197 *Fluorescence emission ( $\lambda_{Exc} = 610 \text{ nm}$ ,  $\lambda_{Em} = 650 \text{ nm}$ ) of  $1 \mu\text{M}$  MG in the absence (blue bars) or*  
 198 *in the presence (red bars) of theophylline (8 mM). Measurements were performed in triplicate at*  
 199 *room temperature in SE buffer containing 3 mM magnesium.*

200 We rationally engineered 20 theoswitch (Thsw) variants with various purine/ pyrimidine  
 201 combinations in the apical loop and different lengths of the connector domain (Table S2 and

202 Figure S2). The sensing response of all Thsw variants was carried out by fluorescence  
203 assay at a single malachite green concentration (1 $\mu$ M) in the absence and in the presence  
204 of the target molecule theophylline at saturating concentration (8 mM). Under these  
205 conditions theoswitches 17.1, 17.3, 18.3, 19.7, 19.9, 19.11, and 19.12 did not show any  
206 significant fluorescence emission meaning that either the theophylline binding site was  
207 affected by the modification of the aptamer or that the kissing interaction could not stabilize  
208 the complex (Figure 3). Some Thsw candidates (18.1, 19.2, 19.4 and 19.10) exhibited a  
209 strong fluorescence signal in the presence as well as in the absence of theophylline (Figure  
210 3) indicating that the formation of the Thsw-Msw complex was sufficient to promote the  
211 binding of the dye even without theophylline leading to a non-specific signal. Therefore,  
212 these variants cannot be exploited for biosensing. Other Thsw variants (17.2, 17.5, 18.2,  
213 19.1, 19.3, 19.5, 19.6, 19.8) showed a theophylline-dependent fluorescence enhancement  
214 that reached almost 20 fold for Thsw19.1.

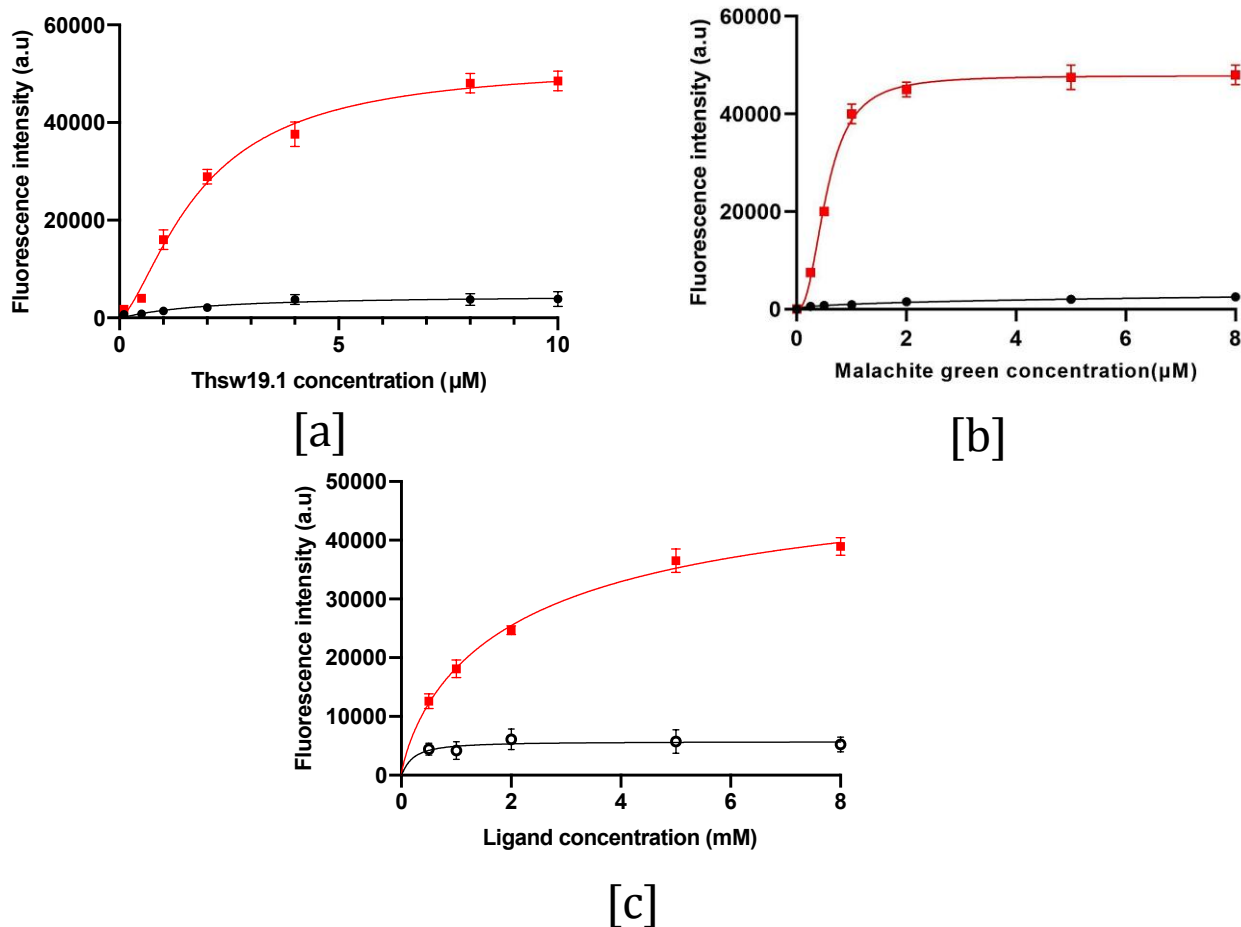
215

216 The Thsw connector between the apical loop and the target molecule binding site and the  
217 base-base combination closing the apical loop plays a critical role in the formation of the  
218 kissing complex as previously demonstrated. (Boiziau et al. 1999; Ducongé and Toulmé  
219 1999; Ducongé et al. 2000). The Thsw19.1 connector consists of 2 base pairs (GC, CG)  
220 and shows a purine-purine (A-A) combination for closing the loop (Figure S2). Purine-purine  
221 combinations were previously demonstrated to favour kissing complex formation, likely due  
222 to a larger aromatic area for stacking interaction and an extended distance between  
223 phosphate residues of the two sugar-phosphate chains, thus weakening the electrostatic  
224 repulsion (Cao and Chen, 2011; Ducongé et al., 2000; Takeuchi et al., 2016). However this  
225 is not a sufficient condition for ensuring specific sensing as Thsw18.1, 18.3, 19.10 and  
226 19.12 also display a purine-purine combination but exhibit poor or non-specific fluorescence  
227 signal. In contrast to Thsw19.1 all these variants have only one base pair in the connector.

228

### 229 Characterization of the malaswitch-theoswitch sensor for theophylline

230 We characterized the binding properties of Thsw19.1 that is the best theophylline  
231 sensing variant with respect to signal intensity. Under the conditions used for the  
232 saturation assay (0.1  $\mu$ M MswG12, 1  $\mu$ M malachite green and 8 mM theophylline), the  
233 plateau was reached in the low micromolar range of Thsw19.1 (Figure 4a). As expected  
234 only a very weak fluorescence signal was observed on the 0-10  $\mu$ M concentration range  
235 in the absence of theophylline indicating the simultaneous requirement of both Msw and  
236 Thsw ligands for complex formation.



237

238 *Figure 4. Fluorescence saturation assays. a) Titration of a MswG12 (0.1 μM)- MG (1 μM) mixture by*  
 239 *the theoswitch 19.1 in the absence (black line) and presence (red line) of 8 mM theophylline. b) MG*  
 240 *saturation assay: titration of a Thsw19.1 (0.1 μM)-MswG12 (4 μM) complex by malachite green in*  
 241 *the presence (red line) and absence (black line) of theophylline. c) Fluorimetric titration of a MG (1*  
 242 *μM), MswG12 (0.1 μM), Thsw19.1 (4 μM) mixture by theophylline (red line) and caffeine (black line).*  
 243 *Fluorescence measurements ( $\lambda_{Exc} = 610 \text{ nm}$ ,  $\lambda_{Em} = 650 \text{ nm}$ ) were performed in triplicate at room*  
 244 *temperature in SE buffer containing 3 mM magnesium..*

245

246 Then we performed the titration of fixed amounts of Thsw19.1 (4 μM), MswG12 (0.1 μM)  
 247 and theophylline (4 mM) by malachite green. Under these conditions half saturation was  
 248 obtained below 1 μM (Figure 4b). Once again almost no fluorescence was detected in the  
 249 absence of theophylline.

250

251 Last, we proceeded to the detection assay of theophylline with our sensor (Figure 4c). The  
 252 MG fluorescence signal increased with the theophylline concentration. Under our conditions  
 253 half-saturation was observed around 1 mM theophylline. As shown on figure 4c the  
 254 Thsw19.1-MswG12 combination does not respond to the addition of caffeine, a compound  
 255 that differs from theophylline by only one methyl group on the N7 position and that is not

256 recognized by the theophylline parent aptamer. The aptaswitch variant therefore retains the  
257 specificity of the parent aptamer : our biosensor is highly specific for theophylline.

258

## 259 **Conclusion**

260 In conclusion, we have designed a malachite green light-up sensor for theophylline. This  
261 was achieved by engineering two aptaswitches from the parent MG and theophylline RNA  
262 aptamers the top parts of which were modified for allowing ligand-dependent kissing  
263 interaction. Our approach led to the development of a label-free, simple sensor to detect a  
264 small size ligand. In earlier studies, several teams developed label-free MG-based sensors  
265 to detect adenosine (Stojanovic and Kolpashchikov, 2004; Xu and Lu, 2009). They  
266 engineered the malachite green aptamer by introducing the adenosine or ATP binding site  
267 and a transducer domain (bridge) between the MG and adenosine binding site. The kissing  
268 aptaswitch combination described here offer an alternative design. This approach does not  
269 require any complex cloning or other expensive technique and could be extended to the  
270 development of sensor for a plethora of small molecules. Indeed we previously engineered  
271 kissing aptaswitches for adenosine and GTP (Durand et al., 2014). They could easily be  
272 converted in light-up sensors using the approach described here. In contrast to strategies  
273 like split fluorescent protein (sFP) based sensor which require complex strategy of  
274 fluorophore maturation and binary light-up aptasensor (BLAS), our strategy is less  
275 expensive and easy to execute (Alam et al., 2017; Debiais et al., 2020; Kolpashchikov and  
276 Spelkov, 2020). However, the sensitivity of our double switch sensor remains rather low.  
277 This could likely be improved by functional screening process (microfluidics, HT-SELEX,  
278 etc.) (Autour et al., 2019; Dao et al., 2016; Sinha et al., 2018).

279

## 280 **Credit author statement**

281 Arghya Sett: Methodology, Investigation, Writing original draft

282 Lorena Zara: Methodology, Investigation, Writing original draft

283 Eric Dausse: Investigation, Supervision

284 Jean-Jacques Toulmé: Conceptualization, Supervision, Funding acquisition, Writing-  
285 Reviewing and Editing,

286

## 287 **Notes**

288 There are no conflicting interests to declare.

289

## 290 **Acknowledgements**

291 We acknowledge the support of the Agence Nationale pour la Recherche in the frame of the  
292 ERA-NET EuroNanoMed-II, (project ER-2016-2360733) and of the Conseil Régional de  
293 Nouvelle Aquitaine (grant 2017-1R30107-00013224).

294

## 295 **Supplementary information**

296

297 Table S1: Sequences of malaswitch variants

298 Table S2: Sequences of theoswitch variants

299 Figure S1: Predicted (Mfold) secondary structure of malaswitch variants.

300 Figure S2: Predicted (Mfold) secondary structure of theoswitch variants.

301

## 302 **References**

- 303 Alam, K.K., Tawiah, K.D., Lichte, M.F., Porciani, D., Burke, D.H., 2017. A Fluorescent Split  
304 Aptamer for Visualizing RNA–RNA Assembly In Vivo. *ACS Synth. Biol.* 6, 1710–1721.  
305 <https://doi.org/10.1021/acssynbio.7b00059>
- 306 Autour, A., Bouhedda, F., Cubi, R., Ryckelynck, M., 2019. Optimization of fluorogenic RNA-  
307 based biosensors using droplet-based microfluidic ultrahigh-throughput screening.  
308 *Methods* 161, 46–53.
- 309 Autour, A., Jeng, S.C.Y., Cawte, A.D., Abdolazadeh, A., Galli, A., Panchapakesan, S.S.S.,  
310 Rueda, D., Ryckelynck, M., Unrau, P.J., 2018. Fluorogenic RNA Mango aptamers for  
311 imaging small non-coding RNAs in mammalian cells. *Nat. Commun.* 9, 656.
- 312 Babendure, J.R., Adams, S.R., Tsien, R.Y., 2003. Aptamers switch on fluorescence of  
313 triphenylmethane dyes. *J. Am. Chem. Soc.* 125, 14716–14717.
- 314 Baugh, C., Grate, D., Wilson, C., 2000. 2.8 Å crystal structure of the malachite green  
315 aptamer1. *J. Mol. Biol.* 301, 117–128.
- 316 Boiziau, C., Dausse, E., Yurchenko, L., Toulmé, J.-J., 1999. DNA Aptamers selected  
317 against the HIV-1trans-activation-responsive RNA element form RNA-DNA kissing  
318 complexes. *J. Biol. Chem.* 274, 12730–12737.
- 319 Bouhedda, F., Autour, A., Ryckelynck, M., 2018. Light-up RNA aptamers and their cognate  
320 fluorogens: from their development to their applications. *Int. J. Mol. Sci.* 19, 44.
- 321 Bouhedda, F., Fam, K.T., Collot, M., Autour, A., Marzi, S., Klymchenko, A., Ryckelynck, M.,  
322 2020. A dimerization-based fluorogenic dye-aptamer module for RNA imaging in live  
323 cells. *Nat. Chem. Biol.* 16, 69–76.

324 Cao, S., Chen, S.-J., 2011. Structure and stability of RNA/RNA kissing complex: with  
325 application to HIV dimerization initiation signal. *RNA* 17, 2130–2143.

326 Chovelon, B., Durand, G., Dausse, E., Toulmé, J.-J., Faure, P., Peyrin, E., Ravelet, C., 2016.  
327 ELAKCA: enzyme-linked aptamer kissing complex assay as a small molecule sensing  
328 platform. *Anal. Chem.* 88, 2570–2575.

329 Dao, P., Hoinka, J., Takahashi, M., Zhou, J., Ho, M., Wang, Y., Costa, F., Rossi, J.J.,  
330 Backofen, R., Burnett, J., Przytycka, T.M., 2016. AptaTRACE Elucidates RNA  
331 Sequence-Structure Motifs from Selection Trends in HT-SELEX Experiments. *Cell Syst.*  
332 3, 62–70. <https://doi.org/10.1016/j.cels.2016.07.003>

333 Debiais, M., Lelievre, A., Smietana, M., Müller, S., 2020. Splitting aptamers and nucleic acid  
334 enzymes for the development of advanced biosensors. *Nucleic Acids Res.* 48, 3400–  
335 3422. <https://doi.org/10.1093/nar/gkaa132>

336 Dolgosheina, E. V, Jeng, S.C.Y., Panchapakesan, S.S.S., Cojocar, R., Chen, P.S.K.,  
337 Wilson, P.D., Hawkins, N., Wiggins, P.A., Unrau, P.J., 2014. RNA mango aptamer-  
338 fluorophore: a bright, high-affinity complex for RNA labeling and tracking. *ACS Chem.*  
339 *Biol.* 9, 2412–2420.

340 Ducongé, F., Di Primo, C., Toulmé, J.J., 2000. Is a closing “GA pair” a rule for stable loop-  
341 loop RNA complexes? *J. Biol. Chem.* 275, 21287–21294.  
342 <https://doi.org/10.1074/jbc.M002694200>

343 Ducongé, F., Toulmé, J.-J., 1999. In vitro selection identifies key determinants for loop–loop  
344 interactions: RNA aptamers selective for the TAR RNA element of HIV-1. *Rna* 5, 1605–  
345 1614.

346 Durand, G., Dausse, E., Goux, E., Fiore, E., Peyrin, E., Ravelet, C., Toulmé, J.J., 2016. A  
347 combinatorial approach to the repertoire of RNA kissing motifs; Towards multiplex  
348 detection by switching hairpin aptamers. *Nucleic Acids Res.* 44, 1–10.  
349 <https://doi.org/10.1093/nar/gkw206>

350 Durand, G., Lisi, S., Ravelet, C., Dausse, E., Peyrin, E., Toulmé, J.J., 2014. Riboswitches  
351 based on kissing complexes for the detection of small ligands. *Angew. Chemie - Int. Ed.*  
352 53, 6942–6945. <https://doi.org/10.1002/anie.201400402>

353 Ellington, A.D., Szostak, J.W., 1990. In vitro selection of RNA molecules that bind specific  
354 ligands. *Nature* 346, 818.

355 Grate, D., Wilson, C., 1999. Laser-mediated, site-specific inactivation of RNA transcripts.  
356 *Proc. Natl. Acad. Sci.* 96, 6131–6136.

357 Guet, D., Burns, L.T., Maji, S., Boulanger, J., Hersen, P., Wenthe, S.R., Salamero, J.,  
358 Dargemont, C., 2015. Combining Spinach-tagged RNA and gene localization to image

359 gene expression in live yeast. *Nat. Commun.* 6, 1–10.

360 Hayat, A., Marty, J.L., Mok, W., Li, Y., 2014. Recent Progress in Nucleic Acid Aptamer-  
361 Based Biosensors and Bioassays. *Sensors* 8, 7050–7084.  
362 <https://doi.org/10.3390/s8117050>

363 James, A.M., Baker, M.B., Bao, G., Searles, C.D., 2017. MicroRNA Detection Using a  
364 Double Molecular Beacon Approach: Distinguishing Between miRNA and Pre-miRNA.  
365 *Theranostics* 7, 634–646. <https://doi.org/10.7150/thno.16840>

366 Jenison, R.D., Gill, S.C., Pardi, A., Polisky, B., 1994. High-resolution molecular  
367 discrimination by RNA. *Science* (80- ). 263, 1425–1429.

368 Kolpashchikov, D.M., Spelkov, A., 2020. Binary (Split) Light-up Aptameric Sensors. *Angew.*  
369 *Chemie Int. Ed.*

370 Neubacher, S., Hennig, S., 2019. RNA Structure and Cellular Applications of Fluorescent  
371 Light-Up Aptamers. *Angew. Chemie Int. Ed.* 58, 1266–1279.

372 Ouellet, J., 2016. RNA Fluorescence with Light-Up Aptamers. *Front. Chem.* 4, 1–12.  
373 <https://doi.org/10.3389/fchem.2016.00029>

374 Paige, J.S., Nguyen-Duc, T., Song, W., Jaffrey, S.R., 2012. Fluorescence imaging of  
375 cellular metabolites with RNA. *Science* 335, 1194.  
376 <https://doi.org/10.1126/science.1218298>

377 Paige, J.S., Wu, K.Y., Jaffrey, S.R., 2011. RNA mimics of green fluorescent protein.  
378 *Science* (80- ). 333, 642.

379 Pfeiffer, F., Mayer, G., 2016. Selection and Biosensor Application of Aptamers for Small  
380 Molecules. *Front. Chem.* 4, 25. <https://doi.org/10.3389/fchem.2016.00025>

381 Pu, Q., Zhou, S., Huang, X., Yuan, Y., Du, F., Dong, J., Chen, G., Cui, X., Tang, Z., 2020.  
382 Intracellular Selection of Theophylline-Sensitive Hammerhead Aptazyme. *Mol. Ther.*  
383 *Nucleic Acids* 20, 400–408. <https://doi.org/10.1016/j.omtn.2020.03.001>

384 Sett, A., Zara, L., Dausse, E., Toulmé, J.-J., 2020. Engineering Light-Up Aptamers for the  
385 Detection of RNA Hairpins through Kissing Interaction. *Anal. Chem.* 92, 9113–9117.  
386 <https://doi.org/10.1021/acs.analchem.0c01378>

387 Shelke, S.A., Shao, Y., Laski, A., Koirala, D., Weissman, B.P., Fuller, J.R., Tan, X.,  
388 Constantin, T.P., Waggoner, A.S., Bruchez, M.P., Armitage, B.A., Piccirilli, J.A., 2018.  
389 Structural basis for activation of fluorogenic dyes by an RNA aptamer lacking a G-  
390 quadruplex motif. *Nat. Commun.* 9, 4542. <https://doi.org/10.1038/s41467-018-06942-3>

391 Sinha, A., Gopinathan, P., Chung, Y.-D., Lin, H.-Y., Li, K.-H., Ma, H.-P., Huang, P.-C.,  
392 Shiesh, S.-C., Lee, G.-B., 2018. An integrated microfluidic platform to perform

393           uninterrupted SELEX cycles to screen affinity reagents specific to cardiovascular  
394           biomarkers. *Biosens. Bioelectron.* 122, 104–112.

395   Stojanovic, M.N., Kolpashchikov, D.M., 2004. Modular aptameric sensors. *J. Am. Chem.*  
396           *Soc.* 126, 9266–9270.

397   Strack, R.L., Song, W., Jaffrey, S.R., 2014. Using Spinach-based sensors for fluorescence  
398           imaging of intracellular metabolites and proteins in living bacteria. *Nat. Protoc.* 9, 146.

399   Takeuchi, Y., Endo, M., Suzuki, Y., Hidaka, K., Durand, G., Dausse, E., Toulmé, J.-J.,  
400           Sugiyama, H., 2016. Single-molecule observations of RNA–RNA kissing interactions in  
401           a DNA nanostructure. *Biomater. Sci.* 4, 130–135.

402   Tombelli, S., Minunni, M., Mascini, M., 2007. Aptamers-based assays for diagnostics,  
403           environmental and food analysis. *Biomol. Eng.*  
404           <https://doi.org/10.1016/j.bioeng.2007.03.003>

405   Tuerk, C., Gold, L., 1990. Systematic evolution of ligands by exponential enrichment: RNA  
406           ligands to bacteriophage T4 DNA polymerase. *Science* 249, 505–510.  
407           <https://doi.org/10.1126/science.2200121>

408   Umar, M.I., Ji, D., Chan, C.-Y., Kwok, C.K., 2019. G-Quadruplex-Based Fluorescent Turn-  
409           On Ligands and Aptamers: From Development to Applications. *Molecules* 24, 2416.  
410           <https://doi.org/10.3390/molecules24132416>

411   Wang, H., Wang, J., Sun, N., Cheng, H., Chen, H., Pei, R., 2016. Selection and  
412           Characterization of Malachite Green Aptamers for the Development of Light-up Probes.  
413           *ChemistrySelect* 1, 1571–1574.

414   Wrist, A., Sun, W., Summers, R.M., 2020. The Theophylline Aptamer: 25 Years as an  
415           Important Tool in Cellular Engineering Research. *ACS Synth. Biol.* 9, 682–697.  
416           <https://doi.org/10.1021/acssynbio.9b00475>

417   Xu, W., Lu, Y., 2009. Label-free fluorescent aptamer sensor based on regulation of  
418           malachite green fluorescence. *Anal. Chem.* 82, 574–578.

419   Zhang, J., Fei, J., Leslie, B.J., Han, K.Y., Kuhlman, T.E., Ha, T., 2015. Tandem Spinach  
420           Array for mRNA Imaging in Living Bacterial Cells. *Sci. Rep.* 5, 17295.  
421           <https://doi.org/10.1038/srep17295>

422   Zimmermann, G.R., Jenison, R.D., Wick, C.L., Simorre, J.-P., Pardi, A., 1997. Interlocking  
423           structural motifs mediate molecular discrimination by a theophylline-binding RNA. *Nat.*  
424           *Struct. Biol.* 4, 644–649.

425   Zimmermann, G.R., Wick, C.L., Shields, T.P., Jenison, R.D., Pardi, a, 2000. Molecular  
426           interactions and metal binding in the theophylline-binding core of an RNA aptamer.  
427           *RNA* 6, 659–667.

**Supplementary information:**

Table S1: Sequences of malaswitch variants

Table S2: Sequences of theoswitch variants

Figure S1: Predicted (Mfold)secondary structures of malaswitch variants.

Figure S2: Predicted (Mfold)secondary structures of theoswitch variants.

Table S1: Sequence of malaswitch variants

The apical part of the MG aptamer (nucleic acid bases in green) was replaced to generate malaswitch (Msw) variants. Nucleic acid bases in Msw complementary to the loop of K3 are shown in pink. Point mutations in the complementary loop of malaswitch variants appear in blue. The kissing motif of K3 is in red and the mutated bases (K3Mut) is in cyan blue.

| Malaswitch candidates | Sequences (5'-3')  |
|-----------------------|--|
| MG aptamer            | GGAUCCCGACUGGCGAGAGCCAGGUAACGAAUGGAUCC                       |
| K3                    | CGAGCCUGGGAGCUCG   |
| K3Mut                 | CGAGCCUGACGAGCUCG  |
| MswK3'                | GGAUCCCGACU <sup>U</sup> CCCAGAGGUAACGAAUGGAUCC              |
| MswG12A20             | GGAUCCCGACU <sup>G</sup> CCCAGAG <sup>A</sup> UAACGAAUGGAUCC |
| MswC12                | GGAUCCCGACU <sup>C</sup> CCCAGAGGUAACGAAUGGAUCC              |
| MswG12                | GGAUCCCGACU <sup>G</sup> CCCAGAGGUAACGAAUGGAUCC              |

Table S2: Sequence of theoswitch variants

The apical part of the theophylline aptamer (nucleic acid bases in yellow) was replaced to generate theoswitch (Thsw) variants. Nucleic acid bases in Thsw complementary to the loop of malaswitch MswG12 are shown in red. Nucleotides conserved in both theophylline aptamer and theoswitch variants appear in blue.

| Theoswitch candidates | Sequences (5'-3')                   |
|-----------------------|-------------------------------------|
| Theophylline aptamer  | GGCGAUACCAGCCGAAAGGCCCUUGGCAGCGUC   |
| Thsw17.1              | GGCGAUACCAACUGGGAGCUCCUUGGCAGCGUC   |
| Thsw17.2              | GGCGAUACCAAACUGGGACCCUUGGCAGCGUC    |
| Thsw17.3              | GGCGAUACCAUCUGGGAAACCCUUGGCAGCGUC   |
| Thsw17.4              | GGCGAUACCACUACUGGGACCCUUGGCAGCGUC   |
| Thsw17.5              | GGCGAUACCAACCUGGGACCCUUGGCAGCGUC    |
| Thsw18.1              | GGCGAUACCAUGACUGGGAACUCUUGGCAGCGUC  |
| Thsw18.2              | GGCGAUACCAGAUCUGGGAGUACUUGGCAGCGUC  |
| Thsw18.3              | GGCGAUACCACUACUGGGAGCCUUGGCAGCGUC   |
| Thsw19.1              | GGCGAUACCAGCACUGGGAGCCCUUGGCAGCGUC  |
| Thsw19.2              | GGCGAUACCAGGACUGGGAGCUCCUUGGCAGCGUC |
| Thsw19.3              | GGCGAUACCACUACUGGGACAGCCUUGGCAGCGUC |
| Thsw19.4              | GGCGAUACCAUGGCUGGGACCUCCUUGGCAGCGUC |
| Thsw19.5              | GGCGAUACCACUACUGGGAAAGCCUUGGCAGCGUC |
| Thsw19.6              | GGCGAUACCACAACUGGGAAUGCCUUGGCAGCGUC |
| Thsw19.7              | GGCGAUACCAGUACUGGGACACCCUUGGCAGCGUC |
| Thsw19.8              | GGCGAUACCACACCUGGGAAUGCCUUGGCAGCGUC |
| Thsw19.9              | GGCGAUACCACUCCUGGGACAGCCUUGGCAGCGUC |
| Thsw19.10             | GGCGAUACCAAGGCUGGGAGCACCUUGGCAGCGUC |
| Thsw19.11             | GGCGAUACCAUGGCUGGGACCUCCUUGGCAGCGUC |
| Thsw19.12             | GGCGAUACCAGGGCUGGGAGCACCUUGGCAGCGUC |

Figure S1. Predicted (Mfold) secondary structures of malaswitch variants:

The bases in pink are complementary to the kissing loop K3 (Figure 1). The mutations are indicated in blue.

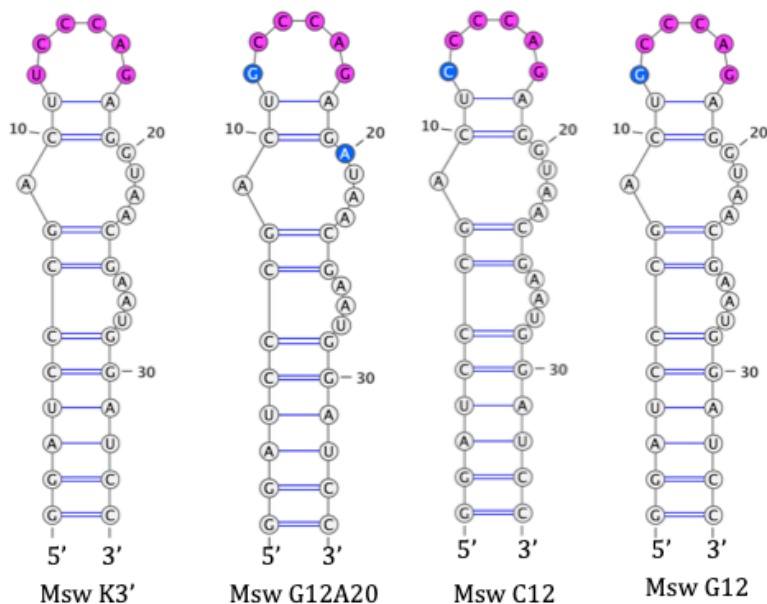
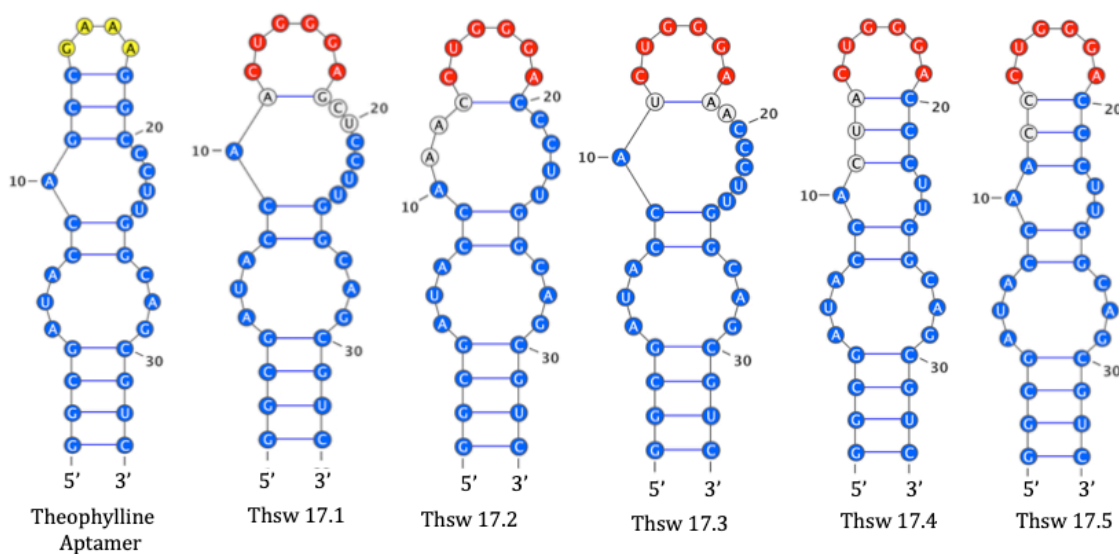
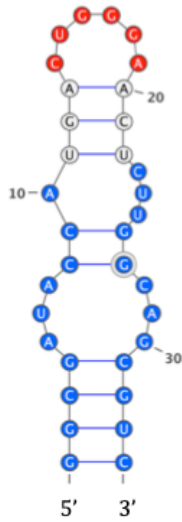


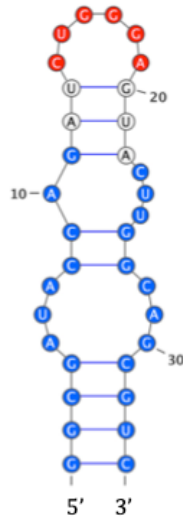
Figure S2: Predicted (Mfold) secondary structures of theoswitch variants

The bases in yellow is the top part of theophylline aptamer which was substituted by a kissing motif (red bases) for generating theoswitch variants. The nucleotides in blue pare resent in both the parent theophylline aptamer and theoswitch variants.

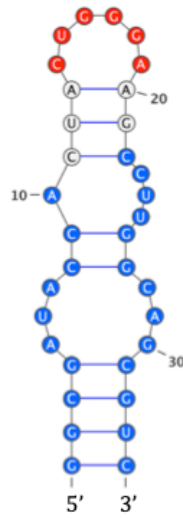




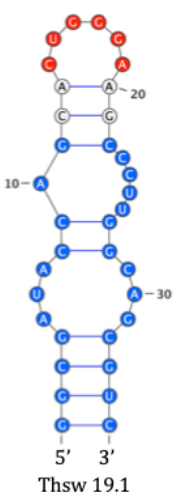
Thsw 18.1



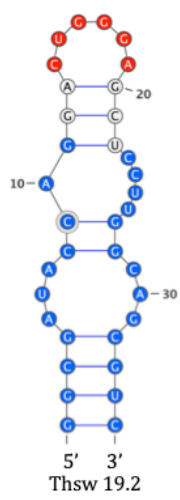
Thsw 18.2



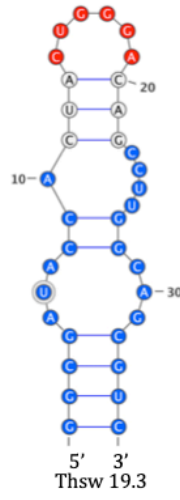
Thsw 18.3



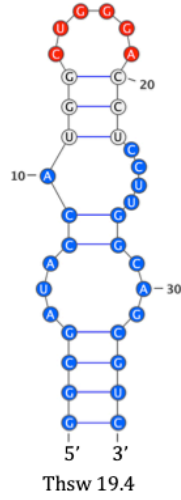
Thsw 19.1



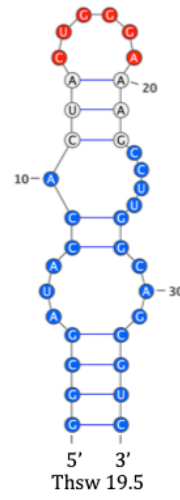
Thsw 19.2



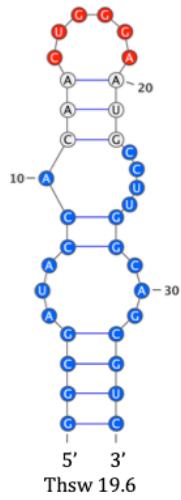
Thsw 19.3



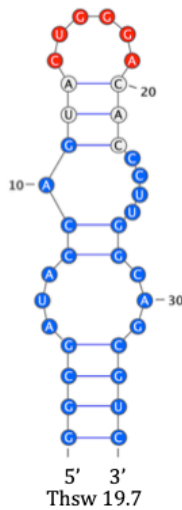
Thsw 19.4



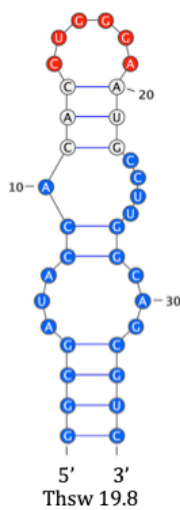
Thsw 19.5



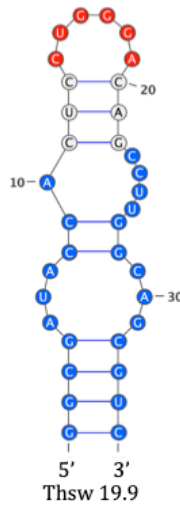
Thsw 19.6



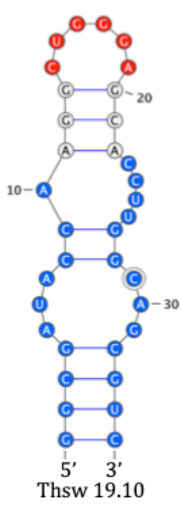
Thsw 19.7



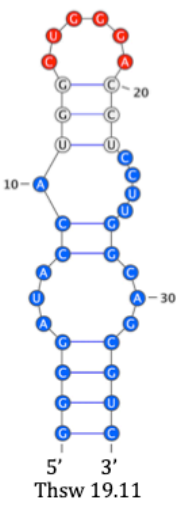
Thsw 19.8



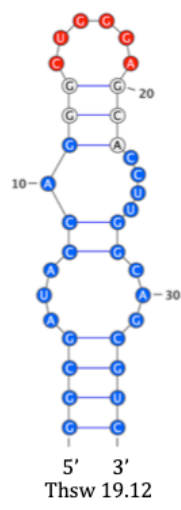
Thsw 19.9



Thsw 19.10



Thsw 19.11



Thsw 19.12

### 3.2 Conclusions

The first attempt to create a small molecular sensor based on light-up and kissing-complex strategies is promising. Firstly, we designed a new malaswitch G12 with an impact on the malachite green fluorescence intensity much higher than the aptamer itself in the presence of the kissing partner. It exhibits very high sensitivity and specificity for the aptakiss K3, with a significant increase in fluorescence (50-fold).

In turn, the second aptaswitch Thsw19.1 shows a higher sensitivity for the MswG12 upon adding theophylline, producing a 20-fold fluorescence increase. The Thsw 19.1 forms a specific fluorescent kissing complex with the malaswitch MG12 only in the presence of theophylline and malachite green. The specificity of this complex is also demonstrated by replacing theophylline with its analogue caffeine, for which no fluorescence emission is observed. Furthermore, this study allowed us to demonstrate how the kissing complex formation is strictly dependent on the length and composition of the connector and the bases that close the loop.

In conclusion, we developed a functional aptaswitch capable of detecting a target in a single fluorescence assay. These fluorescent switches can be easily integrated into a label-free biosensor platform. The results obtained from this first proof-of-concept show that they can be potentially exploited to create aptasensors for the detection of different small molecule targets.

## 4. Anti-Pesticide DNA Aptamers Fail to Recognize their Targets with Reported Micromolar Dissociation Constants

### 4.1 Strategy

As described on the part 3.1, the final aim of my thesis project would consist in realizing an alternative sensing platform for organic pollutant detection, based on a fluorescent double-switch complex. Despite its unique and elegant shape, achieving the rational design for a co-operation between two aptaswitches – presented in the previous part Experimental Section 3. - has proven far from easy. Firstly, before to obtain the double switch effect, it is necessary to require the understanding of a system in which the aptawitch-target affinity must be preserved. Furthermore, before designing the system, it is fundamental to create a homogeneous biosensor platform for verifying the affinity and specificity of the aptamer for its cognate target.

In order to achieve this project and generate aptasensors for pesticides, we focused on two aptamers largely described in literature: SS2-55<sup>59</sup> and SS-24-35<sup>13</sup> (Fig. 25), able to bind four different organophosphorus pesticides: isocarbophos, phorate, omethoate and profenofos.

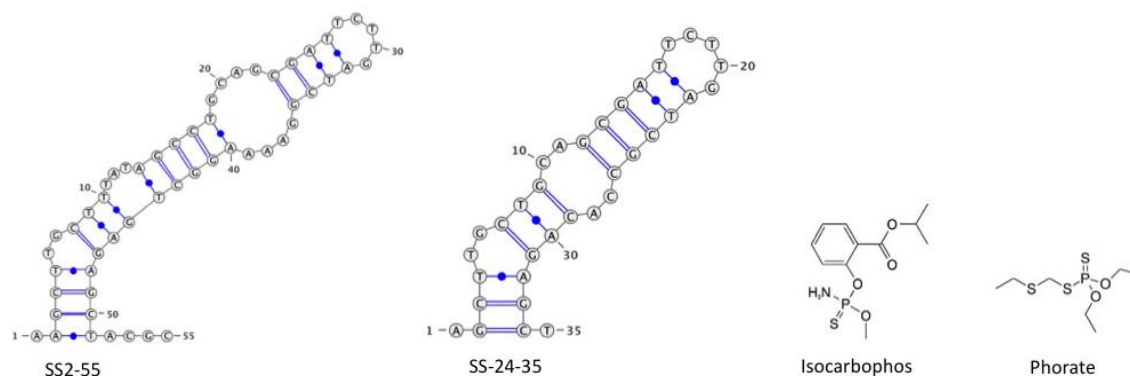


Fig. 25. Secondary structure of organophosphates-aptamer and chemical structure of isocarbophos and phorate.

Among the four targets above mentioned, we focused on two of them: isocarbophos and phorate. These two organophosphorus are used against several species of insect such as insects, mites and other pests, and commonly applied in cotton or food crops including

corn, coffee, fruits and some vegetables. They act as acetylcholinesterase inhibitor and a neurotoxin. They both have a high toxicity to humans and animal kingdom (especially aquatic species and birds). Isocarbophos and phorate have a poor level of water solubility, with a high potential for bioaccumulation. To date, they are considered to be among the most poisonous chemicals commonly used for pest control and their products are labelled with a DANGER signal word. Nevertheless, they continue to be used almost all over the world. Therefore, it is urgent to monitor their presence in the environment with a sensitive approach such as aptasensors.

Several research groups have developed aptasensors for phorate<sup>161,162</sup> and isocarbophos,<sup>163</sup> however, some of them lack assay specificity.

In order to create isocarbophos and phorate double-switch aptasensors, we firstly decided to create two fluorescent aptasensors with the SS2-55 and SS-24-35 aptamers. Fluorescence Anisotropy measurements were used through two displacement reporting routes: one using the SYBR Green intercalator concept<sup>92</sup> and the other based on the fluorescent labelled complementary strand approach.<sup>148</sup> In addition, by way of comparison, other known small-molecule aptamers with similar size and affinity for their targets were also considered.

# **Anti-Pesticide DNA Aptamers Fail to Recognize their Targets with Asserted Micromolar Dissociation Constants**

Lorena Zara<sup>1,2</sup>, Silvia Achilli<sup>1</sup>, Benoît Chovelon<sup>1,3</sup>, Emmanuelle Fiore<sup>1</sup>, Jean-Jacques Toulmé<sup>2</sup>,  
Eric Peyrin<sup>1\*</sup>, Corinne Ravelet<sup>1\*</sup>

<sup>1</sup>Département de Pharmacochimie Moléculaire, Grenoble Alpes University, CNRS, UMR 5063,  
France

<sup>2</sup>Novaptech, 2 Allée du Doyen Georges Brus, 33600 Pessac, France

<sup>3</sup>Service de Biochimie, Biologie Moléculaire, Toxicologie Environnementale, CHU de  
Grenoble-Alpes site Nord- Institut de Biologie et de Pathologie, La Tronche, France

\*corresponding authors: corinne.ravelet@univ-grenoble-alpes.fr ; eric.peyrin@univ-grenoble-  
alpes.fr

**Key-words:** pesticide, aptamers, Fluorescence anisotropy, Isothermal Titration Calorimetry

## **Abstract**

Herein, we originally aimed at developing fluorescence anisotropy biosensor platforms devoted to the homogeneous-phase detection of isocarbophos and phorate pesticides by using previously isolated DNA aptamers. To achieve this, two reporting approaches displaying very high generalisability features were implemented, based on either the complementary strand or the SYBR green intercalator displacement strategies. Unfortunately, none of the transduction methods led to phorate-dependent signals. Only the SYBR green displacement method provided a small output in the presence of isocarbophos, but at an analyte concentration greater than 100  $\mu\text{M}$ . In order to identify the origin of such data, isothermal titration calorimetry (ITC) experiments were subsequently performed. It was shown that aptamers bind neither isocarbophos nor phorate in free solution with the claimed micromolar dissociation constants. This work puts forward some doubts about the previously described aptasensors that rely on the use of these functional DNA molecules. It also highlights the need to carefully investigate the binding capabilities of aptamers after their isolation and to include appropriate control experiments with scrambled or mutated oligonucleotides.

## Introduction

The usage of pesticides in agriculture is well-known to cause very serious problems in the food and environment contamination, putting the health of humanity at risk.<sup>1</sup> Indeed, organophosphorous pesticides (OP), the most used pesticides, vary in their toxicities<sup>2</sup>, but most of them are poisonous and can cause acute or chronic damage to humans.

Currently, the methods used for pesticide detection generally imply gas chromatography, liquid chromatography, and liquid or gas chromatography coupled to mass spectrometry detection (HPLC-MS, GC-MS)<sup>3-5</sup>. Although these approaches are sensitive and trustworthy, most of them are complicated, time consuming, and expensive, and require highly qualified technicians.<sup>6</sup> Thus, rapid, sensitive, specific, and easy-to-use analytical methods are being developed to meet the need for environmental pollution control and early warning. Biosensors are promising in this context due to their advantages of low cost, easy operation, fast response, and high sensitivity. As compared with common antibodies or enzymes used in elaborating biosensors, aptamers display better stability, lower molecular weight, easy modification and low cost, and are considered as excellent candidates for developing aptasensors devoted to the pesticide detection. Hence, there is a great interest for designing new aptasensors able to detect pesticide residues<sup>7</sup> and, to that end, a large number of pesticide-binding aptamers have been recently selected.<sup>8</sup>

Among them, DNA aptamers that bind to four OP isocarbophos, phorate, omethoate and profenofos have been reported in 2012 by Wang and colleagues.<sup>9</sup> *In vitro* selection was performed on the basis of the structure-switching method using an immobilized random ssDNA library. Two ssDNA sequences, **SS2-55** and **SS4-54**, were identified. The authors stated that the apparent dissociation constant between the functional DNA molecules and the four organophosphorus pesticides lies between 0.8 and 2.5  $\mu\text{M}$ . The same authors have subsequently engineered a series of variants that better interact with OP.<sup>10</sup> A molecular beacon (MB) was used for the competitive binding to aptamers and the fluorescence intensity changes of MB was calculated as inhibition ratio. Among them, the aptamer **SS-24-35** obtained from a construct of **SS2-55** and **SS4-54** displayed the highest activity in binding to isocarbophos and profenofos with inhibition ratios of over 85% and 70%, respectively.

These three aptamers, adsorbed or grafted on a sensing surface, have been employed in the design of various heterogeneous-phase biosensors. In 2014, Pang *et al.* developed a rapid Surface Enhanced Raman Spectroscopy (SERS) method to detect and discriminate four specific pesticides (isocarbophos, omethoate, phorate, and profenofos) by using the immobilized **SS2-55** aptamer.<sup>25</sup> More recently, the surface-grafted **SS24-35** aptamer was applied for developing an electrochemical aptasensor to sense the profenofos, phorate, isocarbophos and omethoate analytes.<sup>11</sup> Most attention was focused on the design of colorimetric nanoparticle-based aptasensors. For instance, the detection of six OP (isocarbophos, phosalone, methamidophos, acephate, trichlorfon, dursban),<sup>12</sup> or phorate,<sup>13</sup> was achieved with the **SS2-55** aptamer adsorbed or grafted onto gold nanoparticles (AuNP) surfaces. **SS2-54** and **SS24-35** aptamers were respectively used for AuNP colorimetric detection of isocarbophos<sup>14</sup> and omethoate.<sup>14,15</sup> Li *et al.* also described an aptasensor for the determination of phorate based on **SS2-55**-templated silver nanoclusters.<sup>16</sup>

Among aptamer-based sensors, homogeneous-phase platforms such as fluorescent sensors are very performing, due notably to their high intrinsic sensitivity, high efficiency, simplicity, speed and the capability for automated high-throughput and multiplexed analysis.<sup>17-19</sup> To date, only one study by Zhang et al<sup>10</sup> has focused on the design of FRET-based DNA aptasensors for the isocarbophos and phorate determination. Thereby, the original aim of this study was to elaborate fluorescence anisotropy (FA) systems that would be capable to sense these two OPs. The measurement by FA adds another dimension of observation to the fluorescence-based experiment, providing information on the local environment, fluorescence lifetime and molecular mass. One of the advantages of fluorescence anisotropy studies as compared to fluorescence intensity (FI) ones is that since the measurements are ratiometric in nature, they are not dependent on the actual light intensity values or the fluorophore concentration.

To achieve our goal, we decided to implement two reporting strategies that exhibit the most desirable features in terms of assay generalizability, *i. e.* based on displacement schemes that involve either a complementary strand of the functional oligonucleotide or a DNA intercalator (SYBR Green). These indirect approaches are characterized by their easiness and broad applicability, regardless of aptamer structure. Indeed, significant FA responses have been reported for hairpin (ATP and Hg(II) detection),<sup>20</sup> quadruplex (ochratoxin A detection),<sup>21</sup> or unknown (tyrosinamide detection)<sup>22</sup> motifs.

Unfortunately, regardless the used approach, we found that the afore described OP aptamers did not respond to the presence of analytes with the apparent affinities claimed by the authors. Well-validated small-molecule aptamers directed against L-tyrosinamide, D-arginine-vasopressin or ochratoxin A were concomitantly tested to confirm the generalizability of the FA-displacement methods used. ITC experiments were then carried out to ascertain whether the tested aptamers recognize OP compounds with the reported micromolar dissociation constants. We found that the DNA oligonucleotides (in the micromolar concentration range) are unable to interact with the analytes, even at a concentration as high as 500  $\mu$ M. We finally discussed the requirements to prove the proper functionality of an aptamer, with the need to multiply characterization strategies within more than one assay platform.

## Materials and Methods

### Chemicals

Sodium chloride (NaCl), SYBr green I (SG), L-tyrosinamide (L-Tym), ochratoxin A (OTA) were purchased from Sigma-Aldrich (Saint-Quentin, France). D-arginine-vasopressin (AVP) trifluoroacetate salt were supplied by Bachem (Weil am Rhein, Germany). Magnesium chloride hexahydrate ( $MgCl_2 \cdot 6H_2O$ ) was purchased from Fisher Scientific (Illkirch, France). HCl and NaOH were provided by Carlo Erba (Val de Reuil, France). All chemicals were at least of analytical grade. Water was purified using a Millipore (Bedford, MA) filter with a reverse osmosis cartridge.

Pesticides (isocarbophos and phorate) were purchased from Dr. Ehrenstorfer GmbH and stocked in ethanol at 4°C at 10 mM concentration. L-Tym was prepared in water at 10 mM concentration. A stock solution of AVP was prepared at 1845  $\mu$ M in water. Ochratoxin A was dissolved in methanol to obtain stock solution (2.5 mM).

All DNA samples were from Eurogentec (Seraing, Belgium), stock solutions were made at 1 mM concentration with pure water and stored at -20°C. The sequences are listed in **Table 1**.

Buffers were prepared every week and stored at 4°C. For all experiments, the oligonucleotides dedicated to pesticides or other targets were diluted in 2X or more concentrated buffer (it depends on experiments), denatured at 80°C during 5 min, kept at room temperature for 30 min. Pesticides were added to obtain a final concentration of 5% ethanol. For all the experiments and wells, the binding buffer for **SS2-55** and **SS-24-35** aptamers dedicated to pesticides with a respective length of 55 and 35 mer, consisted of 10 mM Tris, pH 8, 10 mM NaCl, 10 mM KCl, 10 mM MgCl<sub>2</sub> and 5% ethanol. For L-Tym assays, the buffer used was mainly composed with 10 mM Tris, pH 7.5, 25 mM NaCl, 5 mM MgCl<sub>2</sub> with 5% ethanol. For AVP, the binding buffer used was composed of 10 mM Tris, pH 7.5, 50 mM KCl, 3 mM MgCl<sub>2</sub> and 2.5% ethanol. For OTA, the binding buffer consisted of 10 mM Tris, pH 8.5, 120 mM NaCl, 5 mM KCl, 20 mM CaCl<sub>2</sub> and 2.5% ethanol.

### **SYBR Green Displacement**

Titration curves of aptamers ranging from 8 to 512 nM (for **SS2-55** and **SS-24-35**), 1 to 32 nM (for Apt-Tym-38 and Apt-Tym-49), 4 to 8000 nM (for Apt-OTA or Apt-AVP) in the absence and in the presence of respectively 100 µM of isocarbophos and 500 µM of phorate, 100 µM of tyrosinamide, 3 µM of OTA and 500 µM of AVP were performed. After, titration curves of the targets, ranging from (0 to 500 µM for isocarbophos), (0 to 100 µM for L-Tym), (400 to 25 600 µM for OTA) and (6.25 to 100 µM for AVP) were realized with an appropriate concentration of aptamer showing the higher difference of anisotropy between aptamer alone and aptamer with target. The reagents were mixed in the wells in the following order: after denaturation, DNA aptamer and targets were first pre-incubated for 15 min at room temperature or 4°C followed by the addition of SG. The final concentration of SG in the wells was fixed to 1.05 µM as previously reported.<sup>23</sup> Experiments were performed in triplicate. Reading measurement were realised immediately or after 30 minutes of incubation time, depending on experiments realised.

### **Complementary strand displacement**

To establish the titration curves of aptamer (ranging from 20 nM to 1280 nM) in the presence and in the absence of isocarbophos (100 µM or 500 µM), phorate (100 µM) or L-Tym (100 µM), structured aptamers and analyte solutions were mixed into individual wells (final volume = 100 µL). After 15 minutes at room temperature, the complementary strand (CS) (20 nM) was added and the solution was kept at room temperature for 15 minutes in the dark. Blank wells of the microplate received 100 µL of the binding buffer. All experiments were done in triplicate. Finally, the microplate was placed into the microplate reader for the measurement.

### **Fluorescence anisotropy measurements**

The fluorescence anisotropy (FA) was measured in black 96-well Greiner Bio-One microplates (Courtaboeuf, France) using a Tecan Infinite F500 microplate reader (Männedorf, Switzerland). Excitation for SG based assay was set at 485 ± 20 nm and emission was collected with 535 ±

25 nm bandpass filters. For complementary strand displacement, the measurement was done with excitation filters at  $590 \pm 20$  nm and emission filters at  $635 \pm 25$  nm.

Fluorescence anisotropy change  $\Delta r$  was calculated as follows:

$\Delta r = r - r_f$  where  $r$  is the anisotropy of the hybrid (dye-labelled CS or SG with aptamer) in presence of target and  $r_f$  is the anisotropy of the dye-labelled CS or SG with aptamer in absence of target.

## ITC measurements

Calorimetry was performed with a MicroCal iTC200 Titration Calorimeter from Malvern (Palaiseau, France) and the data were analyzed using software Origin, Microcal Analysis Origin Launcher. The experiments were carried out at 15°C. Aptamers and targets were dissolved in the same buffer, (see previous section for binding buffer composition, except for OTA, which was composed of 10 mM Tris, pH 8.5, 120 mM NaCl, 5 mM KCl, 20 mM MgCl<sub>2</sub>, 3.66% ethanol). All the solutions were degassed to avoid air bubbles.

The aptamer concentration in the microcalorimeter cell (0.2 mL) varied from 8 to 30  $\mu$ M. A total of 20 injections of 2  $\mu$ L of target solution at concentrations varying from 300 to 500  $\mu$ M were added at intervals of 120 s while stirring at 750 rpm. Control experiments were performed by injection of target into the buffer solution. At least two independent titrations were run.

## Results

### SYBR green displacement assays

The proof-of-principle of the SG-based FA strategy was previously established using the SG as probe and various functional DNA molecules as recognition elements. Three different model systems involving unstructured (23 mer) and hairpin-like (25 mer and 22 mer T-rich functional DNA) motifs were used for the respective detection of L-tyrosinamide, adenosine and Hg(II) (**Figure 1**).<sup>23</sup> As a function of the target nature and the induced-fit binding process of functional DNA, the mechanism is based on either the SG release or catch upon ligand binding. Therefore, positive or negative FA responses can be observed depending on the relative contributions of direct competition and allosteric switch processes.

This method was first applied using a 55 and a 35 mer aptamers named **SS2-55** and **SS-24-35** for the isocarbophos recognition (**Figure S1A**). As expected, due to the short lifetime of the SYBR Green (in the picosecond range) relative to the time scale of rotation (in the subnanosecond range), the FA signal of the free dye was high, about 0.300 (data not shown). Upon complexation with the aptamer, the FA signal decreased with the dye/base ratio diminishing, as the result of both the considerable increase in  $\tau$  (in the nanosecond range) and a resonance energy homotransfer (RET) effect between closely located dyes within DNA. The titration curves displayed a plateau within the 2-64 nM and 64 to 128 nM ranges for **SS2-55** and **SS-24-35** aptamers, respectively, with a minimal value around 0.090-0.100. After this clear transition, an anisotropy increases higher for **SS2-55** than **SS-24-35** was observed with the DNA size increasing due to the enhancement in the apparent mass. Titration curves were established in the presence of 100  $\mu$ M of isocarbophos (**Figure S1A**) and then compared with those

conducted in the absence of analyte. No difference in anisotropy was observed for **SS2-55** whereas we evidenced an  $\Delta r$  value of about 0.012 with the **SS-24-35** aptamer at 8 nM (**Figure 1**). The distinct sequence length of the two oligonucleotides could explain the different behaviour between the two aptamers. Indeed, a higher length could induce the non-specific binding of SG to nucleobases that would be not implied in the target recognition process, leading to a detrimental effect on the FA response. This interpretation is supported by results reported in **Figure S1B**, observed with Apt-Tym-38 (38 mer) and its truncated version Apt-Tym-23 (23 mer). A release of SG ( $\Delta r$  around 0.010) was recorded with Apt-Tym-38 whereas a greater extent of release occurred with Apt-Tym-23 ( $\Delta r$  around 0.020 for 100  $\mu\text{M}$  of L-Tym).<sup>23</sup> Nevertheless, the results obtained with Apt-Vaso-55 and Apt-Tym-49 indicated that SG displacement strategy is able to produce a FA change even if the sequence of aptamer was long (**Figure S1B**). The minor  $\Delta r$  value of 0.003 at 100  $\mu\text{M}$  isocarboxophos, recorded using the **SS2-55** aptamer (**Figure 1:Iso**) might suggest that the binding interaction of this aptamer was of lower magnitude than those of Apt-Vaso-55 and Apt-Tym-49 with ( $K_d$  of 1.1  $\mu\text{M}$ <sup>24</sup> and 1.7  $\mu\text{M}$ , respectively).<sup>25</sup>

As the temperature change is known to greatly impact the interaction of both the SG dye and the aptamer stability as well as the FA signal,<sup>23</sup> 500  $\mu\text{M}$  of isocarboxophos or phorate was added to **SS-24-35** and reading measurements were performed after 30 min of incubation at 4°C. For isocarboxophos, the  $\Delta r$  value slightly increased with the target increasing concentration and temperature decreasing (from  $\sim 0.010$  to  $\sim 0.020$ ). Unfortunately, no difference in anisotropy was observed in the absence and presence of 500  $\mu\text{M}$  of phorate, showing a negligible  $\Delta r$  value (**Figure 1**). This indicates that phorate is unable to induce SYBR green displacement. The lack of response observed with phorate could originate from its different molecular structure as compared with isocarboxophos. The aromatic residue, only retrieved in isocarboxophos, could be able to interact with DNA through a larger interface and then displace more easily the SYBR green intercalator. It might be suspected that the target binds non-specifically to the functional DNA, explaining in turn the low  $\Delta r$  variation when the isocarboxophos concentration was five-fold increased (from 100 to 500  $\mu\text{M}$ ). In contrast, a much enhanced  $\Delta r$  response was observed at saturation concentration with a variety of previously described aptamers involving hairpin, G-quadruplex or unstructured DNA motifs. The reported  $\Delta r$  values were respectively 0.064, 0.061, -0.070 or -0.030 for Ade, L-Tym, Hg(II) and OTA, respectively (**Figure 1**). Of note, the saturation concentration obtained for Ade (1000  $\mu\text{M}$ ) was lower than that of LTym (20 000  $\mu\text{M}$ ). This difference had been explained by the occurrence of both SG release and capture mechanisms.<sup>23</sup> A similar mechanism for the **SS24-35** aptamer binding could occur.

### Complementary strand displacement assays

Strand displacement assays based on a fluorescence anisotropy signal transduction approach was developed using the **SS-24-35** aptamer, as previously described for numerous compounds such as L-tyrosinamide,<sup>22</sup> ATP,<sup>20</sup> and ochratoxin.<sup>21</sup> This method exploits the ability of nucleic acids to generate duplex structures with complementary sequences (CS). In the absence of the target, base pairing between the complementary sequences of the aptamer and CS is privileged. Upon target addition, the aptamer reorganisation led to the aptamer-CS duplex destabilization, leading to the release of the CS that generates a detectable FA signal decrease.

Herein, two Texas red (TR)-labeled complementary strand (TR-CSA and TR-CSB) (**Table 1**) corresponding in large part to the sequence used in the original aptamer selection,<sup>10</sup> were used as probes. On the basis of previous results obtained for L-tyrosinamide structure-switching assay,<sup>22</sup> the Texas red fluorophore and a 9-mer CS were chosen to design the probe. It has been shown that, for a 12-mer CS, the fluorescein dye slightly raises the assay sensitivity as compared to the TR label, whereas the fluorescein labelled 9-mer CS does not afford the duplex formation with the aptamer. On the other hand, the same 9-mer CS tagged with the TR label is able to successfully form duplex with the functional oligonucleotide and is comfortably displaced upon target binding.<sup>22</sup> In addition to the length and the type of the fluorophore, another important parameter in the signal response is the CS:aptamer ratio.<sup>26</sup> For all the aptamers, the CS probe concentration was set to 20 nM and various aptamer concentrations ranging from 20 to 1280 nM were tested in the absence and presence of targets.

First, to verify that ethanol did not adversely affect the CS displacement, 5% of ethanol was added to the L-tyrosinamide binding buffer. The titration curves (**Figure S2A**) with the Apt-Tym concentration increasing were established using the TR-tagged CS previously described and 100  $\mu$ M of L-tyrosinamide.<sup>22</sup> The addition of the target resulted in a large FA decrease for all the tested aptamer concentrations (with a  $\Delta r$  max value around -0.070 at 1280 nM of Apt-Tym-38). At the 320 nM aptamer concentration (1:16 CS:aptamer ratio), the CS displacement by the free target is optimal, indicating that a large amount of aptamer is favorable to the assay and showing that 5% ethanol affects neither the duplex formation nor the CS displacement. Of note, the aptamer concentration increase led to the  $\Delta r$  enhancement, better than that realised with the 1:1 CS:aptamer stoichiometry (**Figure 2: L-Tym versus L-Tym\***).

For aptamer **SS24-35**, despite the presence of a higher salt concentration, weaker strength hybridization was observed with TR-CSA and TR-CSB as compared with the Apt-Tym-CS-Tym system (data not shown). In contrast to Apt-Tym, no displacement of either complementary strands TR-CSA or TR-CSB was observed for the **SS-24-35** aptamer in the presence of 500  $\mu$ M of isocarbophos (**Figure S2A and Figure 2**) or 100  $\mu$ M of phorate, and this, whatever the tested CS:aptamer ratio. Such finding is quite surprising because this strategy is known to be extremely generalisable and was successfully applied to various aptamers for L-Tym,<sup>22</sup> ATP<sup>20</sup> or OTA,<sup>21</sup> showing  $\Delta r$  value of -0.021, 0.023 or -0.017 respectively with 1:1 or 1:2 (for ATP) CS:aptamer ratio (**Figure 2**). In addition, the molecular beacon employed in the original work of Zhang et al.<sup>10</sup> consisted of 20 bases where 15 of them are common to the two used CS.

The two FA displacement approaches developed herein failed to generate OP-dependent signals with the apparent affinities claimed by the authors. Theoretically, such lack of significant response can originate from two phenomena: (i) an ineffective reporting process and/or (ii) the inaptitude for the DNA molecules to bind the targets with the expected dissociation constants. Although of high generalizability features, the displacement signalling approaches may not work as well as intended in some cases. For example, Juncker et al. have demonstrated that a shorter CS, having a much lower hybridization free energy than the longer CS, displays no induced fit binding and may not be displaced by its target.<sup>27</sup> With this in mind, it might be possible that the 20 mer CS used by Zhang and al.<sup>10</sup> is moved more easily than our designed CS. Furthermore, the sensitivity of the SG displacement approach could be limited if the catch mechanism related to the DNA structuration upon target binding is significantly counterbalanced by a direct competitive effect.<sup>23</sup>

## ITC assays

In order to address the issues, we then decided to characterize the molecular recognition capabilities of the DNA molecules by using Isothermal titration calorimetry (ITC). ITC is a technique that directly measures the energetics associated with the binding of two components. Moreover, since heat is universally generated or absorbed during any molecular interaction, ITC has become a state-of-art label-free analytical method for characterizing small molecule aptamers.<sup>28</sup> When the affinity between the macromolecule and the ligand is comprised between  $10^4 \text{ M}^{-1}$  and  $10^8 \text{ M}^{-1}$  ( $100 \text{ }\mu\text{M} < K_d < 0.01 \text{ }\mu\text{M}$ ), the affinity and the enthalpy of binding can be simultaneously determined in a single experiment. If the affinity between the reactants is too low ( $K_d > 100 \text{ }\mu\text{M}$ ), neither the affinity nor the enthalpy of binding can be reliably determined. Many examples of ITC-based binding affinity calculation for different small molecule-aptamer pairs have been successfully reported in the literature (**Table 2**).

Binding data for a variety of aptamers tested in literature are shown in **Table 2** (in conditions similar to those realised with both OP and aptamers). In general, the aptamer concentration is comprised between 5 to 150  $\mu\text{M}$  and the target concentration ranges from 25 to 900  $\mu\text{M}$ , for dissociation constants comprised between 0.2 to 16  $\mu\text{M}$  (as expected for isocarbophos and phorate). The aptamer Apt-Tym-38 was also tested with 5% of ethanol to verify that this percentage of organic solvent did not impact binding constant affinity determination by ITC.

The ITC profiles at 15°C for the binding of the two pesticides (isocarbophos and phorate) to the two DNA aptamers are presented **Figure 3** and **Figure S3**. Each of the heat burst curves corresponded to a single injection of the target solutions into the DNA solutions. The resulting heat plotted as a function of molar ratio was depicted in the lower panel where data points reflect the experimental injection heats while the solid lines reflect the calculated fits of the data. Unfortunately, the titration of **SS2-55** and **SS24-35** aptamers by isocarbophos or phorate showed only minor heat exchange, in contrast with what is commonly reported in literature and recorded herein for L-Tym and OTA (Figure S4 and S5). The titration of L-Tym to Apta-Tym-38 resulted in negative peaks that reveal exothermic binding. Data processing with the ITC software generated a  $K_d$  value of  $0.5 \pm 2.2 \text{ }\mu\text{M}$  at 15 °C for L-tyrosinamide, in good agreement with the values of  $0.63 \pm 0.06 \text{ }\mu\text{M}$  obtained for Apt-Tym-49 at the same temperature.<sup>29</sup> ITC results exhibit a lower enthalpy variation ( $-9.4 \pm 0.3 \text{ kcal mol}^{-1}$  vs  $-16.1 \pm 0.2 \text{ kcal mol}^{-1}$ ) and a lower  $\Delta S$  value ( $-0.35 \text{ kcal mol}^{-1}$  vs  $-12.6 \text{ kcal mol}^{-1}$ ) as compared with Apt-Tym-49.<sup>29</sup> Apart from the aptamer length difference, these distinct values could be attributed to the presence of 5% ethanol in the buffer. Control experiments performed by injection of L-tyrosinamide into the buffer solution yielded insignificant heats of dilution (**Figure S3**).

From these data, we can conclude that, in homogeneous-phase, neither isocarbophos nor phorate display binding to **SS24-35** or **SS2-55** aptamers with dissociation constants in the micromolar range. These findings could explain the lack of significant displacement-based FA output upon binding of analytes under the current conditions.

## Discussion and Conclusion

Pesticide residue detection is a key approach for the management of pesticide contamination, which requires development of new methods for highly-sensitive detection. Under this

circumstance, novel aptamers have attracted great attention of researchers because of their well-known superiorities. Some publications have now highlighted the need to multiply characterisation techniques of aptamers after the SELEX procedure as well as to carry out control experiments with scrambled sequences and non-cognate compounds to establish the aptamer binding and specificity.

In 2015, Mc Keague et al. have performed a comprehensive examination of a panel of traditional affinity binding assays using a set of aptamers for the small molecule target, ochratoxin A. They proposed a workflow that allows specific recommendations for each step of the *in vitro* procedure (*i.e.* aptamer screening, characterization, and functional validation for optimal integration into Aptamer-Based Applications) that will ensure that new aptamers are entirely and securely characterized.<sup>30</sup> The characterization is a key step of the whole SELEX procedure and the multiplication of different binding evaluation procedures between an aptamer and its target is an essential prerequisite for further aptamer use.

Some model aptamers devoted to small molecules such as adenosine<sup>31</sup>, L-tyrosinamide<sup>32</sup>, cocaine<sup>33</sup>, or ochratoxin A<sup>34</sup> have proved their worth in the development of the different biosensor platforms. As an example, the anti-adenosine aptamer was studied in all directions with different transduction approaches as electrochemical, mass-based<sup>35</sup> and optical like fluorescence anisotropy (FA). For instance, in FA approach, different strategies involving direct<sup>36</sup>, split assembly<sup>37</sup>, kissing assembly<sup>38</sup>, enzymatic protection<sup>39</sup> nanomaterial amplification,<sup>40</sup> protein amplification,<sup>41</sup> recycling amplification,<sup>42</sup> or dye displacement<sup>43</sup> were successfully applied, highlighting the performant selection and the binding recognition properties of such functional DNA molecules.

From the aptamer selection to the biosensor design, there are many check points that guarantee the analytical results, such as the employment of scrambled DNA sequences, the choice of concurrent analytes as controls and independent methods for binding constant determination. Recently, Zhong and Liu have performed large binding assays on the arsenic binding aptamer named Ars-3 using ITC, DNA staining dyes, and gold nanoparticles (AuNPs). After carefully comparing Ars-3 and a few random control DNA sequences, they concluded that Ars-3 does not recognize As(III).<sup>44</sup> Some authors have highlighted that gold nanoparticles can bind to different targets.<sup>45</sup> For example, the adsorption of As(III) on the AuNP surface<sup>46</sup> can produce the exact same color response for colorimetric sensing than the positive assay (+ target) with aptamer, creating artefacts in AuNP-based biosensors. This publication challenges about the characterization of certain aptamers for which there is a lack of controls. More recently, De Wael et al. have compared different analytical methodologies to validate or disprove the binding capabilities of ampicillin-binding aptamer sequences. The target binding potential was evaluated in solution using ITC, native nano-electrospray ionization mass spectrometry and 1H-nuclear magnetic resonance spectroscopy. Here again, the authors concluded that there are no reasons to believe that complexation occurs within the low nM to high mM range.<sup>28</sup>

Regarding the anti-pesticide aptamers investigated in the present work, rare are the studies for which all the controls were carried out. Only one publication related to the OP determination exhibits adequate controls to reveal the binding interaction between the **SS24-35** and

omethoate.<sup>15</sup> For other ones, including the one by Zong et al.,<sup>13</sup> control experiments are missing. In most cases, pesticides analogues are used to test the aptasensor specificity; however, no investigation with scrambled sequences and target alone in the presence of sensing materials is conducted.<sup>11,13,14,47</sup> At best, analogous pesticides and/or scrambled sequences<sup>16</sup> are examined but the effects of the target adsorption onto the AuNP surface are rarely investigated.<sup>12</sup>

The response of an aptamer in solution can be significantly different from that reported with the same functional oligonucleotide immobilized onto a biosensor surface. For examples, several studies on microarrays have reported differences in aptamer affinity when compared with solution-based measurements.<sup>48</sup> Positively charged surfaces, immobilisation densities, aptamer orientations as well as spacer moieties may directly influence aptamer's folding and consequently binding.<sup>49</sup> Manipulation of the conditions (specific incubation times, temperatures and buffer conditions as well as the presence of blocking agents to decrease non-specific binding) can promote the interaction of weak binding sequences with their target, where binding was not previously observed.<sup>50</sup> In addition, surface-based interaction can be improved relative to solution-based binding through enhancement in the local concentration. As shown for IgE in SPRi, the amount of target bound goes through a maximum as function of the aptamer surface density. In the low surface density range, the target binding increases with the aptamer surface density until the limit of steric hindrance is reached in the bound target layer. After that, the bound IgE amount decreases as the aptamer surface density is further increased.<sup>51</sup>

Thus, the results obtained in this study highlighted the necessity to validate the binding potential of new isolated aptamers various and complementary techniques involving homogeneous methods, which avoid surface effects. This is especially important for aptamers that bind to small molecules. Recently, for a published aptamer dedicated to a protein target, the authors went in the right direction by portraying affinity measurements performed with three different techniques combining heterogeneous (SPR) and homogeneous (Microscale Thermophoresis and filter radiolabelling) platform in three independent laboratories as it was advised by Famulok and Mayer.<sup>52,53</sup>

## Acknowledgments

We thank Emilie Gillon and Anne Imberty for respectively providing helpful technical support and discussion about ITC experiments and data analysis.

This work was supported by funding ANRT CIFRE.

## References

- (1) Mahajan, R.; Bonner, M. R.; Hoppin, J. A.; Alavanja, M. C. R. *Environ. Health Perspect.* **2006**, *114* (8), 1205–1209.
- (2) Jia, M.; Wang, Y.; Teng, M.; Wang, D.; Yan, J.; Miao, J.; Zhou, Z.; Zhu, W. *Ecotoxicol. Environ. Saf.* **2018**, *163*, 1–6.
- (3) Rodriguez-Mozaz, S.; de Alda, M. J. L.; Barceló, D. J. *Chromatogr. A* **2004**, *1045* (1–2), 85–92.
- (4) Ferrer, I.; Thurman, E. M. *J. Chromatogr. A* **2007**, *1175* (1), 24–37.

- (5) Wu, L.; Song, Y.; Hu, M.; Zhang, H.; Yu, A.; Yu, C.; Ma, Q.; Wang, Z. *Food Chem.* **2015**, *176*, 197–204.
- (6) Rodriguez-Mozaz, S.; Lopez de Alda, M. J.; Barceló, D. *J. Chromatogr. A* **2007**, *1152* (1–2), 97–115.
- (7) Nguyen, V.-T.; Kwon, Y. S.; Gu, M. B. *Curr. Opin. Biotechnol.* **2017**, *45*, 15–23.
- (8) Liu, M.; Khan, A.; Wang, Z.; Liu, Y.; Yang, G.; Deng, Y.; He, N. *Biosens. Bioelectron.* **2019**, *130*, 174–184.
- (9) Wang, L.; Liu, X.; Zhang, Q.; Zhang, C.; Liu, Y.; Tu, K.; Tu, J. *Biotechnol. Lett.* **2012**, *34* (5), 869–874.
- (10) Zhang, C.; Wang, L.; Tu, Z.; Sun, X.; He, Q.; Lei, Z.; Xu, C.; Liu, Y.; Zhang, X.; Yang, J.; Liu, X.; Xu, Y. *Biosens. Bioelectron.* **2014**, *55*, 216–219.
- (11) Fu, J.; An, X.; Yao, Y.; Guo, Y.; Sun, X. *Sensors. Actuators B.* **2019**, *287*, 503–509.
- (12) Bai, W.; Zhu, C.; Liu, J.; Yan, M.; Yang, S.; Chen, A. *Environ. Toxicol. Chem.* **2015**, *34* (10), 2244–2249.
- (13) Bala, R.; Sharma, R. K.; Wangoo, N. *Anal. Bioanal. Chem.* **2016**, *408* (1), 333–338.
- (14) Liu, D.-L.; Li, Y.; Sun, R.; Xu, J.-Y.; Chen, Y.; Sun, C.-Y. *J. Nanosci. Nanotechnol.* **2020**, *20* (4), 2114–2121.
- (15) Wang, P.; Wan, Y.; Ali, A.; Deng, S.; Su, Y.; Fan, C.; Yang, S. *Sci. China. Chem.* **2016**, *59*, 237–242.
- (16) Li, X.; Shi, J.; Chen, C.; Li, W.; Han, L.; Lan, L.; Guo, Y.; Chang, Y.; Cai, J.; Ding, Y. *New J. Chem.* **2018**, *42* (8), 6293–6298.
- (17) Nutiu, R.; Li, Y. *Methods San Diego Calif* **2005**, *37* (1), 16–25.
- (18) Juskowiak, B. *Anal. Bioanal. Chem.* **2011**, *399* (9), 3157–3176.
- (19) Li, T.; Wang, E.; Dong, S. *Chem. Commun.* **2009**, No. 5, 580–582.
- (20) Goux, E.; Lespinasse, Q.; Guieu, V.; Perrier, S.; Ravelet, C.; Fiore, E.; Peyrin, E. *Methods* **2016**, *97*, 69–74.
- (21) Cruz-Aguado, J. A.; Penner, G. *Anal. Chem.* **2008**, *80* (22), 8853–8855.
- (22) Zhu, Z.; Schmidt, T.; Mahrous, M.; Guieu, V.; Perrier, S.; Ravelet, C.; Peyrin, E. *Anal. Chim. Acta* **2011**, *707* (1), 191–196.
- (23) Chovelon, B.; Fiore, E.; Faure, P.; Peyrin, E.; Ravelet, C. *Biosens. Bioelectron.* **2017**, *90*, 140–145.
- (24) Williams, K. P.; Liu, X.-H.; Schumacher, T. N. M.; Lin, H. Y.; Ausiello, D. A.; Kim, P. S.; Bartel, D. P. *Proc. Natl. Acad. Sci. U. S. A.* **1997**, *94* (21), 11285–11290.
- (25) Ruta, J.; Perrier, S.; Ravelet, C.; Fize, J.; Peyrin, E. *Anal. Chem.* **2009**, *81* (17), 7468–7473.
- (26) Li, Y.; Zhao, Q. *Anal. Chem.* **2019**, *91* (11), 7379–7384.
- (27) Munzar, J. D.; Ng, A.; Corrado, M.; Juncker, D. *Chem. Sci.* **2017**, *8* (3), 2251–2256.
- (28) Bottari, F.; Daems, E.; de Vries, A.-M.; Van Wielendaele, P.; Trashin, S.; Blust, R.; Sobott, F.; Madder, A.; Martins, J. C.; De Wael, K. *J. Am. Chem. Soc.* **2020**, *142* (46), 19622–19630.
- (29) Challier, L.; Miranda-Castro, R.; Barbe, B.; Fave, C.; Limoges, B.; Peyrin, E.; Ravelet, C.; Fiore, E.; Labbe, P.; Coche-Guerente, L.; Ennifar, E.; Bec, G.; Dumas, P.; Mavre, F.; Noel, V. *Anal. Chem.* **2016**, *88* (23), 11963–11971.
- (30) McKeague, M.; De Girolamo, A.; Valenzano, S.; Pascale, M.; Ruscito, A.; Velu, R.; Frost, N. R.; Hill, K.; Smith, M.; McConnell, E. M.; DeRosa, M. C. *Anal. Chem.* **2015**, *87* (17), 8608–8612.
- (31) Huizenga, D. E.; Szostak, J. W. *Biochemistry* **1995**, *34* (2), 656–665.
- (32) Vianini, E.; Palumbo, M.; Gatto, B. *Bioorg. Med. Chem.* **2001**, *9* (10), 2543–2548.
- (33) Stojanovic, M. N.; de Prada, P.; Landry, D. W. *J. Am. Chem. Soc.* **2000**, *122* (46), 11547–11548.
- (34) Cruz-Aguado, J. A.; Penner, G. *Anal. Chem.* **2008**, *80*, 8853–8855.
- (35) Wang, J.; Munir, A.; Zhou, H. S. *Talanta* **2009**, *79* (1), 72–76.
- (36) Perrier, S.; Ravelet, C.; Guieu, V.; Fize, J.; Roy, B.; Perigaud, C.; Peyrin, E. *Biosens. Bioelectron.* **2010**, *25* (7), 1652–1657.
- (37) Zhu, Z.; Ravelet, C.; Perrier, S.; Guieu, V.; Fiore, E.; Peyrin, E. *Anal. Chem.* **2012**, *84* (16), 7203–7211.
- (38) Durand, G.; Lisi, S.; Ravelet, C.; Dausse, E.; Peyrin, E.; Toulme, J.-J. *Angew. Chem.-Int. Ed.* **2014**, *53* (27), 6942–6945.

- (39) Kidd, A.; Guieu, V.; Perrier, S.; Ravelet, C.; Peyrin, E. *Anal. Bioanal. Chem.* **2011**, *401* (10), 3229–3234.
- (40) Xiao, X.; Li, Y. F.; Huang, C. Z.; Zhen, S. J. *Chem. Commun.* **2015**, *51* (89), 16080–16083.
- (41) Kang, L.; Yani, B.; Zhang, X.; Cui, L.; Meng, H.; Mei, L.; Wu, C.; Ren, S.; Tan, W. *Anal. Chim. Acta* **2015**, *879*, 91–96.
- (42) Huang, Y.; Liu, X.; Zhang, L.; Hu, K.; Zhao, S.; Fang, B.; Chen, Z.-F.; Liang, H. *Biosens. Bioelectron.* **2015**, *63*, 178–184.
- (43) Chovelon, B.; Fiore, E.; Faure, P.; Peyrin, E.; Ravelet, C. *Biosens. Bioelectron.* **2017**, *90*, 140–145.
- (44) Zong, C.; Liu, J. *Anal. Chem.* **2019**, *91* (16), 10887–10893.
- (45) Shao, Q.; Hall, C. K. *Langmuir ACS J. Surf. Colloids* **2016**, *32* (31), 7888–7896.
- (46) Zong, C.; Zhang, Z.; Liu, B.; Liu, J. *Langmuir ACS J. Surf. Colloids* **2019**, *35* (22), 7304–7311.
- (47) Pang, S.; Labuza, T. P.; He, L. *The Analyst* **2014**, *139* (8), 1895–1901.
- (48) Martin, J. A.; Chushak, Y.; Chávez, J. L.; Hagen, J. A.; Kelley-Loughnane, N. J. *Nucl. Acids* **2016**, 1–11.
- (49) Urmann, K.; Modrejewski, J.; Scheper, T.; Walter, J.-G. *BioNanoMaterials* **2016**, *18* (1–2).
- (50) Katilius, E.; Flores, C.; Woodbury, N. W. *Nucleic Acids Res.* **2007**, *35* (22), 7626–7635.
- (51) Simon, S.; Bognár, Z.; Gyurcsányi, R. E. *Electroanalysis* **2020**, *32*, 851–858.
- (52) Famulok, M.; Mayer, G. *Chem. Biol.* **2014**, *21* (9), 1055–1058.
- (53) Jauset Rubio, M.; Svobodová, M.; Mairal, T.; Schubert, T.; Künne, S.; Mayer, G.; O’Sullivan, C. K. *Anal. Bioanal. Chem.* **2016**, *408* (3), 875–884.
- (54) Zhang, Z.; Oni, O.; Liu, J. *Nucleic Acids Res.* **2017**, *45* (13), 7593–7601.
- (55) Neves, M. A. D.; Reinstein, O.; Saad, M.; Johnson, P. E. *Biophys. Chem.* **2010**, *153* (1), 9–16.
- (56) Roncancio, D.; Yu, H.; Xu, X.; Wu, S.; Liu, R.; Debord, J.; Lou, X.; Xiao, Y. *Anal. Chem.* **2014**, *86* (22), 11100–11106.
- (57) Reinstein, O.; Yoo, M.; Han, C.; Palmo, T.; Beckham, S. A.; Wilce, M. C. J.; Johnson, P. E. *Biochemistry* **2013**, *52* (48), 8652–8662.
- (58) Reinstein, O.; Neves, M. A. D.; Saad, M.; Boodram, S. N.; Lombardo, S.; Beckham, S. A.; Brouwer, J.; Audette, G. F.; Groves, P.; Wilce, M. C. J.; Johnson, P. E. *Biochemistry* **2011**, *50* (43), 9368–9376.
- (59) Kwon, Y. S.; Nguyen, V.-T.; Park, J. G.; Gu, M. B. *Anal. Chim. Acta* **2015**, *868*, 60–66.
- (60) Pei, W.; Liu, M.; Wu, Y.; Zhao, Y.; Liu, T.; Sun, B.; Liu, Y.; Wang, Q.; Han, J. *Eur. J. Pharm. Sci.* **2020**, *148*, 105319.

**Table 1.** Oligonucleotides sequences. Complementary sequences are in green and red.

| DNA names  | Sequences (from 5' to 3')                                   |
|------------|---|
| SS2-55     | AAGCTTGCTTTATAGCCTGCAGCGATTCTTGATCGGAAAAGGC<br>TGAGAGCTACGC |
| SS-24-35   | AGCTTGCTGCAGCGATTCTTGATCGCCACAGAGCT                         |
| Apt-Tym-38 | TGGAGCTTGGATTGATGTGGTGTGTGAGTGCGGTGCC                       |
| Apt-Tym-49 | AATTCGCTAGCTGGAGCTTGGATTGATGTGGTGTGTGAGTGCG<br>GTGCC        |
| Apt-OTA    | GATCGGGTGTGGGTGGCGTAAAGGGAGCATCGGACA                        |
| Apt-AVP    | TCACGTGCATGATAGACGGCGAAGCCGTCGAGTTGCTGTGTG<br>CCGATGCACGTGA |
| TR-CSA     | TR-CAAGAATCG  |
| TR-CSB     | CTGCAGCAA-TR  |
| CS-Tym     | TR-CACATCAAT  |

**Table 2.** Examples of  $K_d$  determination and enthalpy change estimated by the ITC method for validated small molecule-aptamer systems. Non-exhaustive-list.

| Small molecule                            | Aptamer bases structure | [small molecule] $\mu\text{M}$ | [Aptamer] $\mu\text{M}$ | $K_d$ estimated $\mu\text{M}$                         | $\Delta H$ kcal mol <sup>-1</sup>                        | Ref |
|---|-------------------------|--------------------------------|-------------------------|---|--|-----|
| L-tyrosinamide                            | 49                      | 330                            | 32                      | $0.63 \pm 0.06^*$                                     | $-16.1 \pm 0.2$  | 29  |
|   | 23<br>unknown           | 250                            | 15                      | $0.19 \pm 0.02^*$                                     |  |     |
| Adenosine                                 | 27<br>hairpin           | 500                            | 10                      | $16.4 \pm 1.4$  | $-14.1 \pm 0.5$  | 54  |
| Cocaine                                   | MN4<br>36<br>TWJ        | 280                            | 20                      | $0.3 \pm 0.1$   | $-16 \pm 3$  | 55  |
| Cocaine                                   | 38-GC<br>38<br>TWJ      | 500                            | 20                      | $2.6 \pm 1.0$   | nd   | 56  |
| Quinine                                   | MN4<br>TWJ              | 230–2250                       | 15 to 150               | $0.23 \pm 0.03$                                       | $-14.5 \pm 0.4$  | 57  |
|   |                         | 50                             | 5                       | $0.17 \pm 0.04$                                       | nd   | 28  |
| Argininamide                              | Hairpin<br>24           | 7500                           | 150                     | $0.17 \pm 0.015$                                      | nd   | 28  |
| deoxycholic acid                          | WC<br>36<br>TWJ         | 1200–4200                      | 20 to 85                | $16 \pm 3$  | $-7 \pm 1$   | 58  |
| Iprobenfos<br>Edifenphos                  | EIA2<br>64<br>Hairpin   | 25                             | 0.5                     | $1.67^{**}$<br>$0.038^{**}$                           | nd   | 59  |
| doxorubicin<br>epirubicin<br>daunorubicin | AS1411NT                | 900                            | 5                       | $1.24 \pm 0.042$<br>$2.22 \pm 0.06$<br>$2.3 \pm 0.06$ | $-7.9 \pm 0.021$<br>$-7.9 \pm 0.024$<br>$-6.3 \pm 0.019$ | 60  |

\*At 15°C; TWJ= Three Way junction; nd = not determined

\*\*  $s_D$  not determined

**Figure 1.** Comparison of SG fluorescence anisotropy change  $\Delta r$  value for OP tested and other targets from this study or literature data:<sup>40</sup> In red colour: results obtained with aptamers dedicated to OP pesticide. In green colour: results with well-validated aptamers dedicated to small molecules. In blue colour: data from literature. The dotted line is the maximum standard deviation ( $s_D = 0.007$ ) obtained from experiments conducted in the absence of targets ( $n = 20$ ). **Iso** for 100  $\mu\text{M}$  of isocarbophos with **SS2-55** aptamer, **Iso (100)**, **Iso (500)** and **Pho (500)** for respectively 100, 500  $\mu\text{M}$  of isocarbophos and 500  $\mu\text{M}$  of phorate with **SS24-35** aptamer. **Ade** for 1000  $\mu\text{M}$  of Adenosine, **L-Tym** for 20 000  $\mu\text{M}$  of L-tyrosinamide, **Hg(II)** for 312 nM of  $\text{HgCl}_2$  and **OTA** for 25  $\mu\text{M}$  of ochratoxin A.

Experimental conditions for OP: Binding buffer: 10 mM Tris, pH 8, 50 mM NaCl, 10 mM KCl, 10 mM  $\text{MgCl}_2$  and 5% ethanol, SG: 1.05  $\mu\text{M}$ , Aptamers: 8 nM, reading immediately at room temperature for Iso and Iso (100), Reading after 30 min of incubation at 4°C for Iso (500) and Pho (500).

Experimental conditions for OTA: Binding buffer: 10 mM Tris, pH 8.5, 120 mM NaCl, 5 mM KCl, 20 mM  $\text{CaCl}_2$  and 2.5% ethanol, SG: 1.05  $\mu\text{M}$ , Aptamers: 2  $\mu\text{M}$ , reading immediately at room temperature.

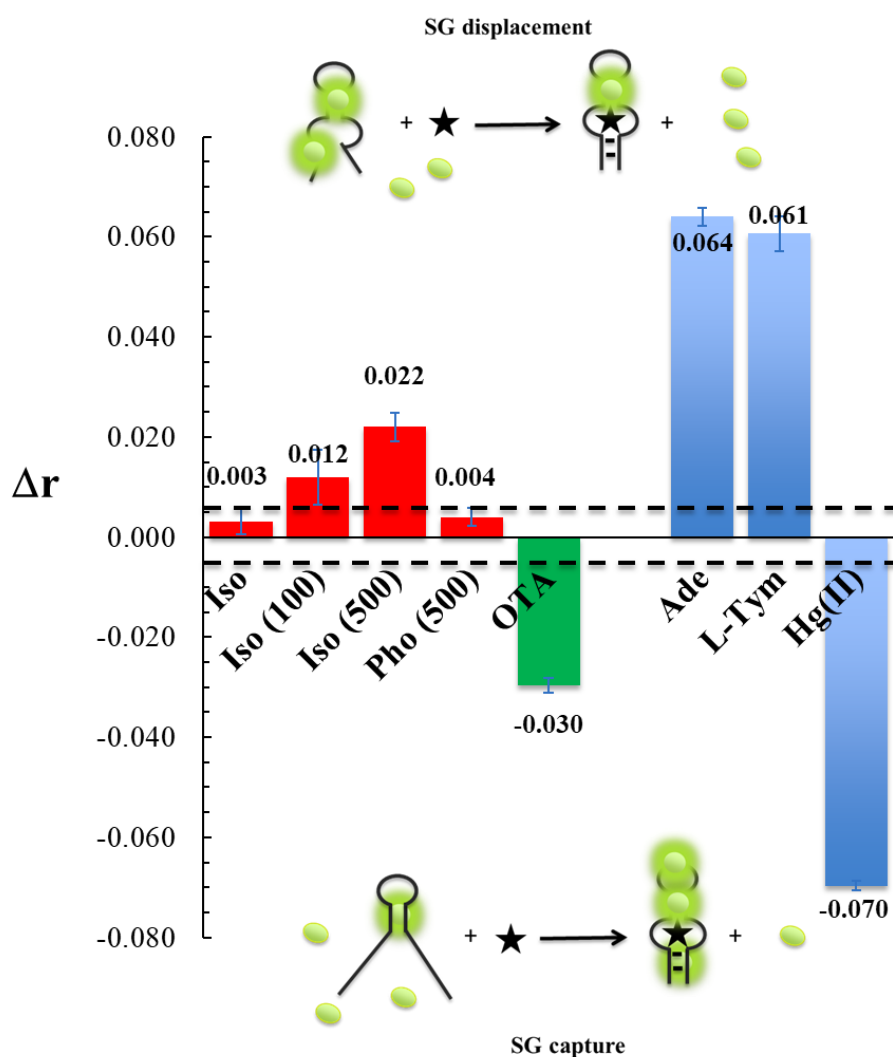


**Figure 2.** Comparison of fluorescence anisotropy change  $\Delta r$  value for 500  $\mu\text{M}$  of isocarbofos and 100  $\mu\text{M}$  of phorate with CS displacement strategy with TR-CSA and TR-CSB on **SS24-35** aptamer and other small molecules from this study or literature data.<sup>22,20,21</sup>

In red colour: results obtained with aptamers dedicated to OP pesticide. In green colour: results with well-validated aptamers dedicated to small molecules. In blue colour: data from literature. The dotted line is the maximum standard deviation ( $s_D = 0.002$ ) obtained from experiments conducted in the absence of targets ( $n=10$ ).

Experimental conditions for isocarbofos and phorate: CS concentration: 20 nM. SS24-35 aptamer: 320 nM; Binding buffer conditions: 10 mM Tris, pH 8, 50 mM NaCl, 10 mM KCl, 10 mM  $\text{MgCl}_2$  and 5% ethanol.

Experimental conditions for L-Tym: CS concentration: 20 nM. Apt-Tym aptamer: 20 nM or 320 nM (for L-Tym\*) with 100  $\mu\text{M}$  of L-tyrosinamide; 10 mM Tris, pH 7.5, 25 mM NaCl, 5 mM  $\text{MgCl}_2$  and 5% ethanol.

**Data literature conditions:**

<sup>22</sup>L-Tym\*\*: CS concentration: 10 nM. Apt-Tym aptamer: 10 nM; L-Tym: 250  $\mu\text{M}$ , 10 mM Tris, pH 7.5, 25 mM NaCl, 5 mM  $\text{MgCl}_2$

<sup>20</sup>ATP: CS= PNA7-TR :200 nM, Aptamer: 400 nM; ATP: 500  $\mu\text{M}$ , 10 mM Tris, pH 8.5, 10 mM NaCl, 10 mM  $\text{MgCl}_2$

<sup>21</sup>Ochratoxin (OTA): CS: 10 nM, Aptamer: 10 nM, OTA: 110 nM, 10 mM TRIS pH 8.5, 120 mM NaCl, 20 mM  $\text{CaCl}_2$ , 5 mM KCl

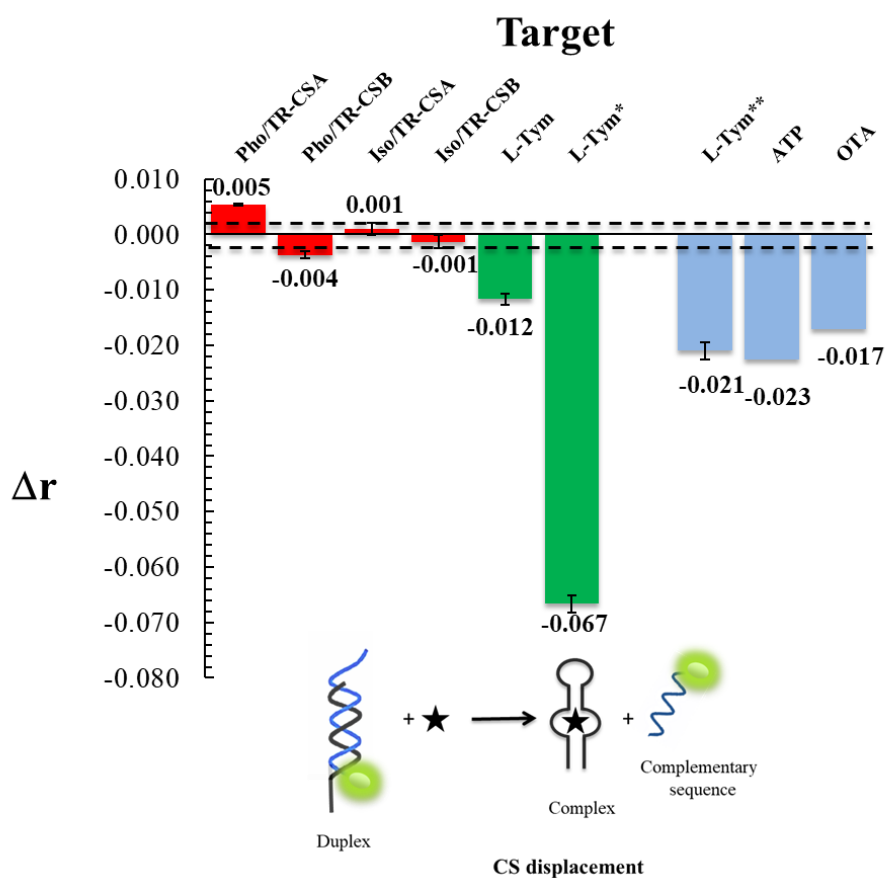
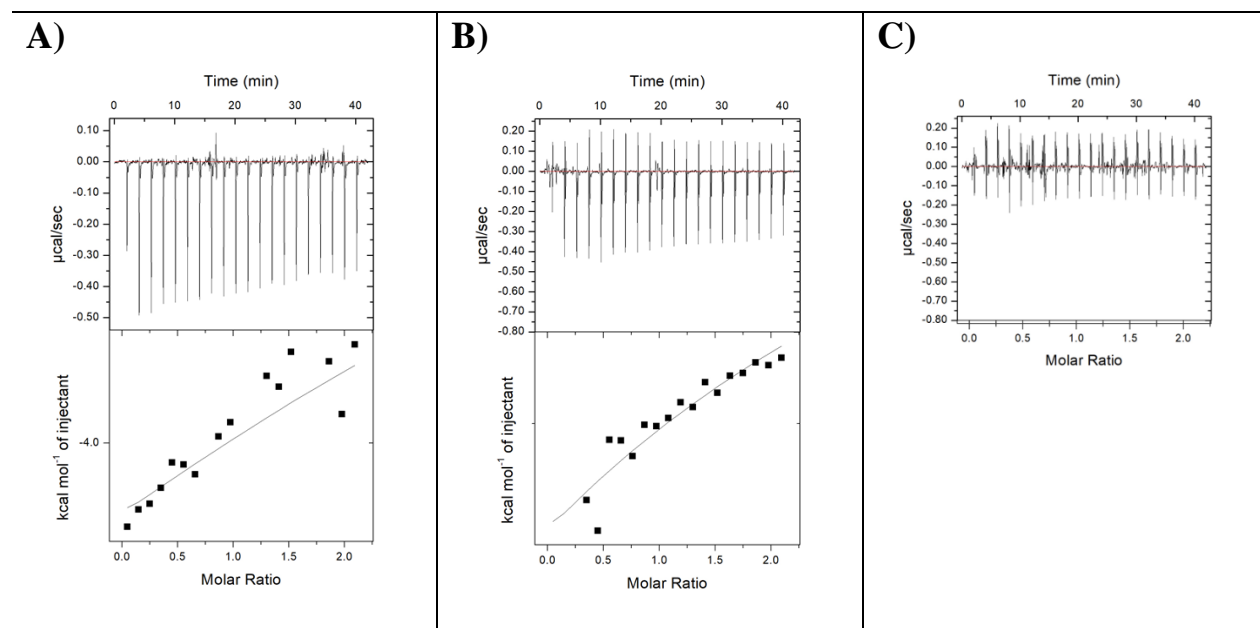


**Figure 3.** ITC analysis of binding affinity of **SS2-55** (30  $\mu\text{M}$ ) **A**) and **SS24-35** (30  $\mu\text{M}$ ) **B**) with 300  $\mu\text{M}$  isocarboxiphos **C**) Control: Titration of isocarboxiphos 300  $\mu\text{M}$  in buffer solution. Experimental conditions: 50 mM Tris, pH 8, 50 mM NaCl, 10 mM KCl, 10 mM  $\text{MgCl}_2$ , 5% Ethanol. Temperature: 15°C.



## Supplementary Information

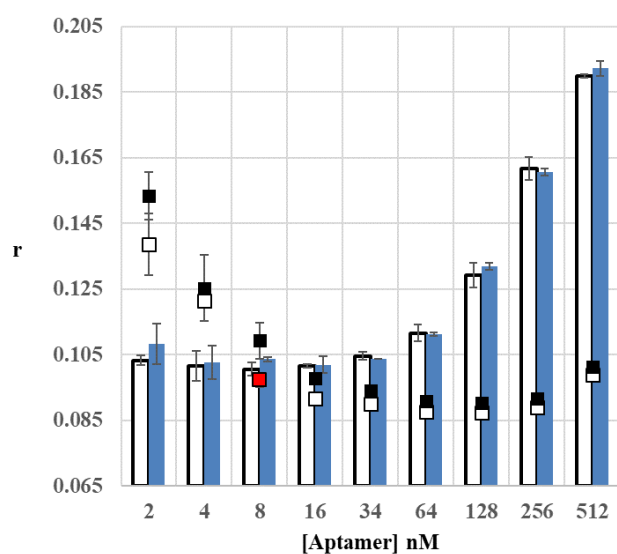
**Table S1:** Mfold predictions of duplex formation at 25°C under aptamer working buffer conditions. Complementary strands are coloured. Free energy and enthalpy are in kcal/mol; entropy is in e.u. (cal/mol/K).

| TR-CSA  | TR-CSB  | CS-Tym   |
|---|---|--|
|   |   |  |
| $\Delta G = -11.6$<br>$\Delta H = -73.3$<br>$\Delta S = -207.1$<br>$T_m = 35.7^\circ\text{C}$ | $\Delta G = -12.0$<br>$\Delta H = -70.5$<br>$\Delta S = -196.2$<br>$T_m = 38.2^\circ\text{C}$ | $\Delta G = -9.8$<br>$\Delta H = -67.0$<br>$\Delta S = -191.8$<br>$T_m = 28.6^\circ\text{C}$ |

**Figure S1. A)** FA anisotropy of SG against **SS2-55** (bars) or **SS24-35** (square) concentration, depicted under aptamer concentration without target (empty symbols) and with 100  $\mu\text{M}$  isocarbophos (Filled symbols). Binding buffer conditions: 10 mM Tris, pH 8, 50 mM NaCl, 10 mM KCl, 10 mM  $\text{MgCl}_2$  and 5% ethanol.

**B)** Comparison of FA anisotropy change of SG for Apt-Vaso-55, Apt-Tym-49, Apt-Tym-38 and Apt-Tym-23 from literature data for respectively 25  $\mu\text{M}$  of arginine vasopressin and 100  $\mu\text{M}$  of L-tyrosinamide. Experimental conditions for arginine vasopressine: SG: 1.05  $\mu\text{M}$ ; Aptamers: 15.6 nM; Binding buffer: 10 mM Tris, pH 7.5, 50 mM KCl, 3 mM  $\text{MgCl}_2$  and 2.5% ethanol; Temperature 25°C; for tyrosinamide: SG: 1.05  $\mu\text{M}$ ; Aptamers: 32 nM; Binding buffer: 10 mM Tris, pH 7.5, 25 mM NaCl, 5 mM  $\text{MgCl}_2$  and 5% ethanol or 2.5% for<sup>23</sup>; Temperature 25°C.

**A)**



**B)**

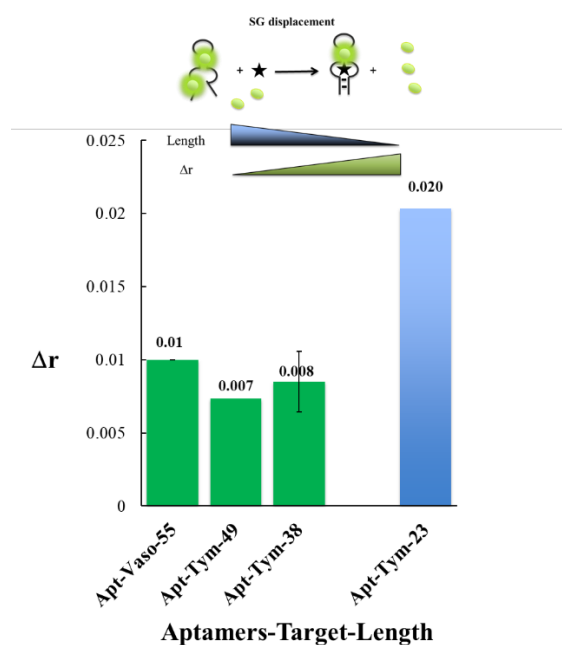


**Figure S2.** Titration curves of CS-Tym (black triangle) with increasing Apt-Tym-38 aptamer concentration with L-tyrosinamide at 100  $\mu$ M. Binding buffer conditions: 10 mM Tris, pH 7.5, 25 mM NaCl, 5 mM MgCl<sub>2</sub> and 5% ethanol. Titration curves of CS-9A (red) and CS-9B (black) with increasing SS-24-35 aptamer concentration with isocarboxiphos at 500  $\mu$ M (square) or with 100  $\mu$ M phorate (circle). Triplicate experiments. CS concentration: 20 nM. Binding buffer conditions: 10 mM Tris, pH 8, 50 mM NaCl, 10 mM KCl, 10 mM MgCl<sub>2</sub> and 5% ethanol.

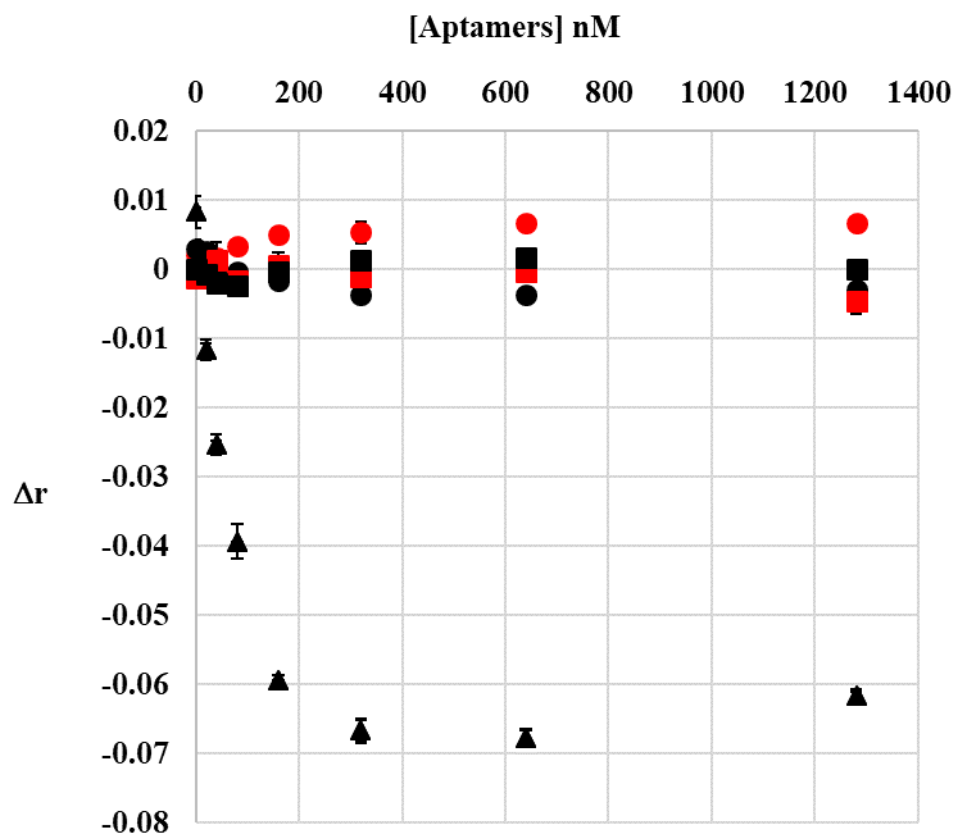


**Figure S3.** ITC analysis of binding affinity of **SS2-55** (30  $\mu\text{M}$ ) **A**) and **SS24-35** (30  $\mu\text{M}$ ) **B**) with 300  $\mu\text{M}$  of phorate. Experimental conditions: 50 mM Tris, pH 8, 50 mM NaCl, 10 mM KCl, 10 mM  $\text{MgCl}_2$ , 5% Ethanol. Temperature: 15°C.

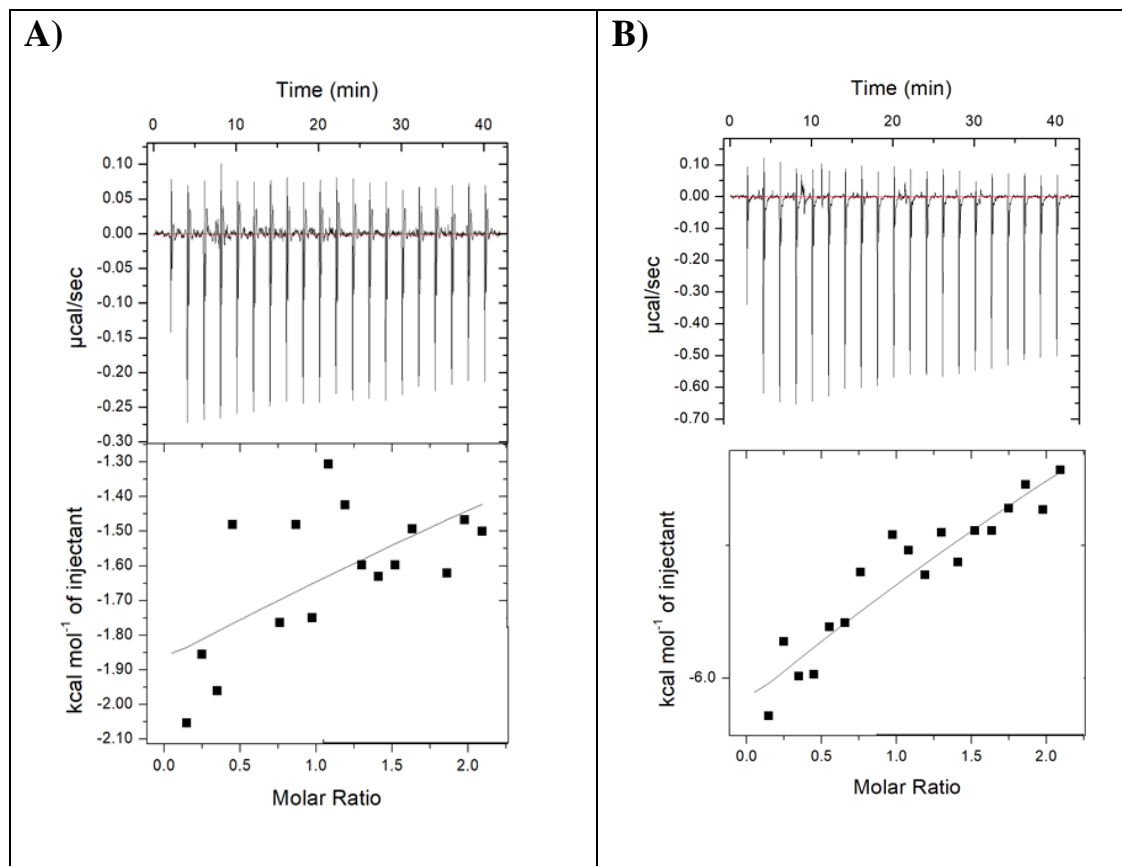


**Figure S4.** **A)** ITC analysis of binding affinity between Apt-L Tym-38 (30  $\mu\text{M}$ ) aptamer and its target (300  $\mu\text{M}$ ) at 15°C. **B)** Blank with 300  $\mu\text{M}$  of tyrosinamide at 15°C. Buffer composition: 10 mM Tris, pH 7.5, 25 mM NaCl, 5 mM  $\text{MgCl}_2$ , 5% Ethanol.

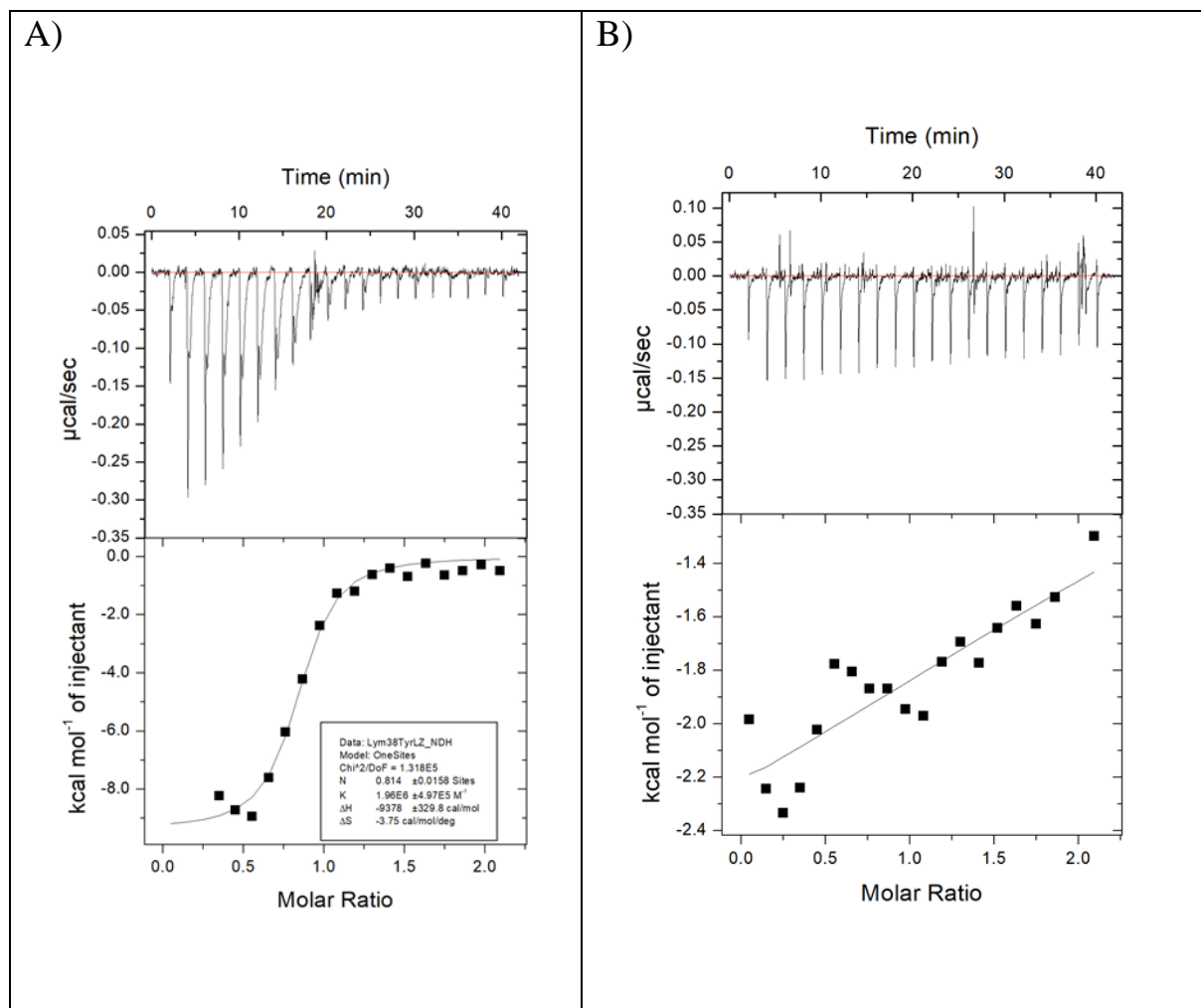
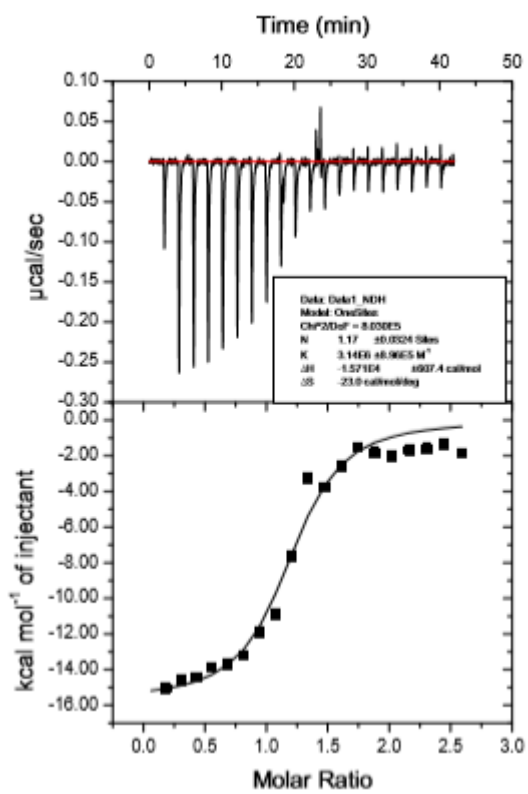


**Figure S5.** ITC analysis of binding affinity between Apt-OTA (8  $\mu\text{M}$ ) aptamer and its target (99  $\mu\text{M}$ ) at 15°C. Buffer composition: 10 mM Tris, pH 8.5, 120 mM NaCl, 5 mM KCl, 20 mM MgCl<sub>2</sub>, 3.66% ethanol.



## 4.2 Conclusions

In conclusion, we have not been capable to develop fluorescent isocarbophos and phorate aptasensors in homogeneous phase. Further experiments by isothermal titration calorimetry (ITC) suggest that aptamers bind neither to isocarbophos or phorate with claimed dissociation constants in the micromolar range.

However, the results obtained are not consistent with those described in the literature. Despite the techniques used in our study are the most common in aptasensors-assay, they have never been tested for these aptamers. Almost all pesticide-aptasensors rely on solid support-based methods, notably gold nanoparticles.<sup>162</sup> The reported works very often lack important information and the conditions used in the experiments are not described (concentrations, buffers..). Likewise, the negative controls necessary to validate the results obtained are in most cases not shown.

# **Conclusions and perspectives**

In order to realize an innovative specific sensor for the detection of pesticides, my project focused on kissing complex and light-up approaches.

Through the combination of these two strategies, we have developed with success new aptasensors specific for different type of targets. To demonstrate their functionality, two proof-of-concepts have been developed. The first one relies on the implementation of a fluorescent kissing-complex able to detect microRNA hairpins and the second one based on the construction of a fluorescent double-switch complex to detect small molecules. Through these works, we have demonstrated the possibility of increasing the specificity of an aptasensor by introducing a double recognition system. Both concepts have proved great specificity for their targets demonstrating that i) they could be extended to the development of sensor for several small molecules, and ii) they can be used as analytical tool in different chemical or biochemical fields.

In order to prove the generalizability of this system, we have recently designed a double-switch system based on RNA-DNA kissing interaction between two new aptaswitches, for the detection of two small targets simultaneously (data not shown). Here again, this system proved to be promising. However, further experiments will be needed to confirm its functionality.

Despite the rather satisfactory results obtained in the approaches mentioned above, the attempt to generate a new aptasensor for pesticide detection was unsuccessful. In fact, chosen pesticide-aptamers proved unsuitable to be converted into aptaswitches. While we failed to create an aptasensor as we hoped, this work allowed us to give a contribution to the aptamer community.

A future perspective would be to investigate the ability of the capture-SELEX to select aptamers towards pesticide as previously described in chapter 1. Another innovate alternative will be to use a high performing separation technique such as capillary electrophoresis. Based on our knowledge, this type of selection for small molecules has never been performed before.

Undoubtedly, the development of a new selection method will take a long and thorough job. In fact, on one hand, capillary electrophoresis is highly performing in the selection of aptamers, on the other, it is a meticulous technique that requires great skills.<sup>164,165</sup> All the conditions, related to the technique (capillary diameter, pressure, voltage, current, temperature, pH, salt concentration..) and the selection strategy (library design, capture sequence, target choice, stringency ...), will have to be set up.

Despite the difficulties to be faced for this, the prospect of a new selection remains a difficult challenge, but I am really confident for the realization of this project, and I believe that this system would open the door for a new, highly performing and rapid selection method for small molecules including pesticides.

# References

1. Nguyen, V.-T. *et al.* Aptamer-based environmental biosensors for small molecule contaminants. *Current Opinion in Biotechnology* **45**, 15–23 (2017).
2. Sudsakorn, S. *et al.* Determination of 1,25-dihydroxyvitamin D2 in rat serum using liquid chromatography with tandem mass spectrometry. *Journal of Chromatography B* **879**, 139–145 (2011).
3. Wu, L. *et al.* Application of Magnetic Solvent Bar Liquid-Phase Microextraction for Determination of Organophosphorus Pesticides in Fruit Juice Samples by Gas Chromatography Mass Spectrometry. *Food Chem* **176**, 197–204 (2015)
4. Singh, K. V. *et al.* Synthesis and Characterization of Hapten–Protein Conjugates for Antibody Production against Small Molecules. *Bioconjugate Chemistry* **15**, 168–173 (2004).
5. Durand, G. *et al.* Riboswitches Based on Kissing Complexes for the Detection of Small Ligands. *Angewandte Chemie International Edition* **53**, 6942–6945 (2014).
6. Goux, E. *et al.* An improved design of the kissing complex-based aptasensor for the detection of adenosine. *Analytical and Bioanalytical Chemistry* **407**, 6515–6524 (2015).
7. Tuerk, C. *et al.* Systematic Evolution of Ligands by Exponential Enrichment: RNA Ligands to Bacteriophage T4 DNA Polymerase. *Science*, **249**, 505–510 (1990).
8. Ellington, AD. *et al.* In vitro selection of RNA molecules that bind specific ligands. *Nature*. **346** 818-822 (1990).
9. McKeague, M. *et al.* Challenges and Opportunities for Small Molecule Aptamer Development. *Journal of Nucleic Acids* **2012**, 1–20 (2012).
10. Stojanovic, M. N. *et al.* Aptamer-Based Folding Fluorescent Sensor for Cocaine. *Journal of the American Chemical Society* **123**, 4928–4931 (2001).
11. Fei, A. *et al.* Label-free impedimetric aptasensor for detection of femtomole level acetamiprid using gold nanoparticles decorated multiwalled carbon nanotube-reduced graphene oxide nanoribbon composites. *Biosensors and Bioelectronics* **70**, 122–129 (2015).
12. Wang, P. *et al.* Aptamer-wrapped gold nanoparticles for the colorimetric detection of omethoate. *Science China Chemistry* **59**, 237–242 (2016).
13. Zhang, C. *et al.* Organophosphorus pesticides detection using broad-specific single-stranded DNA based fluorescence polarization aptamer assay. *Biosensors and Bioelectronics* **55**, 216–219 (2014).
14. Nutiu, R. & Li, Y. Structure-Switching Signaling Aptamers. *Journal of the American Chemical Society* **125**, 4771–4778 (2003).
15. Song, S.-H. *et al.* Aptamer-Based Detection Methodology Studies in Food Safety. *Food Analytical Methods* **12**, 966–990 (2019).
16. Walter, J.-G. *et al.* Aptasensors for Small Molecule Detection. *Zeitschrift für Naturforschung B* **67**, 976–986 (2012).
17. Modh, H. *et al.* Aptamer-Modified Magnetic Beads in Biosensing. *Sensors* **18**, 1041 (2018).

18. Gaudin, V. Advances in biosensor development for the screening of antibiotic residues in food products of animal origin – A comprehensive review. *Biosensors and Bioelectronics* **90**, 363–377 (2017).
19. Shihabi, Z. K. & Friedberg, M. A. Analysis of small molecules for clinical diagnosis by capillary electrophoresis. *Electrophoresis* **18**, 1724–1732 (1997).
20. Kim, Y. S. & Gu, M. B. Advances in Aptamer Screening and Small Molecule Aptasensors. in *Biosensors Based on Aptamers and Enzymes* (eds. Gu, M. B. & Kim, H.-S.) vol. 140 29–67 (Springer Berlin Heidelberg, 2013).
21. Modh, H. B. *et al.* Specific detection of tetanus toxoid using an aptamer-based matrix. *Journal of Biotechnology* **238**, 15–21 (2016).
22. Cho, E. J. *et al.* Applications of Aptamers as Sensors. *Annual Review of Analytical Chemistry* **2**, 241–264 (2009).
23. Chen, A. & Yang, S. Replacing antibodies with aptamers in lateral flow immunoassay. *Biosensors and Bioelectronics* **71**, 230–242 (2015).
24. Bauer, M. *et al.* Anything You Can Do, I Can Do Better: Can Aptamers Replace Antibodies in Clinical Diagnostic Applications? *Molecules* **24**, 4377 (2019).
25. Pfeiffer, F. & Mayer, G. Selection and Biosensor Application of Aptamers for Small Molecules. *Frontiers in Chemistry* **4**, (2016).
26. Paborsky L.R. *et al.* The single-stranded DNA aptamer-binding site of human thrombin. *J Biol Chem*, **268**, 20808-20811 (1993);
27. Jenison, R. *et al.* High-resolution molecular discrimination by RNA. *Science* **263**, 1425–1429 (1994).
28. Hofmann H.P. *et al.* Ni<sup>2+</sup>-binding RNA motifs with an asymmetric purine-rich internal loop and a G-A base pair. *RNA* **3**, 1289-1300 (1997).
29. Cao, X. *et al.* Combining use of a panel of ssDNA aptamers in the detection of *Staphylococcus aureus*. *Nucleic Acids Research* **37**, 4621–4628 (2009).
30. London, G. M. *et al.* Isolation and characterization of 2'-F-RNA aptamers against whole HIV-1 subtype C envelope pseudovirus. *Biochemical and Biophysical Research Communications* **456**, 428–433 (2015).
31. Mayer, G. *et al.* Fluorescence-activated cell sorting for aptamer SELEX with cell mixtures. *Nature Protocols* **5**, 1993–2004 (2010).
32. Tan, S. Y. *et al.* SELEX Modifications and Bioanalytical Techniques for Aptamer-Target Binding Characterization. *Critical Reviews in Analytical Chemistry* **46**, 521–537 (2016).
33. Patel, D. J. *et al.* Structure, recognition and adaptive binding in RNA aptamer complexes. *Journal of Molecular Biology* **272**, 645–664 (1997).
34. Mascini, M. *et al.* Nucleic Acid and Peptide Aptamers: Fundamentals and Bioanalytical Aspects. *Angewandte Chemie International Edition* **51**, 1316–1332 (2012).
35. Darfeuille, F. *et al.* Aptamers Targeted to an RNA Hairpin Show Improved Specificity Compared to that of Complementary Oligonucleotides †. *Biochemistry* **45**, 12076–12082 (2006).
36. Tasset, D. M. *et al.* Oligonucleotide inhibitors of human thrombin that bind distinct epitopes. *Journal of Molecular Biology* **272**, 688–698 (1997).

37. Sullivan, R., Adams, M. C., Naik, R. R. & Milam, V. T. Analyzing Secondary Structure Patterns in DNA Aptamers Identified via CompELS. *Molecules* **24**, 1572 (2019).
38. Tsukiji, S. *et al.* Ribozymes that use redox cofactors. *Pure and Applied Chemistry* **76**, 1525–1536 (2004).
39. Famulok, M. Molecular Recognition of Amino Acids by RNA-Aptamers: An L-Citrulline Binding RNA Motif and Its Evolution into an L-Arginine Binder. *Journal of the American Chemical Society* **116**, 1698–1706 (1994).
40. Wrist, A. *et al.* The Theophylline Aptamer: 25 Years as an Important Tool in Cellular Engineering Research. *ACS Synthetic Biology* (2020) doi:10.1021/acssynbio.9b00475.
41. Geiger, A. RNA aptamers that bind L-arginine with sub-micromolar dissociation constants and high enantioselectivity. *Nucleic Acids Research* **24**, 1029–1036 (1996).
42. Kim, Y. S. *et al.* Isolation and characterization of enantioselective DNA aptamers for ibuprofen. *Bioorganic & Medicinal Chemistry* **18**, 3467–3473 (2010).
43. Shoji, A. *et al.* Modified DNA Aptamer That Binds the ( R )-Isomer of a Thalidomide Derivative with High Enantioselectivity. *Journal of the American Chemical Society* **129**, 1456–1464 (2007).
44. Zhang, Y. *et al.* Recent Advances in Aptamer Discovery and Applications. *Molecules* **24**, 941 (2019).
45. Lee, J. *et al.* Aptamer therapeutics advance. *Current Opinion in Chemical Biology* **10**, 282–289 (2006).
46. Green, L.S. *et al.* Nuclease-resistant nucleic acid ligands to vascular permeability factor/vascular endothelial growth factor. *Chem Biol.* **2**, 683-695 (1995).
47. Gold, L. *et al.* Aptamer-based multiplexed proteomic technology for biomarker discovery. *Nature Precedings* 77 (2010).
48. He, W. *et al.* X-Aptamers: A Bead-Based Selection Method for Random Incorporation of Druglike Moieties onto Next-Generation Aptamers for Enhanced Binding. *Biochemistry* **51**, 8321–8323 (2012).
49. Matsunaga, K. *et al.* Architecture of high-affinity unnatural-base DNA aptamers toward pharmaceutical applications. *Scientific Reports* **5**, (2016).
50. Stoltenburg, R. *et al.* SELEX—A (r)evolutionary method to generate high-affinity nucleic acid ligands. *Biomolecular Engineering* **24**, 381–403 (2007).
51. Mencin, N. *et al.* Optimization of SELEX: Comparison of different methods for monitoring the progress of in vitro selection of aptamers. *Journal of Pharmaceutical and Biomedical Analysis* **91**, 151–159 (2014).
52. Park, J.-W. *et al.* Immobilization-free screening of aptamers assisted by graphene oxide. *Chem. Commun.* **48**, 2071–2073 (2012).
53. Nutiu, R. & Li, Y. In Vitro Selection of Structure-Switching Signaling Aptamers. *Angewandte Chemie International Edition* **44**, 1061–1065 (2005).
54. Lu, C. *et al.* Comparison of MoS<sub>2</sub>, WS<sub>2</sub>, and Graphene Oxide for DNA Adsorption and Sensing. *Langmuir* **33**, 630–637 (2017).
55. Chen, X. *et al.* Screening and Identification of DNA Aptamers against T-2 Toxin Assisted by Graphene Oxide. *Journal of Agricultural and Food Chemistry* **62**, 10368–10374 (2014).

56. Nguyen, V.-T. *et al.* Multiple GO-SELEX for efficient screening of flexible aptamers. *Chem. Commun.* **50**, 10513–10516 (2014).
57. Kwon, Y. S. *et al.* Detection of Iprobenfos and Edifenphos using a new Multi-aptasensor. *Analytica Chimica Acta* **868**, 60–66 (2015).
58. Gu, H. *et al.* Graphene oxide-assisted non-immobilized SELEX of okdaic acid aptamer and the analytical application of aptasensor. *Scientific Reports* **6**, (2016).
59. Wang, L. *et al.* Selection of DNA aptamers that bind to four organophosphorus pesticides. *Biotechnology Letters* **34**, 869–874 (2012).
60. He, J. *et al.* Isolation and Identification of the DNA Aptamer Target to Acetamidrid. *Journal of Agricultural and Food Chemistry* **59**, 1582–1586 (2011).
61. Wang, H. *et al.* Selection and characterization of DNA aptamers for the development of light-up biosensor to detect Cd(II). *Talanta* **154**, 498–503 (2016).
62. Stoltenburg, R. *et al.* Capture-SELEX: Selection of DNA Aptamers for Aminoglycoside Antibiotics. *Journal of Analytical Methods in Chemistry* **2012**, 1–14 (2012).
63. Spiga, F. M. *et al.* More DNA–Aptamers for Small Drugs: A Capture–SELEX Coupled with Surface Plasmon Resonance and High-Throughput Sequencing. *ACS Combinatorial Science* **17**, 326–333 (2015).
64. Zhang, A. *et al.* In Vitro Selection of DNA Aptamers that Binds Geniposide. *Molecules* **22**, 383 (2017).
65. Cruz-Aguado, J. A. & Penner, G. Fluorescence Polarization Based Displacement Assay for the Determination of Small Molecules with Aptamers. *Analytical Chemistry* **80**, 8853–8855 (2008).
66. Kanakaraj, I. *et al.* Biophysical characterization of VEGF–aHt DNA aptamer interactions. *International Journal of Biological Macromolecules* **57**, 69–75 (2013).
67. Baker, B. R. *et al.* An Electronic, Aptamer-Based Small-Molecule Sensor for the Rapid, Label-Free Detection of Cocaine in Adulterated Samples and Biological Fluids. *Journal of the American Chemical Society* **128**, 3138–3139 (2006).
68. McKeague, M. *et al.* Comprehensive Analytical Comparison of Strategies Used for Small Molecule Aptamer Evaluation. *Analytical Chemistry* **87**, 8608–8612 (2015).
69. Mello, F. D. *et al.* Mechanisms and Effects Posed by Neurotoxic Products of Cyanobacteria/Microbial Eukaryotes/Dinoflagellates in Algae Blooms: a Review. *Neurotoxicity Research* **33**, 153–167 (2018).
70. Damalas, C. A. & Eleftherohorinos, I. G. Pesticide Exposure, Safety Issues, and Risk Assessment Indicators. *International Journal of Environmental Research and Public Health* **8**, 1402–1419 (2011).
71. Mostafalou, S. & Abdollahi, M. Pesticides: an update of human exposure and toxicity. *Archives of Toxicology* **91**, 549–599 (2017).
72. García-Cañas, V. *et al.* Present and Future Challenges in Food Analysis: Foodomics. *Analytical Chemistry* **84**, 10150–10159 (2012).
73. Sefah, K. *et al.* In vitro selection with artificial expanded genetic information systems. *Proceedings of the National Academy of Sciences* **111**, 1449–1454 (2014).
74. Song, S. *et al.* Aptamer-based biosensors. *TrAC Trends in Analytical Chemistry* **27**,

108–117 (2008).

75. Hayat, A. & Marty, J. L. Aptamer based electrochemical sensors for emerging environmental pollutants. *Frontiers in Chemistry* **2**, (2014).
76. Munzar, J. D. *et al.* Duplexed aptamers: history, design, theory, and application to biosensing. *Chemical Society Reviews* **48**, 1390–1419 (2019).
77. Hesselberth, J. *et al.* In vitro selection of nucleic acids for diagnostic applications. *Reviews in Molecular Biotechnology* **74**, 15–25 (2000).
78. Ruta, J. *et al.* Noncompetitive Fluorescence Polarization Aptamer-based Assay for Small Molecule Detection. *Analytical Chemistry* **81**, 7468–7473 (2009).
79. Perrier, S. *et al.* Rationally designed aptamer-based fluorescence polarization sensor dedicated to the small target analysis. *Biosensors and Bioelectronics* **25**, 1652–1657 (2010).
80. Kumar Y. V. V. *et al.* Development of a FRET-based fluorescence aptasensor for the detection of aflatoxin B1 in contaminated food grain samples. *RSC Advances* **8**, 10465–10473 (2018).
81. Wang, C. *et al.* A simple aptamer molecular beacon assay for rapid detection of aflatoxin B1. *Chinese Chemical Letters* **30**, 1017–1020 (2019).
82. Zheng, J. *et al.* Rationally designed molecular beacons for bioanalytical and biomedical applications. *Chemical Society Reviews* **44**, 3036–3055 (2015).
83. Stojanovic, M. N. *et al.* Fluorescent Sensors Based on Aptamer Self-Assembly. *Journal of the American Chemical Society* **122**, 11547–11548 (2000).
84. Chen, A. *et al.* Split aptamers and their applications in sandwich aptasensors. *TrAC Trends in Analytical Chemistry* **80**, 581–593 (2016).
85. Yang, C. *et al.* Macrocyclic Host-Dye Reporter for Sensitive Sandwich-Type Fluorescent Aptamer Sensor. *Analytical Chemistry* **87**, 3139–3143 (2015).
86. Park, J.-H. *et al.* High-sensitivity detection of ATP using a localized surface plasmon resonance (LSPR) sensor and split aptamers. *Biosensors and Bioelectronics* **73**, 26–31 (2015).
87. Li, Q. *et al.* Split aptamer mediated endonuclease amplification for small-molecule detection. *Chemical Communications* **51**, 4196–4199 (2015).
88. Guo, T. *et al.* Novel Ratiometric Electrochemical Biosensor Based on a Split Aptamer for the Detection of Dopamine with Logic Gate Operations. *physica status solidi (a)* **217**, 1900924 (2020).
89. Roncancio, D. *et al.* A Label-Free Aptamer-Fluorophore Assembly for Rapid and Specific Detection of Cocaine in Biofluids. *Analytical Chemistry* **86**, 11100–11106 (2014).
90. Le, T. T. *et al.* Determination of minimal sequence for binding of an aptamer. A comparison of truncation and hybridization inhibition methods. *RSC Adv.* **4**, 47227–47233 (2014).
91. Wang, J., *et al.* Aptamer-Based ATP Assay Using a Luminescent Light Switching Complex. *Analytical Chemistry* **77**, 3542–3546 (2005).
92. Chovelon, B. *et al.* A lifetime-sensitive fluorescence anisotropy probe for DNA-based bioassays: The case of SYBR Green. *Biosensors and Bioelectronics* **90**, 140–145 (2017).

93. Dolgosheina, E. V. *et al.* RNA Mango Aptamer-Fluorophore: A Bright, High-Affinity Complex for RNA Labeling and Tracking. *ACS Chemical Biology* **9**, 2412–2420 (2014).
94. Sando, S. *et al.* Light-Up Hoechst–DNA Aptamer Pair: Generation of an Aptamer-Selective Fluorophore from a Conventional DNA-Staining Dye. *ChemBioChem* **8**, 1795–1803 (2007).
95. Grate, D. & Wilson, C. Laser-mediated, site-specific inactivation of RNA transcripts. *Proceedings of the National Academy of Sciences* **96**, 6131–6136 (1999).
96. Paige, J. S. *et al.* RNA Mimics of Green Fluorescent Protein. *Science* **333**, 642–646 (2011).
97. Babendure, J. R. *et al.* Aptamers Switch on Fluorescence of Triphenylmethane Dyes. *Journal of the American Chemical Society* **125**, 14716–14717 (2003).
98. Stojanovic, M. N. & Kolpashchikov, D. M. Modular Aptameric Sensors. *Journal of the American Chemical Society* **126**, 9266–9270 (2004).
99. Chen, J. *et al.* A simple and rapid biosensor for ochratoxin A based on a structure-switching signaling aptamer. *Food Control* **25**, 555–560 (2012).
100. Lau, P. S. & Li, Y. Exploration of Structure-Switching in the Design of Aptamer Biosensors. in *Biosensors Based on Aptamers and Enzymes* (eds. Gu, M. B. & Kim, H.-S.) vol. 140 69–92 (Springer Berlin Heidelberg, 2013).
101. Feagin, T. A. *et al.* Strategies for Creating Structure-Switching Aptamers. *ACS Sensors* **3**, 1611–1615 (2018).
102. Li, D. *et al.* Target-Responsive Structural Switching for Nucleic Acid-Based Sensors. *Accounts of Chemical Research* **43**, 631–641 (2010).
103. Tomizawa, J. Control of *colE1* plasmid replication: The process of binding of RNA I to the primer transcript. *Cell* **38**, 861–870 (1984).
104. Paillart, J. *et al.* Dimerization of retroviral genomic RNAs: structural and functional implications. *Biochimie* **78**, 639–653 (1996).
105. Persson, C. *et al.* Control of replication of plasmid R1: structures and sequences of the antisense RNA, CopA, required for its binding to the target RNA, CopT. *EMBOJ.* **9** 3767–3775 (1990).
106. Ducongé, F. & Toulmé, J.-J. In vitro selection identifies key determinants for loop–loop interactions: RNA aptamers selective for the TAR RNA element of HIV-1. *RNA* **5**, 1605–1614 (1999).
107. Mishra, R. K. *et al.* Targeting nucleic acid secondary structures by antisense oligonucleotides designed through in vitro selection. *Proceedings of the National Academy of Sciences* **93**, 10679–10684 (1996).
108. Boiziau, C. *et al.* DNA Aptamers Selected Against the HIV-1 *trans* -Activation-responsive RNA Element Form RNA-DNA Kissing Complexes. *Journal of Biological Chemistry* **274**, 12730–12737 (1999).
109. Durand, G. *et al.* A combinatorial approach to the repertoire of RNA kissing motifs; towards multiplex detection by switching hairpin aptamers. *Nucleic Acids Research* **44**, 4450–4459 (2016).
110. Goux, E. *et al.* A colorimetric nanosensor based on a selective target-responsive aptamer kissing complex. *Nanoscale* **9**, 4048–4052 (2017).

111. Chovelon, B. *et al.* ELAKCA: Enzyme-Linked Aptamer Kissing Complex Assay as a Small Molecule Sensing Platform. *Analytical Chemistry* **88**, 2570–2575 (2016).
112. Liu, M. *et al.* Aptasensors for pesticide detection. *Biosensors and Bioelectronics* **130**, 174–184 (2019).
113. Zhang W., *et al.* Practical Application of Aptamer-Based Biosensors in Detection of Low Molecular Weight Pollutants in Water Sources. *Molecules* **23**, 344 (2018).
114. Bahreyni, A. *et al.* Fluorometric aptasensing of the neonicotinoid insecticide acetamiprid by using multiple complementary strands and gold nanoparticles. *Microchimica Acta* **185**, (2018).
115. Kim, Y. S. *et al.* Electrochemical detection of 17 $\beta$ -estradiol using DNA aptamer immobilized gold electrode chip. *Biosensors and Bioelectronics* **22**, 2525–2531 (2007).
116. Kim, Y. S. *et al.* A novel colorimetric aptasensor using gold nanoparticle for a highly sensitive and specific detection of oxytetracycline. *Biosensors and Bioelectronics* **26**, 1644–1649 (2010).
117. Bahreyni, A. *et al.* Fluorometric aptasensing of the neonicotinoid insecticide acetamiprid by using multiple complementary strands and gold nanoparticles. *Microchimica Acta* **185**, (2018).
118. Wang, J. *et al.* A novel fluorescent aptasensor for ultrasensitive and selective detection of acetamiprid pesticide based on the inner filter effect between gold nanoparticles and carbon dots. *The Analyst* **143**, 5151–5160 (2018).
119. Bahreyni, A. *et al.* Fluorometric aptasensing of the neonicotinoid insecticide acetamiprid by using multiple complementary strands and gold nanoparticles. *Microchimica Acta* **185**, (2018).
120. Liu, Q. *et al.* Fluorescent aptasensing of chlorpyrifos based on the assembly of cationic conjugated polymer-aggregated gold nanoparticles and luminescent metal-organic frameworks. *The Analyst* (2019)
121. Jiang, M. *et al.* Fluorescence assay for three organophosphorus pesticides in agricultural products based on Magnetic-Assisted fluorescence labeling aptamer probe. *Food Chemistry* **307**, 125534 (2020).
122. Kim, Y. S. *et al.* Electrochemical detection of 17 $\beta$ -estradiol using DNA aptamer immobilized gold electrode chip. *Biosensors and Bioelectronics* **22**, 2525–2531 (2007).
123. Mishra, G. *et al.* Electrochemical Aptasensors for Food and Environmental Safeguarding: A Review. *Biosensors* **8**, 28 (2018).
124. Fei, A. *et al.* Label-free impedimetric aptasensor for detection of femtomole level acetamiprid using gold nanoparticles decorated multiwalled carbon nanotube-reduced graphene oxide nanoribbon composites. *Biosensors and Bioelectronics* **70**, 122–129 (2015).
125. Rapini, R. *et al.* Acetamiprid multidetection by disposable electrochemical DNA aptasensor. *Talanta* **161**, 15–21 (2016).
126. Shi, H., *et al.* Aptamer-based colorimetric sensing of acetamiprid in soil samples: Sensitivity, selectivity and mechanism. *Journal of Hazardous Materials* **260**, 754–761 (2013).
127. Wang, P. *et al.* Aptamer-wrapped gold nanoparticles for the colorimetric detection

- of omethoate. *Science China Chemistry* **59**, 237–242 (2016).
128. Abnous, K. *et al.* A colorimetric gold nanoparticle aggregation assay for malathion based on target-induced hairpin structure assembly of complementary strands of aptamer. *Microchimica Acta* **185**, (2018).
  129. Dou, X. *et al.* A gold-based nanobeacon probe for fluorescence sensing of organophosphorus pesticides. *Analytica Chimica Acta* **891**, 291–297 (2015).
  130. Guo, J. *et al.* Aptamer-based fluorescent screening assay for acetamiprid via inner filter effect of gold nanoparticles on the fluorescence of CdTe quantum dots. *Analytical and Bioanalytical Chemistry* **408**, 557–566 (2016).
  131. Hu, W. *et al.* Fabricating a novel label-free aptasensor for acetamiprid by fluorescence resonance energy transfer between NH<sub>2</sub>-NaYF<sub>4</sub>: Yb, Ho@SiO<sub>2</sub> and Au nanoparticles. *Biosensors and Bioelectronics* **80**, 398–404 (2016).
  132. Bai, W. *et al.* Gold nanoparticle-based colorimetric aptasensor for rapid detection of six organophosphorous pesticides: Colorimetric aptasensor for six organophosphorous pesticides detection. *Environmental Toxicology and Chemistry* **34**, 2244–2249 (2015).
  133. Yang, Z. *et al.* A facile label-free colorimetric aptasensor for acetamiprid based on the peroxidase-like activity of hemin-functionalized reduced graphene oxide. *Biosensors and Bioelectronics* **65**, 39–46 (2015).
  134. Fan, L. *et al.* A highly selective electrochemical impedance spectroscopy-based aptasensor for sensitive detection of acetamiprid. *Biosensors and Bioelectronics* **43**, 12–18 (2013).
  135. Ahmad, I. *et al.* Photostability and Photostabilization of Drugs and Drug Products. *International Journal of Photoenergy* **2016**, 1–19 (2016).
  136. Bouhedda, F. *et al.* Light-Up RNA Aptamers and Their Cognate Fluorogens: From Their Development to Their Applications. *International Journal of Molecular Sciences* **19**, 44 (2017).
  137. Trachman, R. J. *et al.* Structural Principles of Fluorescent RNA Aptamers. *Trends in Pharmacological Sciences* **38**, 928–939 (2017).
  138. Baugh, C. *et al.* 2.8 Å crystal structure of the malachite green aptamer 1 1 Edited by J. A. Doudna. *Journal of Molecular Biology* **301**, 117–128 (2000).
  139. Nguyen, D. H. *et al.* Binding to an RNA Aptamer Changes the Charge Distribution and Conformation of Malachite Green. *Journal of the American Chemical Society* **124**, 15081–15084 (2002).
  140. Ouellet, J. RNA Fluorescence with Light-Up Aptamers. *Frontiers in Chemistry* **4**, (2016).
  141. Kolpashchikov, D. M. Binary Malachite Green Aptamer for Fluorescent Detection of Nucleic Acids. *Journal of the American Chemical Society* **127**, 12442–12443 (2005).
  142. Bhadra, S. & Ellington, A. D. A Spinach molecular beacon triggered by strand displacement. *RNA* **20**, 1183–1194 (2014).
  143. Song, W. *et al.* Imaging bacterial protein expression using genetically encoded RNA sensors. *Nature Methods* **10**, 873–875 (2013).
  144. DasGupta, S. *et al.* Spinach RNA aptamer detects lead( II ) with high selectivity. *Chemical Communications* **51**, 9034–9037 (2015).

145. Zhao, Q. *et al.* Aptamer Binding Assays and Molecular Interaction Studies Using Fluorescence Anisotropy - A Review. *Analytica Chimica Acta* (2020) doi:10.1016/j.aca.2020.05.061.
146. Perrier, S. *et al.* Panoply of Fluorescence Polarization/Anisotropy Signaling Mechanisms for Functional Nucleic Acid-Based Sensing Platforms. *Analytical Chemistry* **90**, 4236–4248 (2018).
147. Sharma, A. K. *et al.* Enzyme-Linked Small-Molecule Detection Using Split Aptamer Ligation. *Analytical Chemistry* **84**, 6104–6109 (2012).
148. Zhu, Z. *et al.* Optimization of the structure-switching aptamer-based fluorescence polarization assay for the sensitive tyrosinamide sensing. *Analytica Chimica Acta* **707**, 191–196 (2011).
149. Chovelon, B. *et al.* A lifetime-sensitive fluorescence anisotropy probe for DNA-based bioassays: The case of SYBR Green. *Biosensors and Bioelectronics* **90**, 140–145 (2017).
150. Slavkovic, S. *et al.* Structure–affinity relationship of the cocaine-binding aptamer with quinine derivatives. *Bioorganic & Medicinal Chemistry* **23**, 2593–2597 (2015).
151. Challier, L. *et al.* Multianalytical Study of the Binding between a Small Chiral Molecule and a DNA Aptamer: Evidence for Asymmetric Steric Effect upon 3'- versus 5'-End Sequence Modification. *Analytical Chemistry* **88**, 11963–11971 (2016).
152. Sakamoto, T. *et al.* Thermodynamic study of aptamers binding to their target proteins. *Biochimie* **145**, 91–97 (2018).
153. Turnbull, W. B. & Daranas, A. H. On the Value of  $c$ : Can Low Affinity Systems Be Studied by Isothermal Titration Calorimetry? *Journal of the American Chemical Society* **125**, 14859–14866 (2003).
154. Slavkovic, S. & Johnson, P. E. Isothermal titration calorimetry studies of aptamer-small molecule interactions: practicalities and pitfalls. *OPEN ACCESS* **2**, 7 (2018).
155. Neves, M. A. D. *et al.* Defining the secondary structural requirements of a cocaine-binding aptamer by a thermodynamic and mutation study. *Biophysical Chemistry* **153**, 9–16 (2010).
156. Zhang, Z. *et al.* New insights into a classic aptamer: binding sites, cooperativity and more sensitive adenosine detection. *Nucleic Acids Research* **45**, 7593–7601 (2017).
157. Lee, H. *et al.* Biogenesis and regulation of the let-7 miRNAs and their functional implications. *Protein & Cell* **7**, 100–113 (2016).
158. Hu, J. *et al.* Serum miR-206 and other muscle-specific microRNAs as non-invasive biomarkers for Duchenne muscular dystrophy. *Journal of Neurochemistry* **129**, 877–883 (2014).
159. Sett, A., Zara, L. *et al.* Engineering Light-Up Aptamers for the Detection of RNA Hairpins through Kissing Interaction. *Analytical Chemistry* **92**, 9113–9117 (2020).
160. Zimmermann, G. R. *et al.* Molecular interactions and metal binding in the theophylline-binding core of an RNA aptamer. *RNA* **6**, 659–667 (2000).
161. Li, X. *et al.* One-step, visual and sensitive detection of phorate in blood based on a DNA–AgNC aptasensor. *New Journal of Chemistry* **42**, 6293–6298 (2018).
162. Bala, R. *et al.* Development of gold nanoparticles-based aptasensor for the

colorimetric detection of organophosphorus pesticide phorate. *Analytical and Bioanalytical Chemistry* **408**, 333–338 (2016).

163. Pang, S. *et al.* Development of a single aptamer-based surface enhanced Raman scattering method for rapid detection of multiple pesticides. *Analyst* **139**, 1895-1901 (2014).

164. Zhu, C. *et al.* Evolution of multi-functional capillary electrophoresis for high-efficiency selection of aptamers. *Biotechnology Advances* 107432 (2019).

165. Mendonsa, S. D. & Bowser, M. T. In Vitro Evolution of Functional DNA Using Capillary Electrophoresis. *Journal of the American Chemical Society* **126**, 20–21 (2004).



## **Aptamer biosensor development for small molecule detection**

**Abstract.** Nowadays, there is an urgency to detect small molecules (molar mass < 1000 g/mol) such as pesticides, toxins, antibiotics or drug residues to protect both human and environment health. It is very important to create a cost effective and simple to use sensor system able to rapidly quantify small molecules, with high efficiency of measurements. In this context, aptamers that are RNA or DNA oligonucleotides displaying high affinity and specificity for their cognate target can be used as molecular recognition element in biosensors. These biosensors called aptasensors can provide a valid and interesting alternative to conventional methods. The aim of this thesis consists in engineering new specific aptasensors based on the coupling of two strategies: light-up and kissing-complex. Firstly, we designed a fluorescent aptamer-based sensing specific of two microRNA precursors: let-7b and miR206. In a second time, based on this construct, we create a label free fluorescent double-switch aptasensor to detect theophylline. Finally, in the third work, two aptamer-based fluorescence anisotropy approaches, using the displacement concept, are investigated to detect pesticides including isocarbophos and phorate.

**Key words:** Nucleic acid aptamers, aptasensors, small molecules, pesticides, kissing complex, light-up, fluorescence anisotropy, isothermal titration calorimetry

## **Développement de biocapteurs à base aptamères pour la détection de petites molécules**

**Résumé:** De nos jours, il est urgent de créer des biocapteurs peu coûteux, efficaces et simples à utiliser, capables de quantifier et de détecter rapidement des petites molécules (masse molaire <1000 g / mol) telles que les pesticides, les toxines, les antibiotiques ou les médicaments, pour protéger, à la fois la santé humaine et l'environnement. Les aptamères sont des oligonucléotides en série ARN ou ADN présentant une affinité et une spécificité élevées pour leur cible. Ils peuvent être utilisés comme éléments de reconnaissance moléculaire dans des biocapteurs, appelés aptacapteurs. Ces derniers offrent une alternative prometteuse aux méthodes conventionnelles pour la détection des petites molécules. L'objectif de cette thèse est de concevoir de nouveaux aptacapteurs spécifiques basés sur le couplage de deux stratégies : « light-up » et « kissing-complexe ». Dans un premier temps, une détection à base d'aptamères fluorescents spécifiques de deux précurseurs de microARN, let-7b et miR206, a été développée. Suivant ce concept, un aptacapteur fluorescent à double reconnaissance capable de détecter la théophylline a été par la suite créé. Enfin, deux approches utilisant la méthode d'anisotropie de fluorescence et le déplacement d'un brin complémentaire de l'aptamère ou d'un intercalant de l'ADN ont été appréhendées pour la détection de deux pesticides, l'isocarbophos et le phorate.

**Mots clés:** aptamères, aptacapteurs, petites molécules, pesticides, kissing-complexe, light-up, anisotropie de fluorescence, calorimétrie de titrage isotherme.